Design of Economic and Open Source Incubator for Developing Countries

by

Miguel A. Ortiz

A Report Submitted to the Faculty of the

Milwaukee School of Engineering

In Partial Fulfillment of the

Requirements for the Degree of

Master of Science in Engineering

Milwaukee, Wisconsin

May 2020

Abstract

The purpose of this document is to describe in detail the capstone project that was completed to fulfill the graduation requirements for a Master of Science in Engineering degree at the Milwaukee School of Engineering (MSOE). The goal of the project was to develop a low-cost incubator for newborns that can be built and maintained in developing nations to support the reduction of newborn deaths caused by hypothermia. For this project, the term “low-cost” was defined as any incubator for which the manufacturing cost is less than four thousand American dollars ($4,000.00). Following the review of an extensive literature on incubators, including an assessment of current products and solutions, the design of a control system for temperature and humidity for a low-cost infant incubator was carried out, along with the design of a physical enclosure. The design process featured a careful evaluation of relevant International Electrotechnical Commission (IEC) standards to ensure that the design would meet requirements associated with the standards. A mathematical model of the control system was developed and simulated using MATLAB and Simulink, respectively. SolidWorks was employed to design the enclosure, and ANSYS was used to verify the materials performance of the design. The use of additive manufacturing was investigated as the means of manufacturing the incubator, but was rejected because of cost. A complete Bill of Materials (BoM) was developed to verify that the proposed incubator can be produced at a cost less than the design goal of four thousand American dollars.

Table of Contents

List of Figures

List of Tables

Nomenclature

Symbols

$A -$ Surface Area of the Baby

$A_f -$ Total Fin Area

$A_t -$ Area of Surface in Contact with the Fluid

$C_c -$ Coefficient of Volumetric Heat Transfer

$C_p -$ Specific Heat Coefficient of Air

$C_v -$ Convective Heat Transfer Coefficient

$F_k -$ Cubic Meters of Blood per Second in the Core Layer

$F_s -$ Cubic Meters of Blood per Second in the Skin Layer

$h_c -$ Heat Conduction Coefficient

$h_v -$ Heat Convection Coefficient

I_0 and I_1 $-$ Modified, Zero − Order Bessel Function

$k -$ Conduction Coefficient

$L -$ Length of the Convection Surface

$\dot{m} -$ Mass Flow per Unit of Time

$N -$ Number of Fins

$Nu_L -$ Nusselt Number

$P -$ Fin Perimeter

$q_a -$ Total Heat Absorbed per Unit of Time

q_{hf} − Total Heat Transfer due to Convection

$Re_L -$ Reynolds Number

$T_a(t)$ − Ambient Temperature as a Function of Time

$T_b(t)$ − Temperature of Blood as a Function of Time

$T_{bh}(t)$ − Temperature of the Surface of the Heating Element

$T_{fin}(t)$ − Final Temperature of the Air Flow as a Function of Time

$T_i(t)$ − Initial Temperature of the Air Flow as a Function of Time

$T_k(t)$ − Core Temperature as a Function of Time

$T_m -$ Temperature of the Resting Surface of the Incubator

$T_s(t)$ − Temperature of Skin as a Function of Time

$T_\infty(t)$ − Temperature of the Cooling Fluid

V − Volume of the Baby's Body

w − Width of the Fin

$\alpha_o O_o(t)$ − Basal Metabolic Heat as Function of Oxygen Consumption

β_R − Coefficient of Radiation Heat Transfer

ε_v − Fraction of the Surface Area Exposed to Convection

ε_c − Fraction of the Surface Area Exposed to Conduction

$\eta_f =$ Fin Efficiency

ρ_b − Density of Blood

ρ_s − Density of Skin

ω_s − Specific Heat of Skin

u_∞ − Speed ofthe Cooling Fluid

ω_b − Specific Heat of Blood

Abbreviations/Acronyms

CAD	-	Computer Aided technology
FEA	-	Finite Element Analysis
FDA	-	Food and Drug Administration
FF	-	Functional Failure
ICE	-	International Electrotechnical Commission
NTE	-	Neutral Thermal Environment,
RCM	-	Reliability Centered Maintenance
UNICEF	-	The United Nations International Children's Emergency Fund
WHO	-	World Health Organization

Introduction

World Health Organization (WHO) data show that prematurity in newborns is the prevalent cause of death among children less than five years old in the world, as shown in Figure 1.

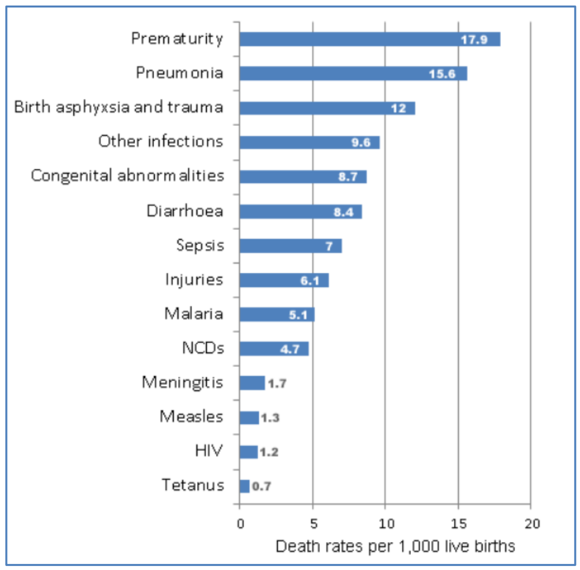

Figure 1. Causes of Death Among Children Under Five Years Old [1].

Even though substantial progress has been made around the globe in reducing the mortality rate, around 5.4 million children die annually, mostly from preventable causes, with 2.5 million deaths occurring in the first month of life, as is shown in Figure 2.

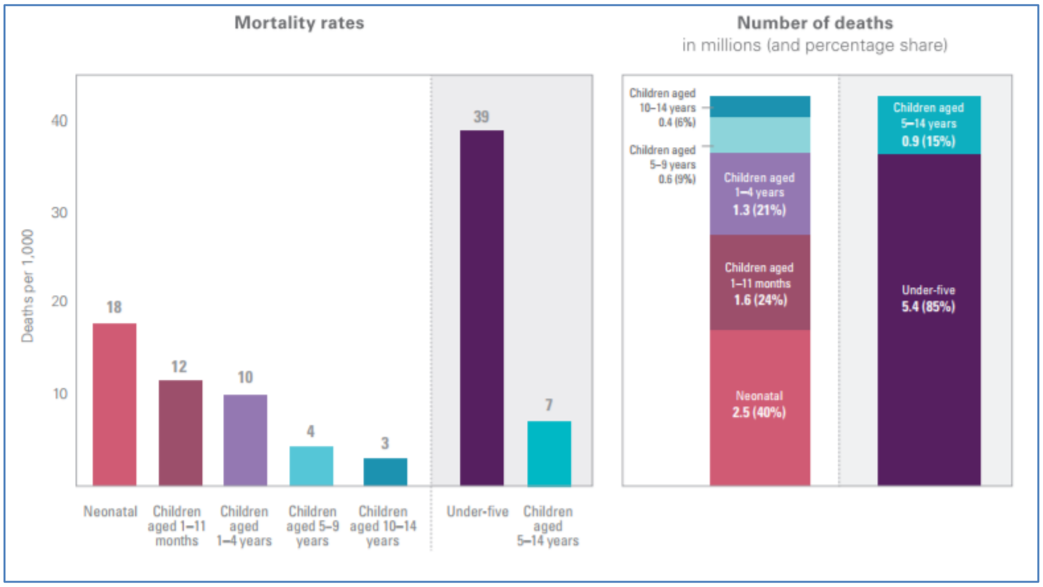

Figure 2. Risk of Dying by Age [2].

Chances of survival are positively correlated with a country's wealth, as shown in Table 1, meaning that where a child is born will impact a child's survival probability. Children born in wealthier countries have higher chances to survive than children born in less wealthy countries

Additional research shows that half of the world's newborns die at home, and more than 99% of all deaths in this category die in developing countries [3].

Table 1. Levels and Trends of the Mortality Rate for Children Under Five Years Old, by Region [2].

	Under-five mortality rate (deaths per 1,000 live births)							Decline (per cent)	Annual rate of reduction (per cent)		
Region	**1990**	**1995**	**2000**	**2005**	**2010**	**2015**	**2017**	**1990-2017**	**1990-2017**	**1990-2000**	**2000-2017**
Sub-Saharan Africa	182	174	156	128	102	82	76	58	3.2	1.6	4.2
Northern Africa and Western Asia	75	62	51	41	33	29	27	64	3.7	3.9	3.7
Northern Africa	84	71	60	49	39	33	31	63	3.6	3.4	3.8
Western Asia	65	54	43	34	27	24	23	65	3.9	4.2	3.7
Central and Southern Asia	124	108	91	75	60	47	43	65	3.9	3.1	4.4
Central Asia	72	73	63	47	35	26	23	68	4.2	1.4	5.8
Southern Asia	126	109	92	76	61	48	44	65	3.9	3.2	4.4
Eastern and South-Eastern Asia	57	49	40	29	22	17	16	73	4.8	3.6	5.5
Eastern Asia	51	45	34	23	15	10	9	82	6.4	3.9	7.9
South-Eastern Asia	72	59	49	40	33	28	26	64	3.8	3.9	3.7
Latin America and the Caribbean	55	43	33	26	24	18	18	68	4.2	5.1	3.7
Oceania	35	33	33	32	28	24	23	36	1.6	0.5	2.3
Australia and New Zealand	10	7	6	6	5	4	4	60	3.4	4.1	3.1
Oceania (exc. Australia and New Zealand)	74	69	66	64	58	51	48	35	1.6	1.0	2.0
Europe and Northern America	14	12	10	8	7	6	6	59	3.3	3.8	3.1
Europe	15	13	10	8	7	6	5	66	4.0	3.9	4.0
Northern America	11	9	8	8	7	7	7	41	1.9	2.8	1.4
Landlocked developing countries	168	157	139	110	85	66	61	64	3.8	1.9	4.8
Least developed countries	176	159	137	111	90	71	66	62	3.6	2.4	4.3
Small island developing States	79	70	62	56	80	45	42	46	2.3	2.4	2.2
World	**93**	**87**	**77**	**64**	**52**	**42**	**39**	**58**	**3.2**	**1.9**	**4.0**

Note: All calculations are based on unrounded numbers.

A more in-depth analysis of the potential causes of death for newborns shows that hypothermia is very common among all infants born, especially in developing countries, and it is a major underestimated challenge for newborn survival in developing countries [3]. Although, by itself, hypothermia is not a direct cause of death, it contributes to a substantial proportion of neonatal mortality globally, mostly as a comorbidity of severe neonatal infections, preterm birth, and asphyxia [3].

Several factors have been identified as contributors to hypothermia in newborns, including the following:

- Environmental factors: The risk of moderate to severe hypothermia increases by 41% for each 5 degrees Celsius decrease in ambient temperature [4].
- Physiological factors: Premature babies are particularly vulnerable to heat loss since they have up four times greater surface per weight than an adult [5].
- Behavioral factors: Cultural practices, like early bathing, contribute to the heat loss in newborns in all types of environments [6].
- Economic factors: Most of the health care facilities in developing countries do not have the resources to provide thermal protection for newborns [7].

Most of the health care facilities in developing countries lack the resources to have proper incubators for newborns [8], which leads to the situations shown in Figure 3.

Figure 3. Newborns in a Public Hospital in Honduras [9].

Commercial incubator costs range from USD $3,000 to $15,000 [10]. Some models are shown in Figure 4.

Figure 4. Commercial Incubators [10].

The purpose of this project is to determine if it is possible to design a standard–compliant and maintainable baby-controlled-Incubator [11]. Using open-source technology with a manufacturing cost of less than four thousand dollars for developing nations that do not have restrictions on the importing of medical devices is a way to support the reduction of infant mortality in impoverished regions around the globe.

Many designs of low-cost incubators have been proposed previously. What this project explored is the possibility to create a design that allows developing nations to build, assemble, and maintain incubators in a reliable and inexpensive way with local and available resources.

This paper addresses the following topics:

- Design of the temperature control system and the humidification system for the incubator: This section describes a proposed control system for the incubator's temperature and humidity.
- Design of the physical enclosure: A proposed design for the physical enclosure of the incubators is presented in this section of the paper.
- Manufacturability and cost: A complete Bill of Materials (BoM) and manufacturing cost for the proposed design is presented, as well as the manufacturing processes that will be required for the production of the incubator.

The following limitations are acknowleged for this project:

- The proposed design is intended to be compliant with some of the requirements defined by the International Electrotechnical Commission (IEC) standards for medical devices [11, 12]. However, the proposed design is meant for regions without restrictions regarding the import of medical devices. A comprehensive list of the global status of importing requirements for different countries can be found on the World Health Organization (WHO) website [13, 14].
- There are different types of incubators; this project focused on developing a design for a Baby-Controlled-Incubator. The IEC defines a Baby-Controlled-Incubator as: "An Air CONTROLLED INCUBATOR which has the additional capability of automatically controlling the incubator air temperature in order to maintain the temperature as measured by a skin TEMPERATURE SENSOR according to the CONTROL TEMPERATURE set by the operator" [11].

In this project, concepts and methods from thermodynamics, mechanics of materials, Finite Element Analysis (FEA), Additive Manufacturing (AM), and simulation were employed to determine if it is possible to design an affordable option for a Baby-Controlled-Incubator for developing nations. In addition, MATLAB, Simulink, Solidworks, and ANSYS software were employed in the design of the different mechanisms and control systems associated with the incubator.

Background

Medical Equipment Challenges in Developing Nations

The high mortality rate in developing nations is a very well-known phenomenon that has been the focus of global organizations like the World Health Organization (WHO), the United Nations International Children's Emergency Fund (UNICEF), and others [2, 6, 7, 15].

Hypothermia is one of the main contributors to the high mortality rates among premature babies around the globe.

Usually, the proposed solutions to deal with this problem focus very little on engineering solutions that can decrease the cost of health care services through the design of equipment that addresses the particular challenges faced by developing nations.

The author became aware of this gap while visiting his home country, Honduras, and discussing the terrible conditions in a public hospital with a resident doctor. During this interchange, the author realized that the Honduran public health care system experiences some challenges in maintaining the equipment that arrives as a donation from developed nations.

Once a failure occurs in the equipment, the public facilities do not have either the resources or technical knowledge within the organization to restore the equipment, which usually remains non-operational. One main contributory factor to the low reliability of donated equipment is the lack of a good quality energy grid, which increases the rate of failure of electronic components, which are difficult to diagnose and repair.

This whole conversation led the author to the realization that developing nations need low-cost, very reliable, and simple-designed machines to help them to solve their health care needs. The medical equipment available in developing nations is designed for very sophisticated markets, which are highly regulated, with excellent support infrastructures, including technical skills and Maintenance Repair and Operations (MRO). These markets are also associated with strong economies with high incomes, where health care is a for-profit business.

In this project, the goal was to demonstrate the feasibility of developing a solution for treating infant hypothermia in developing nations through the design of a low-cost baby-controlled incubator that can be manufactured by local industries in the target regions.

Thermoregulation and Hypothermia

Ellis [16] provides a detailed explanation of the hypothermia process for premature babies. Hypothermia is caused by the inability of premature babies to balance between heat generation and heat loss; this balancing process is called thermoregulation.

The heat generation in premature babies is restricted by their limited amount of brown fat and glycogen, and their inability to make physiological or behavioral changes to increase the production of heat.

The heat loss is generated by the substantial body surface area that allows for a significant heat transfer mechanism.

In her work, Ellis [16] describes the main heat transfer mechanism for premature babies:

- Evaporation: Humidity evaporating on the skin surface, causing heat loss.
- Conduction: Heat transfer by direct contact of the baby's skin with cooler surfaces.
- Convection: Loss of heat by the circulation of cold air in contact with the baby's skin
- Radiation: Loss of heat by the transmission of energy through electromagnetic waves

Principles of Operations of Infant Incubators

Hypothermia in premature babies is treated by providing a Neutral Thermal Environmnent, which is defined by the ideal range temperature at which the infant is neither gaining nor losing heat with minimun oxygen consumption. This temperature range differs from one baby to another, but the consensus is that this range is between 36.5 degrees Celsius to 37 degrees Celsius [16].

As stated by Ellis [16], incubators remain the preferred option to treat hypothermia. Most incubators work on the same principle:

A fan takes air from the environment through filters, and the incubator’s temperature is increased by means of an electrical heater, which is controlled by the skin temperature of the baby.

Humidity is measured and adjusted by adding evaporated water to the air stream. Oxygen is also measured and supplied through a control valve.

The conditioned air flows into the chamber of the incubator to keep the enclosed chamber at the appropriate temperature to ensure the infant’s temperature remains within the range of Neutral Thermal Environment (NTE).

A portion of the air then exits the chamber, and the remaining flow goes back to the conditioning cycle again.

Figure 5 shows a schematic diagram of the working principle described in this section.

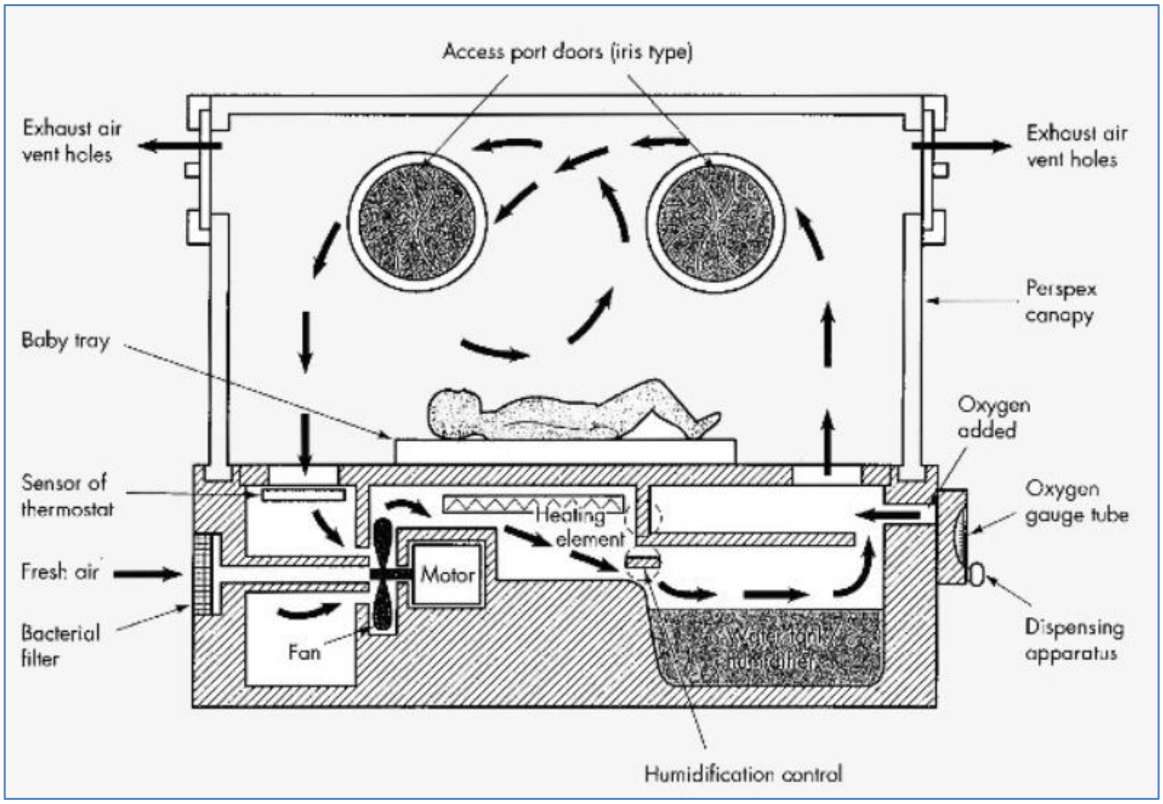

Figure 5. Principle of Operation of an Infant Incubator [17].

Alternative Proposed Solutions to the Problem

Different initiatives have been implemented as a potential solution for low-cost incubators.

Solution 1: MOM Incubator

The MOM incubator [18] is a design proposed by James Robers, an engineering graduate from the University of Loughborough in the United Kingdom. This solution consists of an inflatable chamber that can be deployed easily to provide heat, humidity, and phototherapy

This design (see Figure 6) was awarded the James Dyson Award in 2018. The proposed design is intended to be a low-cost incubator for refugee camps; its main purpose is to serve as a temporary transport from the refugee camps to a proper care facility. This model cannot be classified as a baby-controlled incubator [11] because it lacks a sensor on the baby’s skin to control the temperature; rather, its control loop is based on the chamber’s temperature.

Figure 6. MOM Incubator [18].

Solution 2: Embrace Warmers

An additional solution to fight hypothermia in developing countries is the Embrace Warmer [19], which is a portable infant warmer that provides heat to premature babies (see Figure 7). This device is meant to be an affordable option to provide temperature stability in ambulances and hospitals. It does not provide any humidity or oxygen control, and it does not feature technology that can define a temperature setpoint.

Figure 7. Infant Warmer Device by Embrace [19].

This review of previous attempts to solve the infant hypothermia problem helps to demonstrate the unique contribution of this capstone project. This capstone project has resulted in the conceptual development of a solution for a baby-controlled incubator that can potentially be manufactured and maintained for use in health facilities in developing regions. These features set apart the proposed solution in this paper from other available solutions.

Safety and Security Concerns

One of the main concerns for incubator design is a functional failure (FF) of the temperature control system that could lead to a fatal consequence for the newborn [20]. Adherence to all applicable safety standards was therefore considered in the design phase of this project to mitigate the identified risks. The applicable standards are identified in the “Literature Review” section in this document.

Extensive simulation was additionally used to develop and to verify the feasibility of the incubator prototype.

Ethical Treatment of Human Subjects

No human subject testing was conducted in this project. Instead, the prototype design was developed, tested, and verified with computer simulations to assess the feasibility of the proposed solution.

Review of Literature

Significance of the Topic

The problem of designing low-cost incubators has been recognized as a priority to reduce the mortality rate for newborns in developing countries [5, 6]. Several organizations are working toward the same goal of delivering a low-cost solution for this problem. The World Health Organization (WHO), United Nations (UN), International Children's Emergency Fund (UNICEF), and other important health organizations recognize the importance of finding an effective solution to the hypothermia problem for developing countries [2, 5, 18, 21, 22, 23].

An important observation concerning these current initiatives aimed at developing low-cost incubators is that none of them indicate that they are focused on developing internal capabilities to ensure their solution is sustainable from the operational perspective. That is, none of the initiatives features an objective to create the capability for end-users to build and maintain the designed incubators. This lack of operational perspective will never eliminate the dependency on external support to continue to build new incubators as demand increases. A better and more sustainable long-term solution is to enable developing countries to build and to maintain their equipment going forward.

Design Standards

The U.S. Food and Drug Administration (FDA) recognizes the standards generated by the International Electrotechnical Commission (IEC) as valid to design medical equipment

[21]. Throughout the duration of this capstone project, the following two IEC standards were referenced:

- IEC – 60601-1-1-2: Medical Electric Equipment – Part 1-2: Part 1-2: General Requirements for Safety - Collateral standard: Electromagnetic Compatibility - Requirements and Tests.
- IEC – 60601-2-19: Medical Electric Equipment: Part 2-19: Particular Requirements for the basic safety and essential performance of Infant Incubators.

In addition to reviewing the standards listed above, a third standard was also considered for this project:

- BS EN 13976-1:2018: Rescue Systems-Transportation of Incubators – Part 1: Interface Requirements.

After reviewing this standard, it was concluded that it is not applicable for the scope of this capstone project, because it provides guidance on the mechanical and electrical interfaces required for designing mobile incubators. The scope of the present project is to design a fixed incubator.

Modeling of Hypothermia

Understanding thermal regulation and heat transfer mechanisms for premature babies is extremely important in the design of a proper incubator. A review was undertaken of mathematical models proposed by Pereira e*t al*. [22] and by Fraguela e*t al*. [23]. Both models provide a rigorous mathematical approach for determining heat loss in premature babies.

Control Variables

IEC defines an infant incubator as a "ME Equipment having a compartment which provides with the means to control the environment of the infant primarily by heated air within the compartment" [11].

The main variable of control under this definition is air temperature. In addition to this variable, for this capstone project, humidity control was considered as part of the scope of the design.

Hitu *et al*. [24] provide a framework to control multiple parameters using the microcontroller Arduino; their work focuses on how to connect and to control incubators using sensors for temperature, humidity, and CO_2.

Methods

Temperature Control Design

One of the most critical design considerations for this project is the temperature stability of the infant inside the incubator. The IEC incubator standard defines the following requirements for this variable [11]:

- The steady temperature of the incubator measured ten cm above the center of the mattress surface should not vary more than one degree Celsius.[1]
- Control temperature should be within thirty-five degrees Celsius to thirty-seven degrees Celsius, and shall always exceed the ambient temperature by at least three degrees Celsius.[2]

Most of the design work was performed with simulations to avoid the need for human-testing procedures and regulations. Therefore, the design of a temperature system in compliance with the requirements listed above was developed with modeling of the heat transfer mechanism inside an incubator using MATLAB, Simulink, and ANSYS software.

The work of Fraguela e*t al.* [23] on the mathematical modeling of a heat transfer mechanism for premature babies was deemed appropriate to accomplish this objective, because of the simplicity of the proposed model and the numerical control matrix already developed in the paper, which could be used to build a Simulink model. The paper by Pereira *et al*. [22] provides an alternative approach to model the heat transfer mechanism

---

[1] Section 201.3.212, page 10.
[2] Section 201.5.4, page 11.

at a more granular level by providing a mathematical model for heat transfer among five boundaries in a newborn baby: Skin, Fat, Muscle, and Bone. However, this model features more complexity than what was required for the scope of this capstone project and it lacks a system dynamic control matrix that can be used in Simulink software to conduct design simulations.

Fraguela *et al*. [23] assume that the body of a premature newborn baby consists of two layers:

- Core or Kernel (K), which includes tissues, bones, and internal organs.
- Surface (S), which includes fat and skin.

They also assert that the primary source of heat for a premature baby is basal metabolism, which is defined by Merrian-Webster as:

“The turnover of energy in a fasting and resting organism using energy solely to maintain vital cellular activity, respiration, and circulation as measured by the basal metabolic rates.”

Moreover, the most critical heat transfer mechanism is blood circulation. Fraguela *et al*. [23] also assume that the basal metabolism is uniform in the core layer. Their model also considers that the primary heat losses for a premature baby are:

- Evaporative losses through respiration in the core layer and in the skin.
- Conduction heat loss through the skin that is in contact with the resting surface.
- Convection heat exchange between the surface layer and the circulation inside the chamber of the incubator.

- Radiation heat exchange between the surface layer and the walls of the incubator.

Under these considerations, Fraguela *et al*. [23] propose a model consisting of ordinary differential equations (ODE) to represent the energy balance. In each equation, the left-hand terms represent the rate of accumulation of thermal energy per unit volume due to the change of temperature in the tissue or blood. The right-hand terms contain the sources and losses of heat.

Rate of accumulation of thermal energy per unit volume in the core layer of the baby is equal to conduction heat between the circulatory system and the core plus the generated heat by metabolism minus the heat loss through breathing:

$$\boldsymbol{\rho_k \omega_k \frac{\partial T_k(t)}{\partial t} = C_{bk}(T_b(t) - T_k(t)) + \alpha_o O_o(t) - [CR_1 - CR_2 T_a(t)]} \tag{1}$$

where

$\boldsymbol{\rho_k}$ **= density of the skin**,

ω_k = specific heat of the core layer,

$\frac{\partial T_k(t)}{\partial t}$ = rate of change of the core temperature,

and

$$\boldsymbol{C_{bk} = \rho_b \omega_b F_k}, \tag{2}$$

where

ρ_b = density of blood,

ω_b = specific heat of blood,

F_k = cubic meters of blood per second in the core layer,

$T_b(t)$ = temperature of blood as a function of time,

$T_a(t)$ = ambient temperature as a function of time,

$T_k(t)$ = core temperature as a function of time,

$\alpha_o O_o(t)$ = basal metabolic heat as function of oxygen consumption,

and

$$\boldsymbol{CR_1 - CR_2 T_a(t) = \textbf{heat loss through breathing.}} \tag{3}$$

The rate of accumulation of thermal energy per unit volume in the circulatory layer of the baby is defined by the conduction heat transfer between the circulatory system and the core, and also the heat conduction between the circulatory system and the skin layer:

$$\boldsymbol{\rho_b \omega_b \frac{\partial T_b(t)}{\partial t} = C_{bk}(T_k(t) - T_b(t) + \; C_{bs}[T_s(t) - T_b(t)]}, \tag{4}$$

where

$\frac{\partial T_b(t)}{\partial t}$ = rate of change of temperature in the circulatory layer,

$$\boldsymbol{C_{bs} = \; \rho_b \omega_b F_s}, \tag{5}$$

where

F_s = cubic meters of blood per second in the skin layer,

and

$T_s(t)$ = temperature of skin as a function of time.

Rate of accumulation of thermal energy per unit volume in the skin layer of the baby is determined by the amount of heat conducted from the circulatory system to the skin, minus the addition of the following losses: heat transfer loss through conduction from the skin to the resting surface in the incubator, conduction heat loss between the skin to the environment, the radiation loss between the skin and the incubator environment and the heat loss through evaporation. Thus:

$$\rho_s \omega_s \frac{\partial T_s(t)}{\partial t} = C_{bS}\big(T_b(t) - T_s(t)\big) - [C_c(T_s(t) - T_m) + C_v[T_s(t) - T_a(t)] + \beta_R[(T_s(t) + 273.15)^4 - (T_r(t) + 273.15)^4] + \boldsymbol{C_{e1} T_s(t) - C_{e2} T_a(t) - C_{e3}}], \quad (6)$$

where

ρ_s = density of skin,

ω_s = specific heat of skin,

$\frac{\partial T_s(t)}{\partial t}$ = rate of change of the skin temperature,

and

$$\boldsymbol{C_c = \frac{A\varepsilon_c h_c}{V}} \textbf{ is the coefficient of volumetric heat transfer}, \quad (7)$$

where

A = is the surface area of the baby,

h_c = heat conduction coefficient,

ε_c = fraction of the surface area exposed to conduction,

V = volume of the baby's body,

$T_m =$ temperature of the resting surface of the incubator,

and

$$C_v = \frac{A\varepsilon_v h_v}{V} \text{ is the convective heat transfer }, \tag{8}$$

where

$\varepsilon_v =$ fraction of the surface area exposed to convection,

$h_v =$ heat convection coefficient,

$C_{e1}, C_{e2},$ and C_{e3} are constant terms to determine evaporation rate,

and

$\beta_R =$ coefficient of radiation heat transfer.

Equations (1), (2), and (3) can be simplified and normalized as follows:

$$\boldsymbol{M1}\frac{\partial \boldsymbol{T_k(t)}}{\partial \boldsymbol{t}} = \boldsymbol{M2}(\boldsymbol{T_b}(\boldsymbol{t}) - \boldsymbol{T_k}(\boldsymbol{t})) + \boldsymbol{M5O_o}(\boldsymbol{t}) - [\boldsymbol{M4} - \boldsymbol{M3T_a}(\boldsymbol{t})] \ , \tag{9}$$

$$\boldsymbol{M6}\frac{\partial \boldsymbol{T_b(t)}}{\partial \boldsymbol{t}} = \boldsymbol{M2}(\boldsymbol{T_k}(\boldsymbol{t}) - \boldsymbol{T_b}(\boldsymbol{t}) + \boldsymbol{M7}[\boldsymbol{T_s}(\boldsymbol{t}) - \boldsymbol{T_b}(\boldsymbol{t})], \tag{10}$$

$$O \quad M8\frac{\partial T_s(t)}{\partial t} = M7\big(T_b(t) - T_s(t)\big) - [M9(T_s(t) - T_m) + M10[T_s(t) - T_a(t)] + M11[(T_s(t) + k)^4 - (T_r(t) + k)^4] + \boldsymbol{M12T_s(t) - M13T_a(t) - M14}], \quad (11)$$

The values of the "M" coefficients were determined by Fraguela *et al.* [23] and are shown in Table 2.

Table 2. Coefficient Values for the Incubator System of Equations [23].

$M_1 = 39909.638889$
$M_2 = 738150$
$M_3 = 3150.500874$
$M_4 = 3055.192723$
$M_5 = 346.722892$
$M_6 = 41008.3333$
$M_7 = 295260$
$M_8 = 26465.2777$
$M_9 = 34.86330253$
$M_{10} = 5976.627216$
$M_{11} = 7.4514$
$M_{12} = 2004.8121$
$M_{13} = 1643.0594$
$M_{14} = 195.54196$
$k = 7.38243$

Additional assumptions are made by Fraguela *et al*. [23] in order to determine the coefficients shown in Table 2.

- The temperature of the resting surface is kept constant at 30º C.
- The average consumption of oxygen is 3.9 ml/kg-min, corresponding to an infant weighing 1.2 kg.
- The temperature of the care unit is constant and equal to 20º C.

Using the mathematical model developed by Fraguela *et al.* [23], a Simulink model was created to solve the coupled differential equation and to serve as the simulation to validate the design of the air-heating mechanism and control system of the incubator. The Simulink models associated with this project have all been placed on GitHub [25].

This mathematical model for heat transfer was recreated using Simulink; the model is shown in Figure 8.

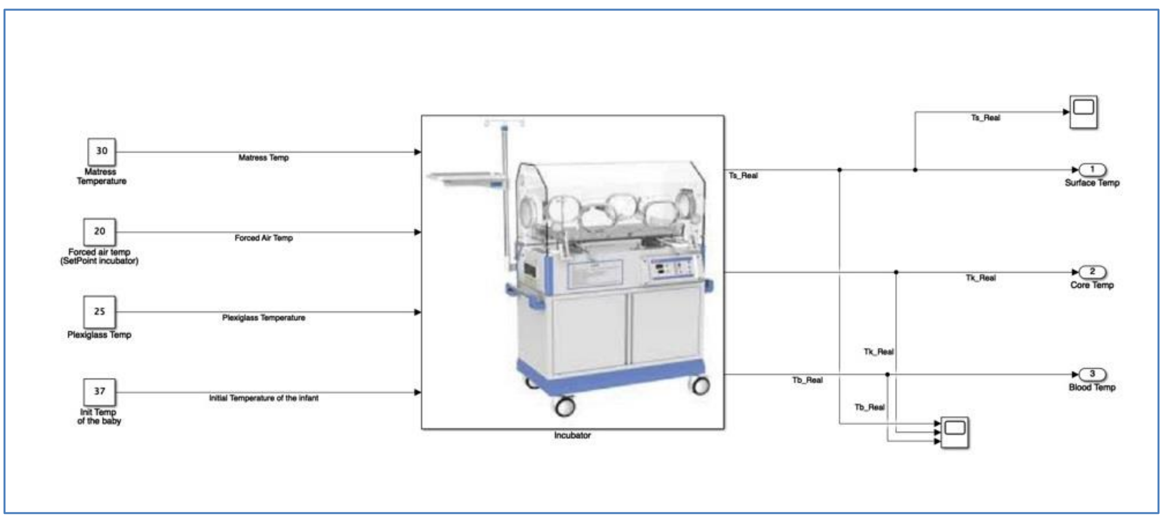

Figure 8. Simulink Model of the Infant Incubator for Temperature Control [25].

The incubator system has four inputs:

- The initial temperature of the baby.
- The surface's temperature that is in contact with the baby is assumed constant at 30º C, using an electrical heating mechanism that is outside of the scope for this project.
- The temperature of the incubator's cover is also considered as a constant with a value equal to 25º C.
- The temperature of the forced air that enters the incubator and that will be used to control the skin temperature of the infant remains in the range of thermal neutrality.

A detailed view of the heat transfer subsystems of the incubator model is shown in Figure 9. The Simulink file is available in a Github repository [25].

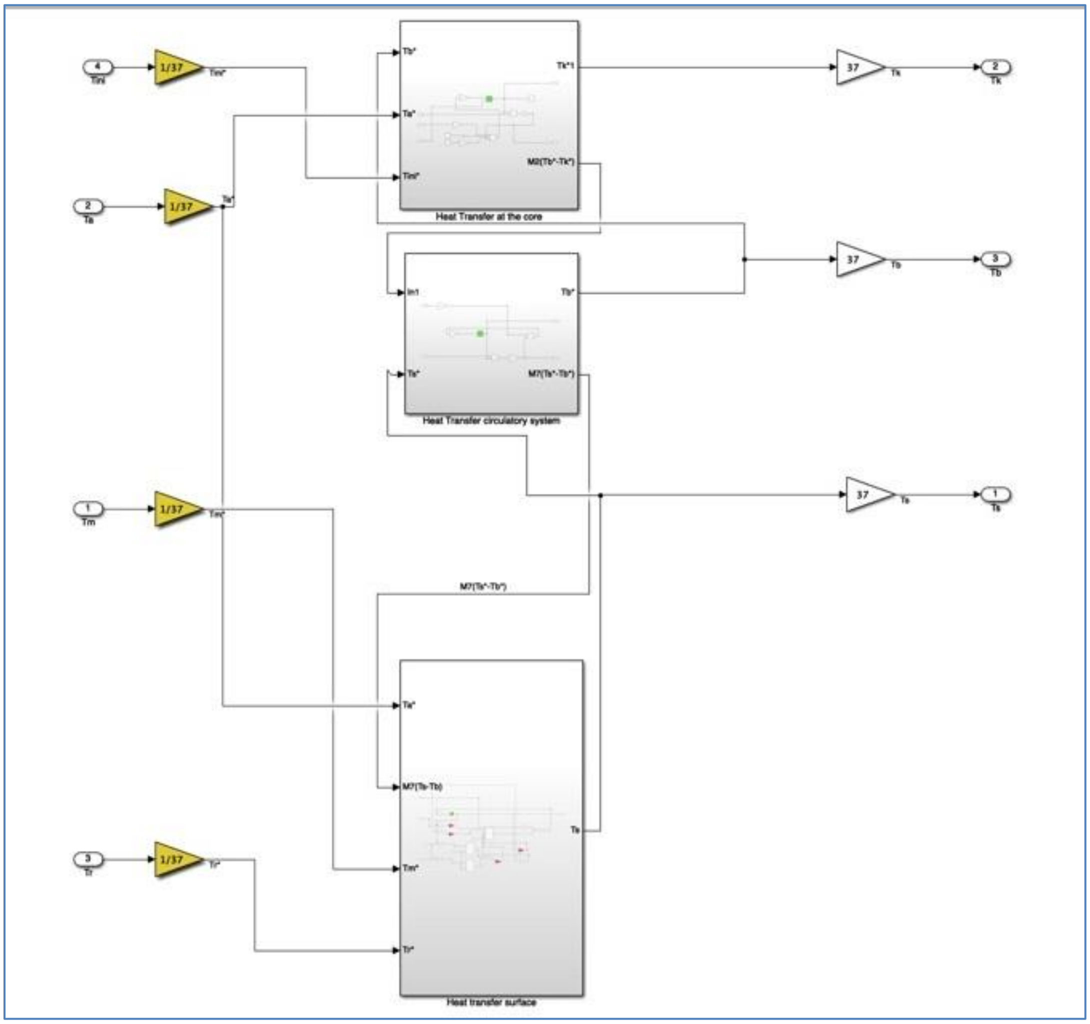

Figure 9. Incubator Heat Transfer Subsystems [25].

An initial simulation showed that if the system is left uncontrolled, the temperature of an infant with an initial temperature of 37º C. will decay in a period of 22 hours to 22º C., as shown in Figure 10. This drop in temperature would have fatal consequences for the infant.

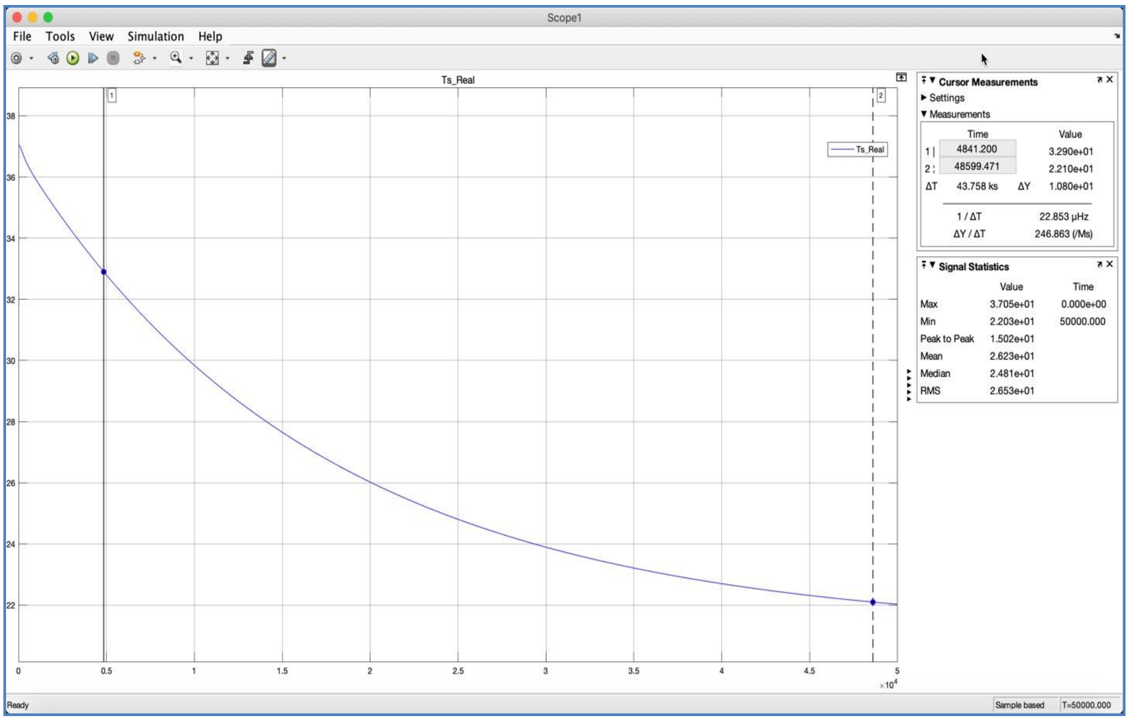

Figure 10. Skin Temperature of an Infant without Temperature Control.

Since the system equation used to model the incubator is not linear because of the heat radiation terms, it was necessary to linearize the system around an operating point.

This process was conducted using the Linear Analysis tool in Simulink. The operating point is defined according to the following criteria:

- The steady state of the skin (surface) temperature.
- The average of the temperature range of the Neutral Thermal Environment (NTE), proposed by Fraguela *et al.* [23], which is the ideal temperature inside of the incubator to avoid hypothermia: (36.8 ºC to 37.3 ºC). The value of the average temperature NTE is 37.05 ºC.

The results of the linearization are shown in Figure 11.

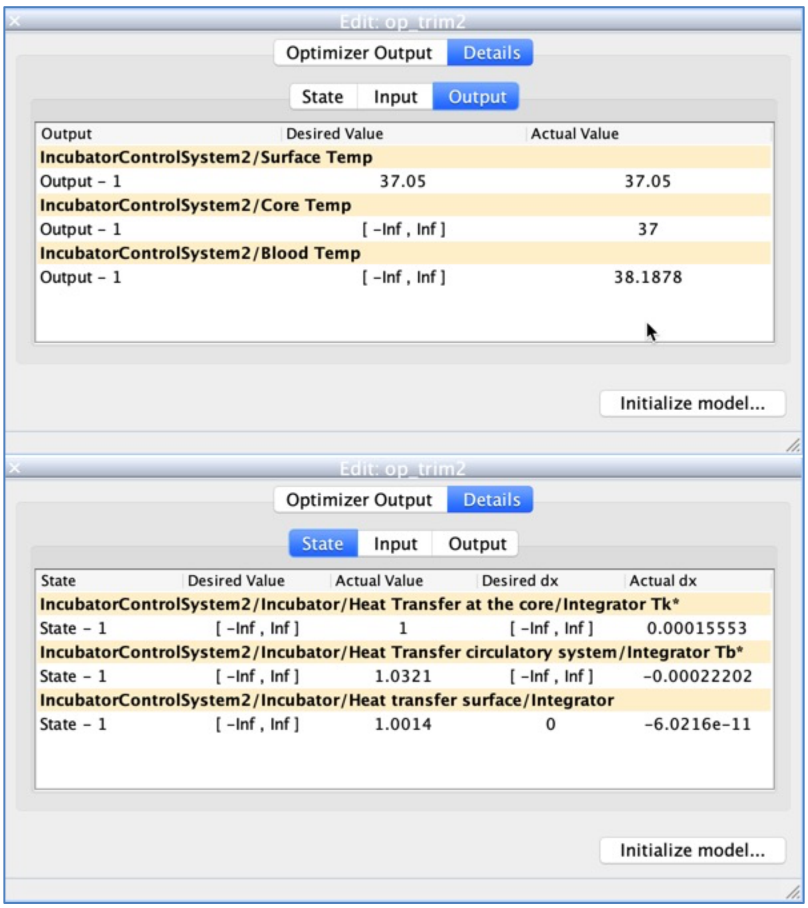

Figure 11. Linearization Results of the Incubator Model Using MATLAB.

The step response of the new linearized model is shown in Figure 12. Here, the input and output labels are as follows:

- Input 1: Temperature of the resting surface: Mattress Temperature
- Input 2: Temperature of the forced air
- Input 3: Temperature of the plexiglas cover
- Input 4: Initial temperature of the infant

The output labels are:

- Output 1: Temperature of the infant skin (surface)
- Output 2: Core temperature of the baby
- Output 3: Temperature of the circulatory layer (blood)

The output temperature to determine hypothermia is the skin's temperature (Input 1), and from Figure 12, it is possible to determine that the inputs that have a significant contribution to the step response of the skin temperature are Input 1 and 2. Therefore, the focus of the incubator design in this capstone project was to determine the precise control mechanism for these inputs to ensure the incubator can sustain a temperature within the NTE.

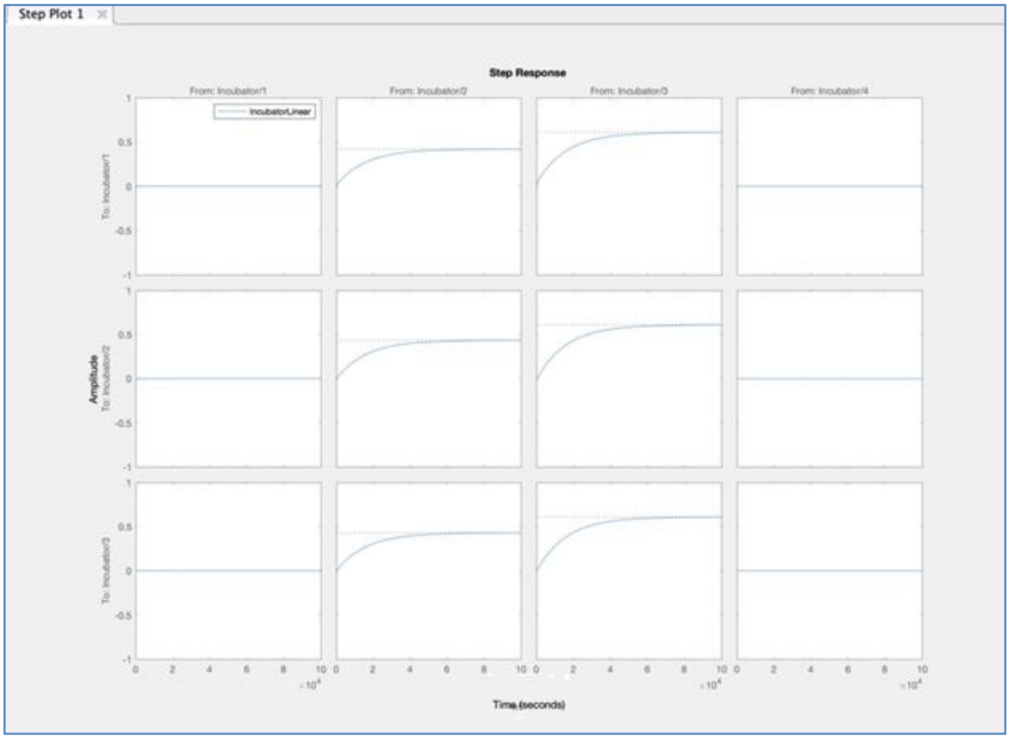

Figure 12. Step Response of the Linearized Incubator System [25].

The linearized model representation in Simulink, based on design conventions indicated by Nise [27], is shown in Figure 13.

.

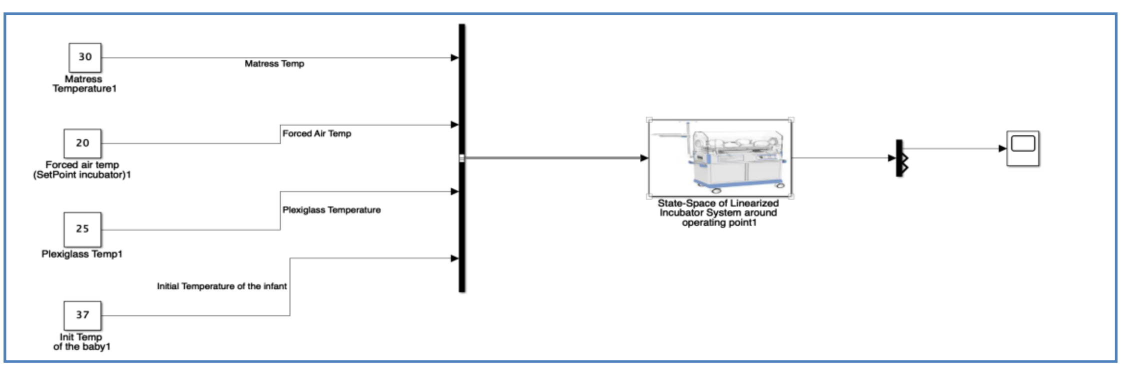

Figure 13. Linearized Representation of the Incubator System in Simulink.

Before moving forward with the incubator design, it was necessary to determine if the system is observable and controllable.

For any Line Time-Invariant System (LTI), F. G. Franklin, J. D. Powell, and A. Emami-Naeimi [26] define *observability* as: “The ability to deduce information about all the modes of the system by monitoring only the sensed outputs.”

Norman S. Nise [27], referring to *controllability*, writes: “If an input to a system can be found that takes every state variable from a desired initial state to a desired final state, the system is said to be controllable: otherwise, the system is uncontrollable.”

To properly design a control system for the variables of interest, it was necessary to determine if the linearized model of incubator is controllable and observable. Using MATLAB functionality, it was possible to demonstrate that the linear representation of the system is both controllable and observable, as shown in Figure 14.

```
linsys = IncubatorLinear #Linearize System representation of the incubator

Co = ctrb(linsys) #This commands calculates the controllability matrix of the
system
Co = 3×12
10^-5 ×
          0    0.0593         0         0         0   -0.0003         0
0    0.0000    0.0000    0.0000         0
          0         0         0         0    0.0000    0.0007    0.0009
0   -0.0000   -0.0000   -0.0000         0
     0.0010    0.2162    0.4424         0   -0.0000   -0.0007   -0.0015
0    0.0000    0.0000    0.0000         0

#The system is controllable if Co has full rank, meaning that the number of
uncontrollable states is equal to zero, as define by the following equation:

unco = length(A)-rank(Co)

unco = 0 #Therefore, the system is controllable.

Ob = obsv(linsys) # #This commands calculates the controllability matrix of the
system

Ob = 9×3
          0         0   37.0000
   37.0000          0         0
          0   37.0000         0
          0    0.1147   -0.1246
   -0.1901    0.1901          0
    0.1850   -0.2590    0.0740
    0.0006   -0.0012    0.0006
    0.0019   -0.0023    0.0004
   -0.0022    0.0030   -0.0008
#The system is observable if Ob has full rank, meaning that the number of unobservable
states is equal to zero, as define by the following equation:

unobs = length(A)-rank(Ob)

unobs = 0 #Therefore, the system is controllable.
```

Figure 14. Controllability and Observability Analysis for the Linearized System [25].

Now that a proper way to simulate the behavior of the infant's temperature inside an incubator was verified, the development of the heating systems and their corresponding controllers was next addressed as the main scope of the project. The schematic diagram of the incubator control system design is shown in Figure 15.

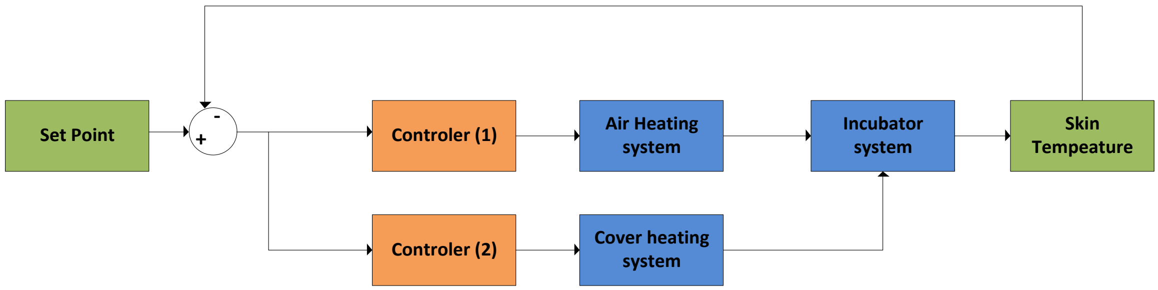

Figure 15. Schematic Diagram of the Control System for the Incubator.

As a first step, the design of the air heating system for the incubator was undertaken.

The system's purpose is to increase the incubator's temperature to an appropriate level to keep its inside temperature within the operating range.

The operating assumptions considered for the design are as follows:

- Minimum environmental temperature expected: 20º C.
- Thermal properties of air remain constant within the temperature range: [20º C. to 40º C.].

Applying the principle of conservation of energy, it is known that for any airflow, the heat required to increase its temperature is given by:

$$\boldsymbol{q_a = \dot{m}C_p\left(T_f(t) - T_i(t)\right)}, \tag{12}$$

where

$q_a =$ total heat absorbed per unit of time,

$\dot{m}$ = mass flow per unit of time,

C_p = specific heat coefficient of air,

$T_{fin}(t)$ = final temperature of the air flow as a function of time,

and

$T_i(t)$ = initial temperature of the air flow as a function of time.

Solving for $T_f(t)$ in Equation (12), the following result is obtained:

$$\frac{\boldsymbol{q_a}}{\boldsymbol{\dot{m}C_p}} + \boldsymbol{T_i(t)} = \boldsymbol{T_f(t)}. \tag{13}$$

After conducting an energy balance, it is possible to deduct that the heat transfer gained by the airflow (q_a) must be equal to the convection heat transferred from the heating element to the airflow (q_h), which is given by the Newton Cooling Equation:

$$\boldsymbol{q_h = hA_t(T_{bh}(t) - T_\infty(t))}, \tag{14}$$

where

$\boldsymbol{q_h}$ = **total heat transfer due to convection**,

h = convection coefficient,

A_t = area of surface in contact with the fluid,

$T_{bh}(t)$ = temperature of the surface of the heating element,

and

$T_{\infty}(t)$ = temperature of the cooling fluid.

Equation (14) expresses the general case for convective heat. For this project, the initial decision was to use a more efficient transfer surface for the heating mechanism. The initial decision was to use a heating element with fins to increase the efficiency of the heat transfer process.

Incropera *et al.* [28] provide a formula for total heat transfer when using fins and also a tabulation of the surface efficiencies for different geometries, as shown in Figure 16.

Based on the simplicity of manufacture and the higher level of fin efficiency, the triangular geometry was selected. The material chosen for the heating mechanism was Aluminum Alloy 2024 T-6, with the thermophysical properties shown in Table 3.

Table 3. Thermophysical Properties for Aluminum Alloy 2024-T6 [28].

ρ (Kg/m3)	C_p (J/Kg. K)	k (W/m. K)
2770	875	177

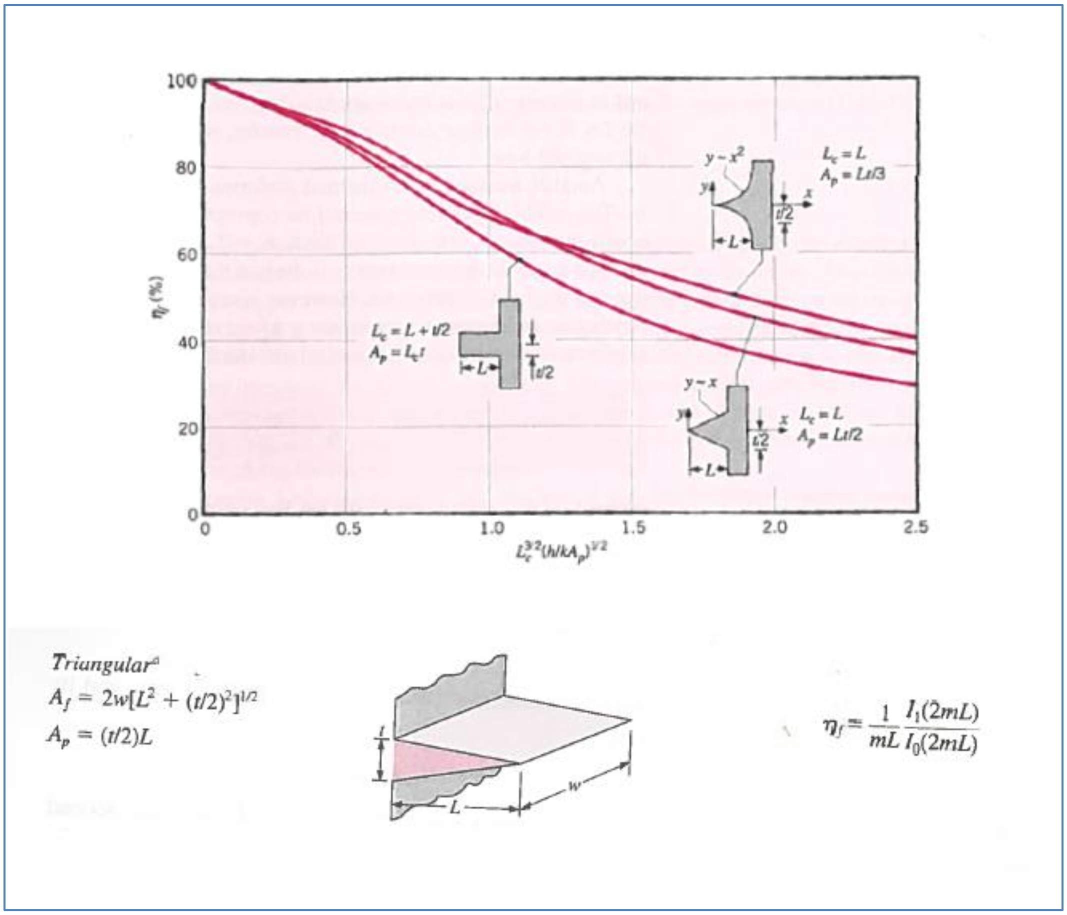

Figure 16. Properties of Fin Elements [28].

Therefore,

$$q_{hf} = hA_t[1 - \frac{NA_f}{A_t}(1 - \eta_f)]\theta_b, \quad (15)$$

where q_{hf} = total heat transfer due to convection,

h = **convection coefficient**,

A_t = total surface area of the element,

A_f = total fin area,

t = thickness of the fin,

L = length of the fin,

w = width of the fin,

N = number of fins.

And,

$\boldsymbol{\eta_f} =$ **fin efficiency**,

where

$$\boldsymbol{m} = \sqrt[2]{\frac{\boldsymbol{hP}}{\boldsymbol{kA_c}}}, \tag{16}$$

$P =$ fin perimeter,

$k =$ conduction coefficient,

I_0 *and* I_1 = modified zero − order Bessel Function.

Finally,

$$\boldsymbol{\theta_b} = (\boldsymbol{T_b} - \boldsymbol{T}_\infty). \tag{17}$$

It was assumed that the heat transfer due to radiation and conduction could be omitted to simplify the analysis. Therefore, the total heat transfer from convection must be equal to the heat transfer generated by the heating element, which is given by the following energy balance:

$$\boldsymbol{E_{generated} - E_{transfer} = E_{stored}}, \tag{18}$$

$$\boldsymbol{E_{generated} = I^2 R}, \tag{19}$$

$$\boldsymbol{E_{transfer} = q_{hf}}. \tag{20}$$

Inserting Equation (15), (19), and (20), into Equation (18), and rearranging terms, the following equation is obtained:

$$\boldsymbol{\frac{\partial T_{bh}(t)}{\partial t} = \frac{I^2 R - hA_t\left[1 - \frac{NA_f}{A_t}\left(1 - \eta_f\right)\right]\left(T_{bh}(t) - T_\infty\right)}{\rho c V}}, \tag{21}$$

where

$T_{bh}(t)$ = temperature of the surface of the heating element,

ρ = density of the heating element material,

c = specific heat of the heating element material,

and

$V =$ volume of the heating element.

Equation (21) was used to model the surface temperature of the heating element, which was then used in Equation (13) to determine the temperature of the air at the exit of the heating systems.

One additional challenge was the determination of the convection coefficient (h), which is a variable dependent on the geometry of the heating surface, its temperature, and the thermal properties of the cooling fluid.

Incropera *et al*. [28] provide the following empirical formulas to determine *h*. For this capstone project, the flat surface approximation method was used, and also, the suggested airflow speeds suggested by Fraguela *et al*. [23]. Thus:

$$\boldsymbol{Re_L = \frac{u_\infty L}{\nu(T_f)}}, \tag{22}$$

$$\boldsymbol{Nu_L = 0.664 Re_L^{\frac{1}{2}} \mathrm{Pr}(T_f)^{\frac{1}{3}}}, \tag{23}$$

$$\boldsymbol{h = \frac{Nu_L k_a(T_f)}{L}}, \tag{24}$$

where

$Re_L =$ Reynolds number,

$u_\infty =$ speed of the cooling fluid,

$L =$ length of the convection surface,

$\nu(T_f) =$ kinematic viscosity as a function of T_f,

$\Pr(T_f) =$ Prandlt number as a function of T_f,

$Nu_L =$ Nusselt number,

$k_a\,(T_f) =$ conduction coefficient for the cooling fluid as a function of T_f,

and

$$\boldsymbol{T_f} = \frac{(\boldsymbol{T_b}(\boldsymbol{t}) + \boldsymbol{T}_\infty)}{\boldsymbol{2}}. \tag{25}$$

Therefore, the calculation of the convective coefficient h is coupled to the temperature solution of the heating surface $T_b(t)$.

Simulink was next employed to design the heating elements using the above equations, including Equation (21).

Figure 17 shows the complete system created in Simulink to numerically solve the coupled set of equations; the Simulink file is available in a Github repository [25].

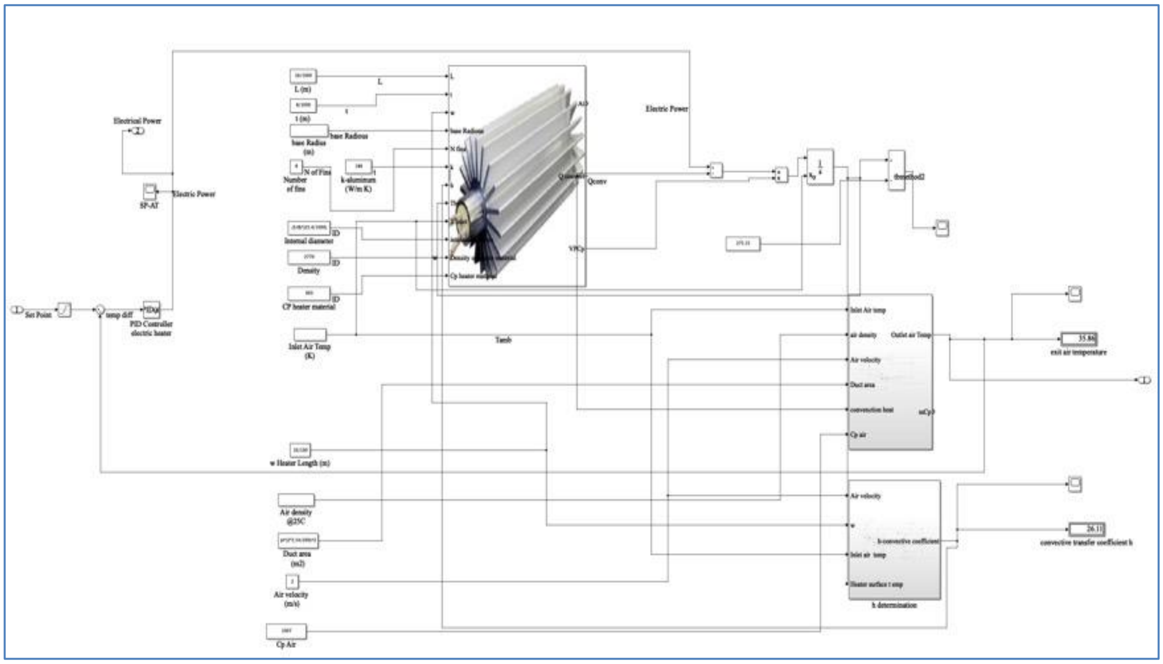

Figure 17. Heating Element Design Using Simulink [25].

The following design characteristics were considered:

$u_\infty = 2\ m/s$, Speed of the cooling fluid,

$\rho_{air} = 0.7364\ kg/m^3$, Density of air at 25ºC, and 5000 m altitude,

Diameter of the heat transfer chamber = 0.0508 m

$w = 0.010\ m$, Width of the fin,

$T_i(t) = 25\ ^\circ C$, Initial temperature of the air flow,

$N = 8$, Number of fins,

$t = 0.008\ m$, Thickness of the fin,

$L = 0.016\ m$, Length of the fin,

An integrated system was created in Simulink, as shown in Figure 18. This model complies with the IEC definition for a baby-controlled incubator[3] [11]. As required by the standard, the model features control of the incubator temperature based on the measurement of the skin temperature through a control loop.

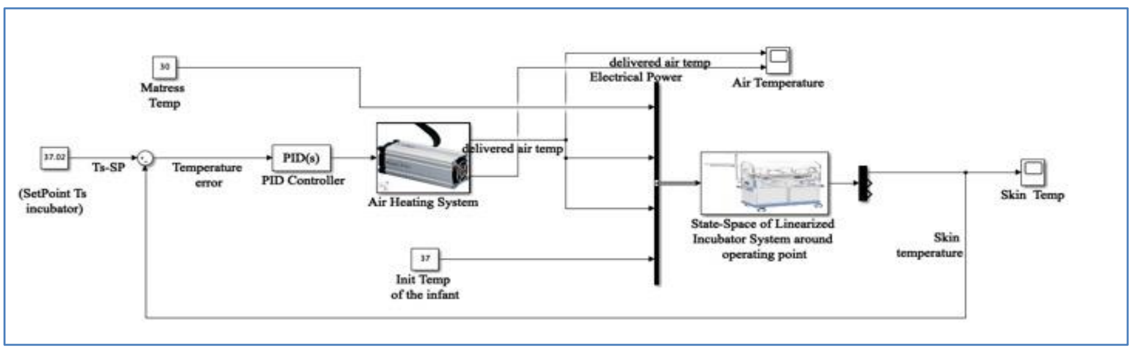

Figure 18. Incubator System Including the Heating Subsystem [25].

In the model, it is assumed that the air temperature inside the incubator and the glass temperature are the same in steady-state condition, and therefore, there is only one control loop required for both variables.

In addition, the Simulink model determines the level of current required to maintain the baby's skin temperature within the Neutral Thermal Environment (NTE).

[3] Section 201.3.204, page 8.

For the proposed air-heating design, a Proportional, Integral and Derivative (PID) control mechanism was designed to provide more flexibility in determining the appropriate roots for the characteristic equation of the dynamic system [26].

As defined by Franklin *et al*. [26], the proportional control (P) provides a feedback control signal that is linear and proportional to the difference between the setpoint and the actual state, which is called the error.

Integral control (I) provides a feedback control signal that is proportional to the summation of all past values of the error value. The Integral control enables the minimization of the error in the steady-state condition, and also minimizes the steady-state response to random disturbances of the system.

The Derivative control (D) generates a feedback control signal that is proportional to the rate of change of the error value. The goal of Derivative control is to improve the closed-loop system stability, speeding up the transient response, and reducing overshoot.

The PID control equation is:

$$\boldsymbol{U(t) = K_p e(t) + K_i \int_{t_0}^{t_1} e(t) dt + K_d \frac{de(t)}{dt}}, \tag{26}$$

where,

$U(t)$ = feedback control signal,

K_p = Proportional term,

K_i = Integral term,

K_d = Derivative term,

and

$e(t)$ = error as a function of time.

There are several methods to determine the right terms in Equation (26) based on the design requirements. Bucz *et al*. [29] provide a holistic overview of the different algorithms that are available to accomplish this objective, which is commonly known as *PID tuning*.

In this project, the built-in tuning capabilities in MATLAB were employed to design a PID control that meets the design criteria defined by the IEC Standard, which establishes the following requirements for temperature control [11]:

- The steady temperature of the incubator measured 10 cm above the center of the mattress surface should not vary more than one degree Celsius.[4]
- Control temperature should be within 35 degrees Celsius to 37 degrees Celsius, and shall always exceed the ambient temperature by at least three degrees Celsius.[5]
- The steady temperature is achieved when the incubator's temperature does not vary by more than one degree Celsius over a period of one hour.[6]

[4] Section 201.3.207, page 9.
[5] Section 201.5.4, page 11.

- For a baby-controlled incubator, the range of control temperature shall be from 35 degrees Celsius or less and to not more than 37.5 degrees Celsius.[7]

Default PID values provided by MATLAB were used to start the design of the appropriate PID controller for the air-heating element.

Figure 19 shows the time response of the air temperature as a function of time for the default PID values (P = 1, I = 1, and D = 0) provided by MATLAB, based on the predefined setpoint of 37.5 degrees Celsius, which shows that the response of the system does not comply with the IEC requirements [11] for steady-state temperature conditions[8] and the allowed range of temperature control.[9]

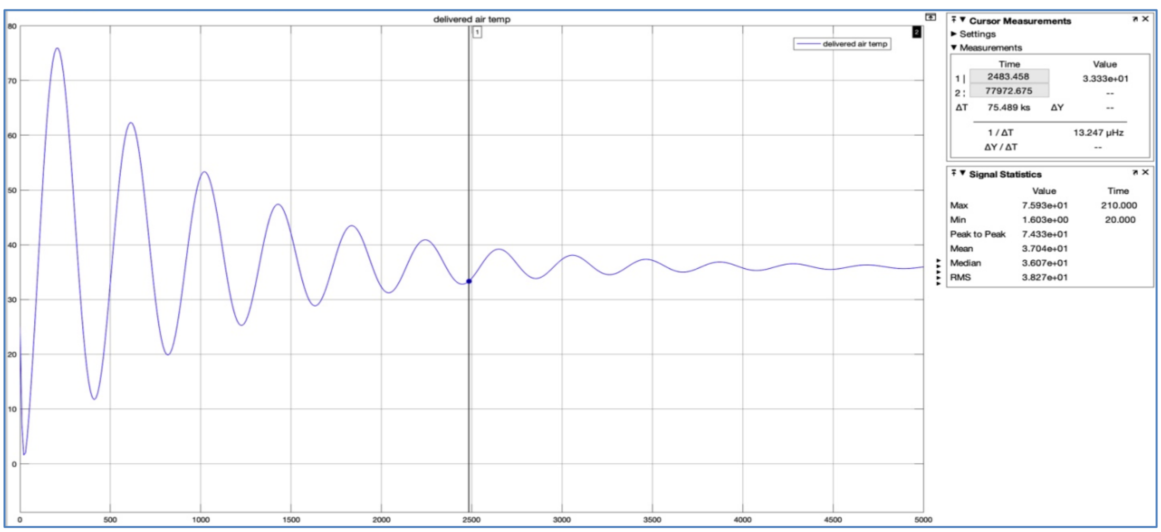

Figure 19. Initial PID Configuration for the Controllers [25].

The system would reach temperature values higher than 40 degrees Celsius, which would be unsafe for an infant.

---

[6] Section 201.3.212. page 10.
[7] Section 201.15.4.2.2.102, page 25.
[8] Section 201.3.212. page 10.
[9] Section 201.15.4.2.2.102, page 25.

To correct this situation, it was decided to limit the output of the control signal to a safe limit, between 30 and 39 degrees Celsius. The saturation block in Simulink emulates the control limit for both the cut-off thermostat and the controller's limiting capabilities, as defined in section 201.15.4 of the IEC standard for incubators [11]. The enhanced temperature response can be observed in Figure 20.

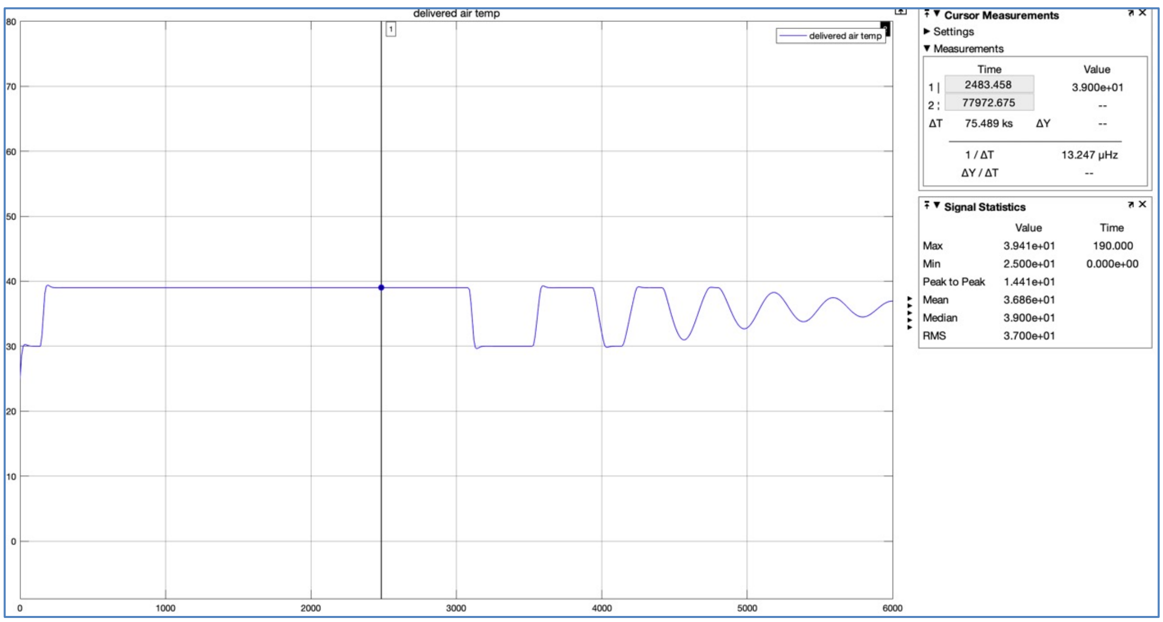

Figure 20. Heated-Air Temperature as a Function of Time [25].

Even with this adjustment, the temperature behavior obtained did not meet the steady-state temperature requirement[10], and the delivered temperature of the air did not stabilize to ± 1 degrees Celsius within one hour (3600 s). To correct this situation, the PID tuning tool available in Simulink was used to improve the steady-state error and transient response.

[10] Section 201.3.212. page 10.

Figure 21 shows the last results of a series of iterations from the PID tuner tool in Simulink. It was concluded that the saturation boundaries imposed on the system limit the controllability of the system, and the PID tuning process resulted in a very small improvement of the temperature range. However, the obtained response was within the requirements of operation, and therefore, the results were considered appropriate for the intended design.

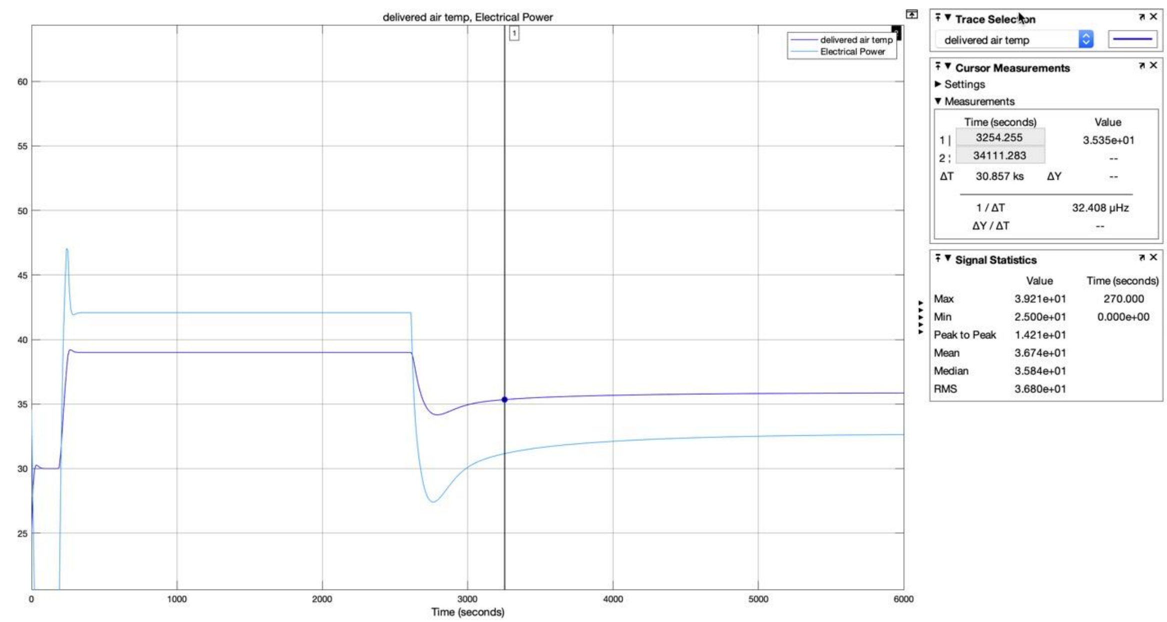

Figure 21. PID Temperature Commands with Limits [25].

From the results shown in Figure 21, it is possible to determine that the maximum amount of heating power required from the electrical heater is 51 watts, and the delivered air temperature does not exceed 40 degrees Celsius.

The optimized final value for the PID control for the proposed design is shown in Figure 22, which is the optimal value that can be used by the Arduino Microcontroller to provide the proportional output to the solid state relays (SSRs), as discussed previously.

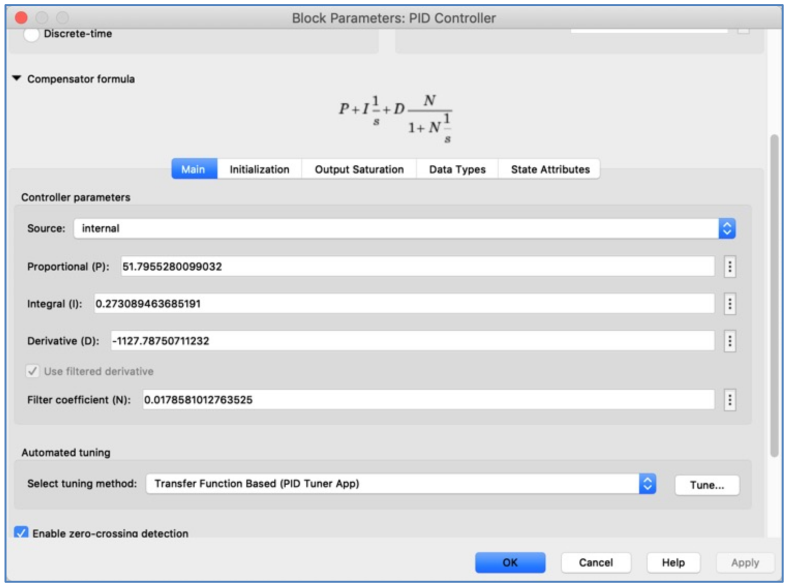

Figure 22. Optimized PID Configuration Using PID Tuner Tool [25].

The expected skin temperature values using the optimized PID control are shown in Figure 23.

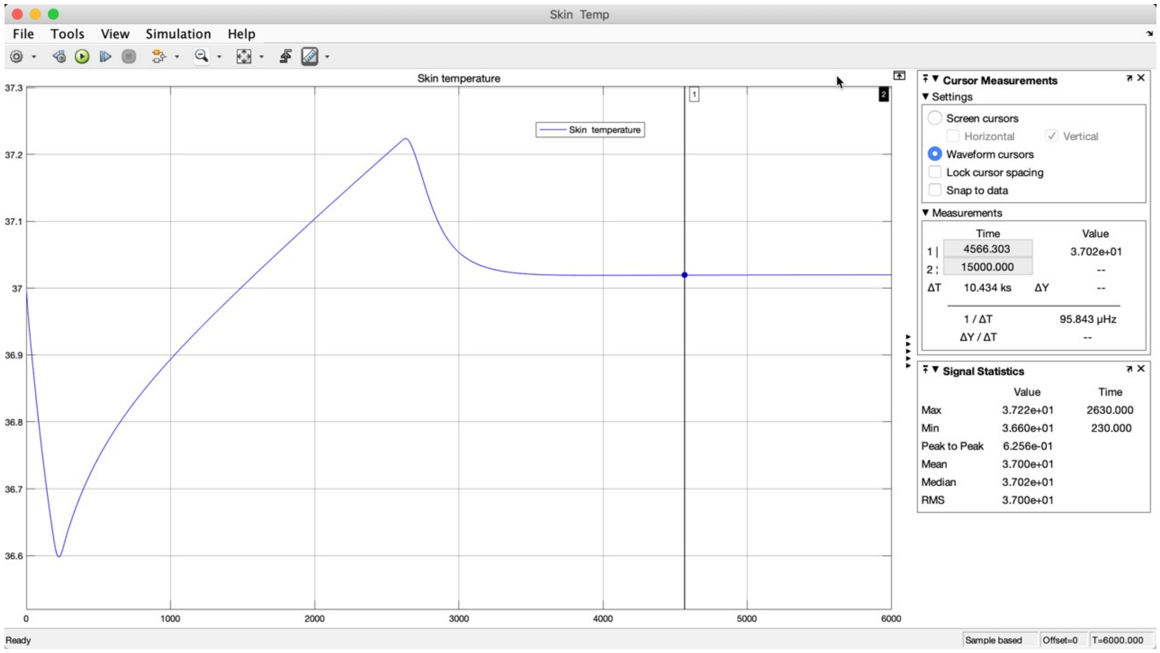

Figure 23. Optimized Response of the Incubator System [25].

Figure 24 features a schematic of the heater control system, which helps to explain the rationale for the selection of critical components.

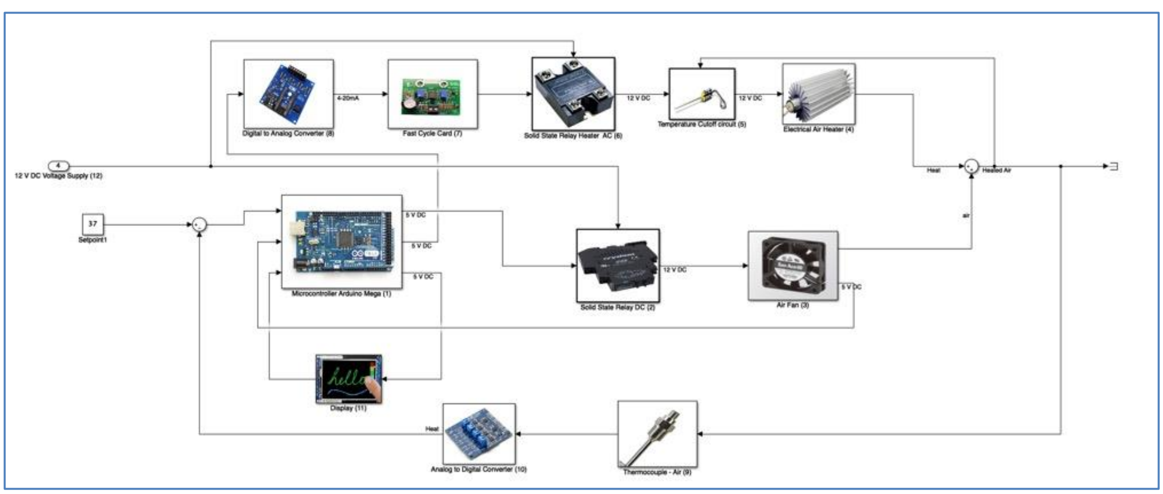

Figure 24. Schematic of the Heater Control System.

Microprocessor

An Arduino Mega microprocessor [30] has been selected because it is widely available, and the amount of support documentation explaining how to connect it to different devices and components is extensive. This makes the device an excellent choice to meet the requirements of open technology. The Arduino Mega model has been selected because it features 54 digital pins, 16 analog inputs, and four serial communication ports, which provide enough capacity to connect all devices intended for the proposed incubator design.

Analog to Digital Converters (ADC) for Thermocouples

Temperature measurement devices like thermocouples produce a small voltage that is not readable directly by most microprocessors. Therefore, it is necessary to use signal amplifiers to get readable voltages. In addition, the ADC device selected for this project provides "Cold Junction Compensation" [31] for different types of thermocouples and safety features like detection of the "Open Thermocouple" Failure Mode [32].

Solid State Relays (SSRs)

SSRs are no-contact relays that allow the interruption of an electrical circuit at very high-speed and high-frequency rates; the SSRs also provide a way to electrically isolate the control input circuit from the output control signals – thus providing a way to protect control circuits from any failure in the output circuit. The SSR manufacturer, Omron Corporation [33], provides a detailed explanation of the principles of operation for SSRs. The SSR device will allow the microprocessor to control the air heating element safely and also allow precise control of the temperature. In addition, for this project, a Proportional Control SSR is used, which provides proportional power to the load (0 to 100%) based on a proportional input value (generally 4 to 20 mA), therefore providing precise control of the heating element and extending its useful life. Crydom Corporation [34] also provides a detailed explanation of the principle behind proportional control. As shown in Figure 25, when the SSR receives a proportional control signal of 50%, it will deliver the output voltage at the peak of each AC half-cycle, thus applying 50% of the power load to the heating element. The Watlow models of SSRs [35] and Fast Cycle Card [36] were selected for this project because of their commercial availability, proven quality, and robust technical support.

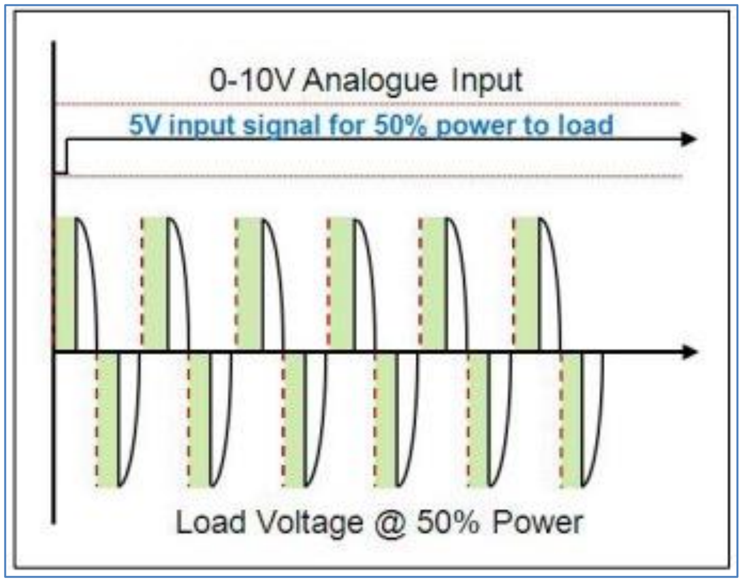

Figure 25. Phase-Angle Control [34].

Fast Cycle Card

To handle the SSR’s fast cycle requirements, it is recommended to include a Fast Cycle Input Card; this card receives a proportional signal (4 to 20 mA) from the microprocessor and then turns on and off the input signal to the SSR to provide the required proportional output.

Digital to Analog Converter (ADC)

Arduino microprocessors cannot supply the proportional control signal (4 to 20 mA) required for field instrumentation. Therefore, it is necessary to add an interface that will convert the digital commands of the microprocessor to a useful 4 to 20 mA control signal required by the Fast Cycle Card described previously.

Heating Element

Initially, it was determined that the optimal design for the air heating element should feature triangular fins. However, once the optimal design was achieved, it was realized that cartridge heaters with triangular fins are not commercially available, and therefore, it was decided to opt for an alternative solution. After researching different options, it was determined that a Compact Fan Heater from OMEGA [37] would be suitable. This model complies with the power and control requirements for the incubator.

Table 4 provides a bill of materials (BoM) to build the heating system design in this section. As indicated in the Results section of this report, the information contained in the BoM was used to determine if the proposed design achieved the objective of this project.

Table 4. Bill of Materials for the Air Heating System.

Component ID	Component Description	OEM number	Quantity	Unitary Cost (USD $)	Total Cost (USD $)	Reference
1	Microcontroller*	Arduino: 7630049200067	1	38.50	38.50	[30]
2	Solid State Relay DC	Sensata-Crydom DR24D03	1	33.42	33.42	[38]
3 & 4	Electrical heater	Omega: FCH-FGC10262R	1	170.25	170.25	[37]
5	Temperature Cut-off device	Selco: OM-160	1	25.00	25.00	
6	Solid State Relay AC	Watlow: SSR-100-10-AC1	2	30.00	30.00	[35]
7	Fast Cycle Card	Watlow: RPC-5399-42-000	1	116	116	[36]
8	Digital to Analog Converter	NCD: PR33-27	1	129.95	129.95	[39]
9	Thermocouple	Omega: M12JSS-M3-U-200-F	1	59.00	59.00	[40]

Table 4. Bill of Materials for the Air Heating System (continued).

10	Analog to Digital Converter*	Maxim Integrated: MAX31855	1	59.95	59.95	[41]
11	TFT Display	Adafruit: 2050	1	39.95	39.95	[42]
12	12 V DC Power Supply	Planet Technology: PWR-15-12	1	19.00	19.00	[43]
Total Cost for the Heating System					**696.02**	

Humidity Control

Humidity control plays an essential role in neonatal treatment. Harpin *et al.* [44] conducted a study to demonstrate that despite the use of maximum air temperatures settings in incubators, premature babies are incapable of maintaining a skin temperature within the NTE interval, because of the high evaporative water loss caused by their poorly developed epidermis. Therefore, humidification is an effective way of decreasing this type of heat loss.

The IEC standard [11] requires that relative humidity values shall have an accuracy of ± 10 % of an actual measured value when the temperature control is set between 32 °C and 36 °C.[11]

The humidification process for the proposed design consists of a water-filled chamber where an electrical resistance provides the necessary heat to evaporate water to increase the relative humidity until it reaches the setpoint value measured in the center of the enclosure.

For this project, an operating range for relative humidity (RH) control between 40% and 80% was selected based on the guidelines provided by the WHO [45]. The humidification system was designed to increase humidification from the lowest level of control (40% RH) to the max setpoint value (80% RH) in no more than 50 minutes, which is the expected stabilization time of the skin temperature of the baby [44]. There is not a time requirement for stable conditions for HR in the IEC standard [11] . Thus, it was determined that using the temperature stabilization time is appropriate.

[11] Section 201.12.1.109, page 19.

From the temperature control design, the following parameters can be designed:

Air conditions: defined at 25 ° C.

Duct diameter: 0.0508 m.

Air velocity: 2 m/s.

The volumetric flow is given by Equation (27):

$$\dot{\mathbf{Q}} = \boldsymbol{V} * \boldsymbol{A} \text{ ,} \tag{27}$$

where

V = fluid velocity,

A = area of the duct.

Therefore, the volumetric flow of heating air for the proposed incubator is:

$$\dot{\mathrm{Q}} = 2 * \pi * \left(\frac{0.0508}{2}\right)^2 \cong 4.05E - 3\frac{m^3}{s} \cong 0.24 \ \frac{m^3}{min} \ \cong 14 \ \frac{m^3}{hour} \text{ .}$$

Based on a benchmark of the dimensions of commercial incubators available in the market, it was decided to pursue a maximum volume design of 0.5 m^3. Therefore, the amount of time required to condition the whole volume of the incubator would be given by Equation (28):

$$\mathbf{t} = \frac{\textbf{\textit{Total Incubator volume}}}{\textbf{\textit{volumetric flow}}} \,. \tag{28}$$

Thus,

$$\mathrm{t} = \frac{0.5\, m^3}{4.05E{-}3\ {m^3}/{s}} \cong 123.5\ s \ \cong 2\ min.$$

Using the values from above, it was possible to start the design of the humidity control system.

The overall objective of the humidification system is to increase air moisture from 30% to 80% in 50 minutes. To determine this amount, an online psychrometric chart provided by Wolfram was used, and is shown in Figure 26.

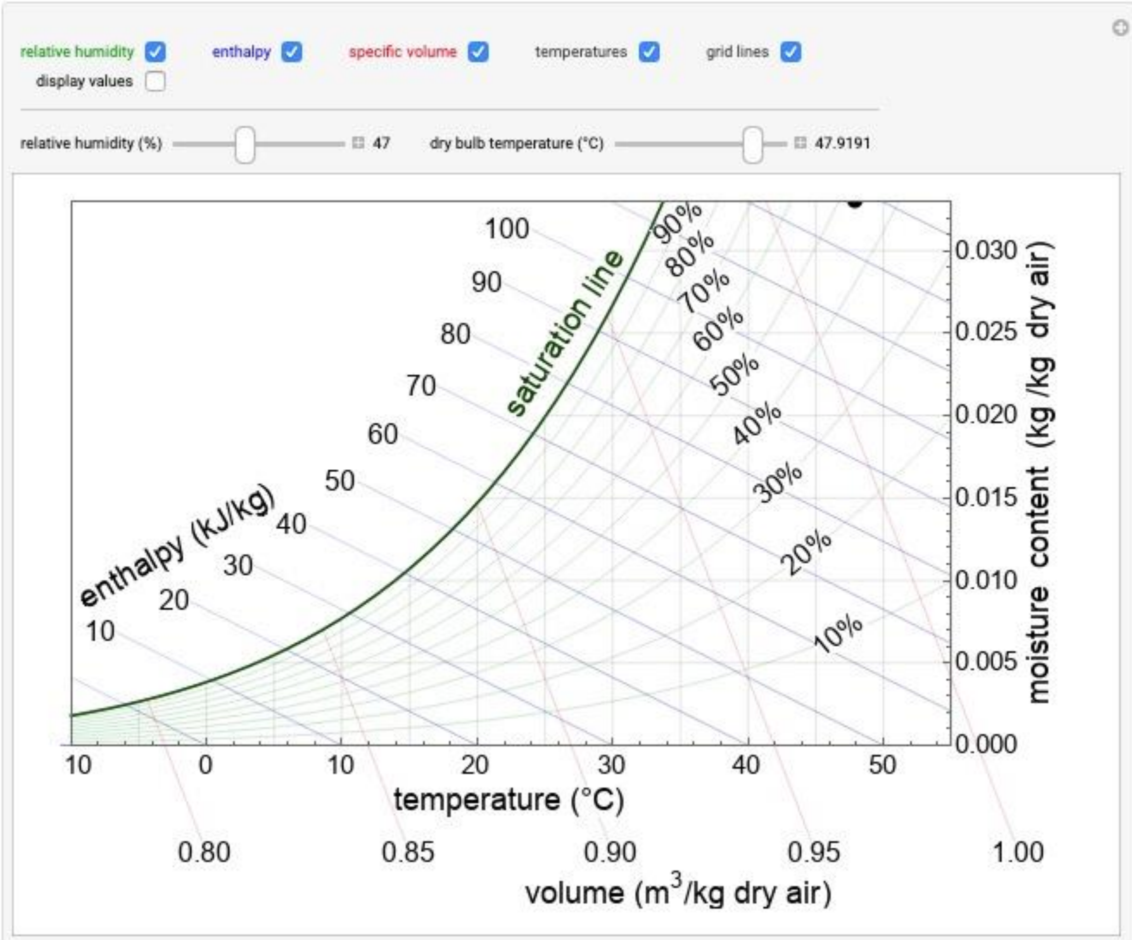

Figure 26. Psychrometric Chart from Wolfram [46].

The psychrometric chart is a graphical representation of the physical and thermodynamic properties of air.

The humidity conditioning process was based on the worst-case scenario (lowest operating temperature and RH, 25° C and 15%, respectively, and highest required setpoint for both variables, 37° C and 80%).

1. Intake air temperature is increased via the heating element from the initial condition 25° C and 30% RH (Step 1 in Figure 27) to 37 °C.

2. Since the air temperature is increased, the initial RH percentage of the air-vapor mixture is decreased to 15 % (Step 2 in Figure 27).

3. After the air temperature increases, saturated steam is added via the humidification chamber, where another heating element provides the required heat to evaporate the water in the chamber until the setpoint for HR is achieved. In Step 3 in Figure 27, this process is shown for a value of 80% RH.

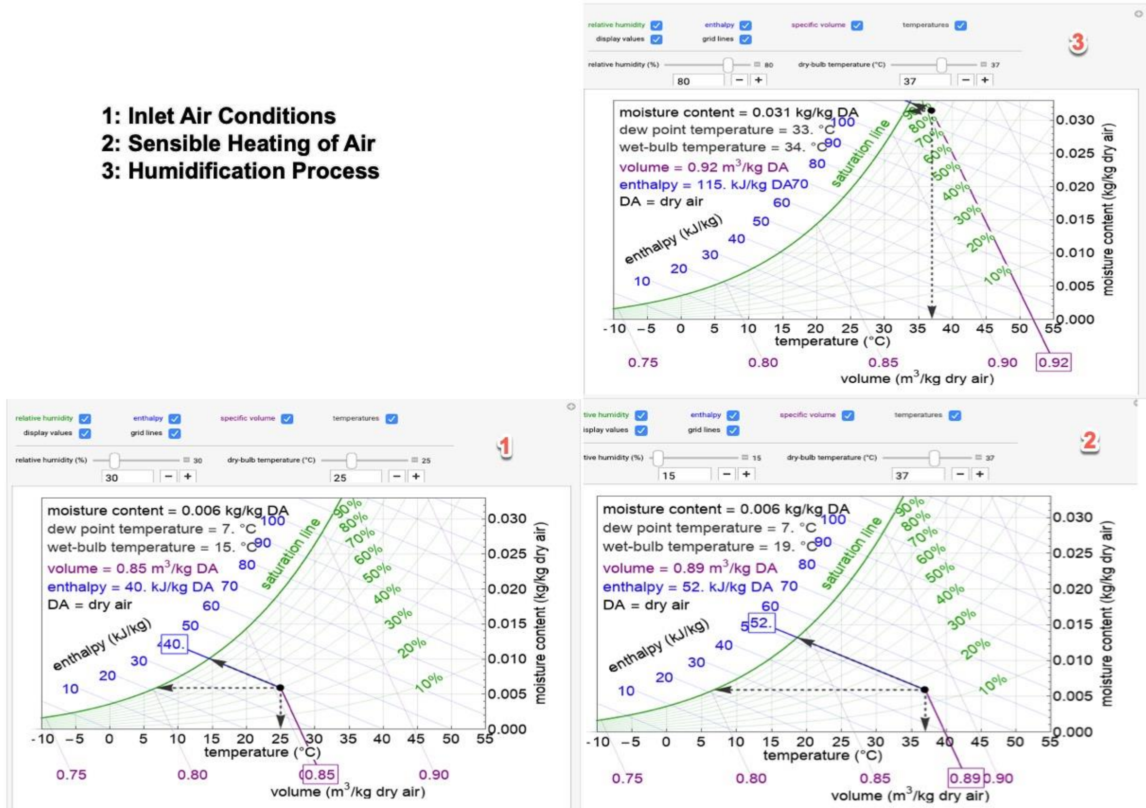

Figure 27. Air Humidification Process.

Based on the psychrometric data from Figure 27, it was possible to determine the size of the heating element for the humidifier as follows:

To increase humidification from 15% to 85%, the moisture content must be increased by:

$$\mathbf{\Delta m = m_{i+1} - m_i} \ , \tag{29}$$

where

Δm = increased moisture content by kg of dry air,

m_{i+1} = moisture content at the end of the humidification process,

m_i = moisture content at begining of the humidification process,

The use of Equation (29) yields the following value:

$\Delta m = 0.031 - 0.06 = 0.029\ {}^{kg}/_{kg\ Dry\ Air}.$

The total mass of water required to increase Δm can be estimated using the following equation:

$$\mathbf{m_w = \dot{Q} * \rho_{air} * \Delta m} \ , \tag{30}$$

where

m_w = mass flow of water,

$\dot{Q}$ = volumetric flow of air,

ρ_{air} = density of air at 37° C.

Based on the calculated airflow and using Equation (30), the total mass flow of water required to increase the humidification of the air from 37% to 80% RH is calculated:

$$\mathrm{m}_w = 4.05E - 3\frac{m^3}{s} * 1.138 \ {kg}/{m^3} * 0.029 \ {kg}/{kg\ Dry\ Air},$$

$$\mathrm{m}_w = 1.34\mathrm{E} - 04 \ {kg\ of\ water}/{s} \cong 0.481 \ {kg\ of\ water}/{h}.$$

Since the objective is to achieve the humidification value in 50 minutes, subtracting the 2 minutes required for ensuring a full exchange of the incubator's volume, the target time to complete the humidification process is 48 minutes (80% of one hour). The value obtained previously is adjusted accordingly to reflect the new evaporation rate:

$$\mathrm{m}_{wadj} = \frac{4.81\mathrm{E}{-01}}{0.8} \cong 0.6 \ {kg\ of\ water}/{h}.$$

And,

$$\mathbf{Q} = \mathbf{m}_t * \boldsymbol{C_p} * \boldsymbol{\Delta}\mathbf{T} \quad (31)$$

where

$\mathrm{Q} = \text{heat},$

$\mathrm{m}_t = \mathrm{m}_{\mathrm{wadj}} + \text{ amont of water in the reservoir} = \text{ total mass of water},$

$C_p = \text{specific heat of water} \frac{\mathrm{kJ}}{\mathrm{kg}},$

$\Delta\mathrm{T} = \text{temperature difference}.$

It was decided to limit the capacity of the water reservoir to 5 kg of water, based on the humidification needs the system would require for refilling the reservoir every eight hours. Then, the heating power required to heat the whole calculated mass of water (plus 0.6 kg for safety purposes) from 25° Celsius to 100° Celsius is determined by Equation (31):

$$Q = 5600 \, {}^{g}/_{h} * \; 4.186 \, {}^{J}/_{g\,°C} * (100 - 25) \text{degrees Celsius} \; \cong 1570 \; {}^{\text{kJ}}/_{h}.$$

The latent heat of evaporation required for the change of phase is determined by:

$$\mathbf{Q}_{\boldsymbol{l}} = \dot{\mathbf{m}} \; * \; \boldsymbol{h}_{\boldsymbol{e}} \; , \qquad (32)$$

where

Q_{l} = latent heat of evaporation,

h_{e} = evaporation heat of water = 2256 ${}^{\text{kJ}}/_{\text{kg}}$,

$\dot{\text{m}}$ = mass flow.

Thus,

$$\text{Q}_{l} = 0.6 \; {}^{kg}/_{h} * \; 2256 \; {}^{kJ}/_{kg} \cong 1354 \; kJ/h.$$

Adding Q and Q_{l} , the total heat power (P) is obtained for the humidificator system:

$$\text{P} = 1354 + 1570 = 2924 \; {}^{kJ}/_{h} \cong 812 \text{ W}.$$

For this project, it was decided to use 1000 W, 120 V AC, and 9 A to provide a safety factor for the calculated resistor and also to accommodate the commercial heaters available in the market.

The schematic for the control system of the humidification is shown in Figure 28. The Arduino Controller (1) receives the setpoint value, and based on the value reading from the humidity sensor, sends a control signal to the solid state relay (2) to power the electrical heater (4) until the setpoint value for the relative humidity is reached. A thermocouple (5) is placed inside the water reservoir to monitor the temperature of the heated water and detect any anomaly during the heating process. The thermocouple sends its signal to an analog to digital converter (6), so it can be read by the microcontroller (1). A thermal cutoff device (3) has also been considered as part of the design to avoid any overheating in the humidification chamber.

Considering the high tolerance of relative humidity measurement specified by the IEC standard (±10%)[12] [11], it was decided to use an on-off control mechanism for the heater element, thus simplifying the design and reducing the cost of total system.

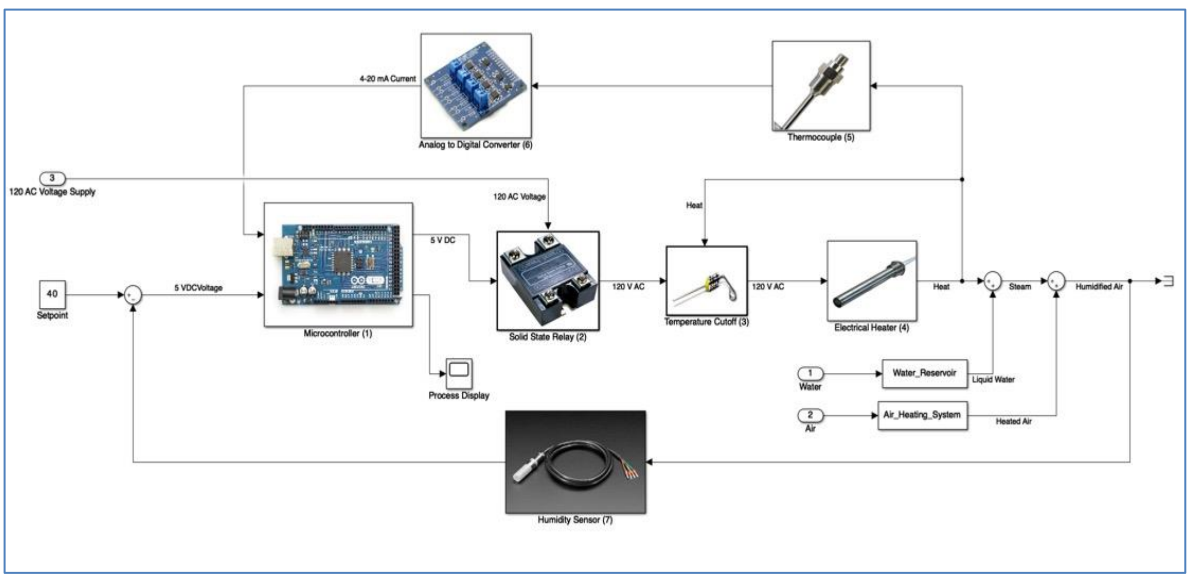

Figure 28. Control System for Incubator's Humidity.

[12] Section 201.12.1.109, page 19.

Figure 29 shows the prototype concept for the humidification chamber. Polytetrafluoroethylene (PTFE) was selected as the material of choice due to its materials property of withstanding high temperature and its usability for medical purposes.

The overall dimensions for the chamber are shown in Figure 30.

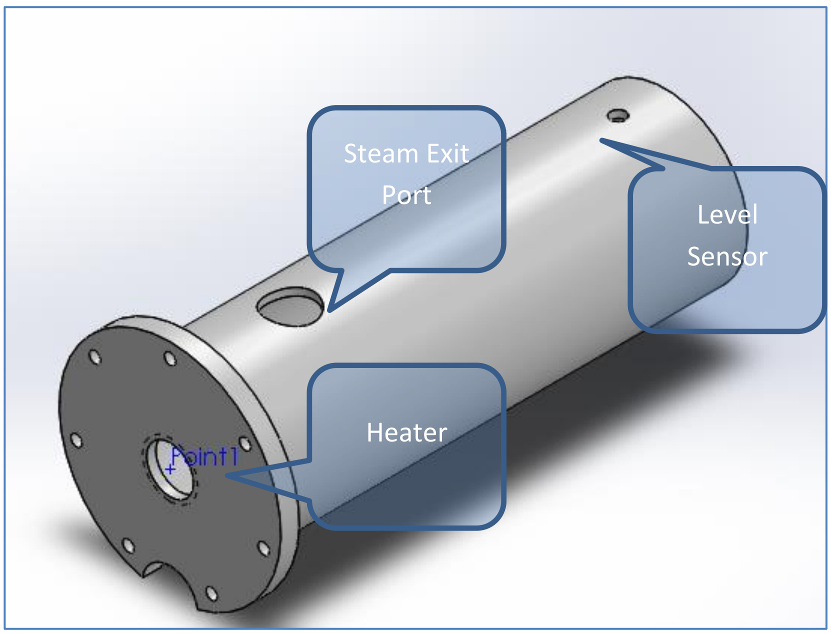

Figure 29. Isometric View Humidifaction Chamber.

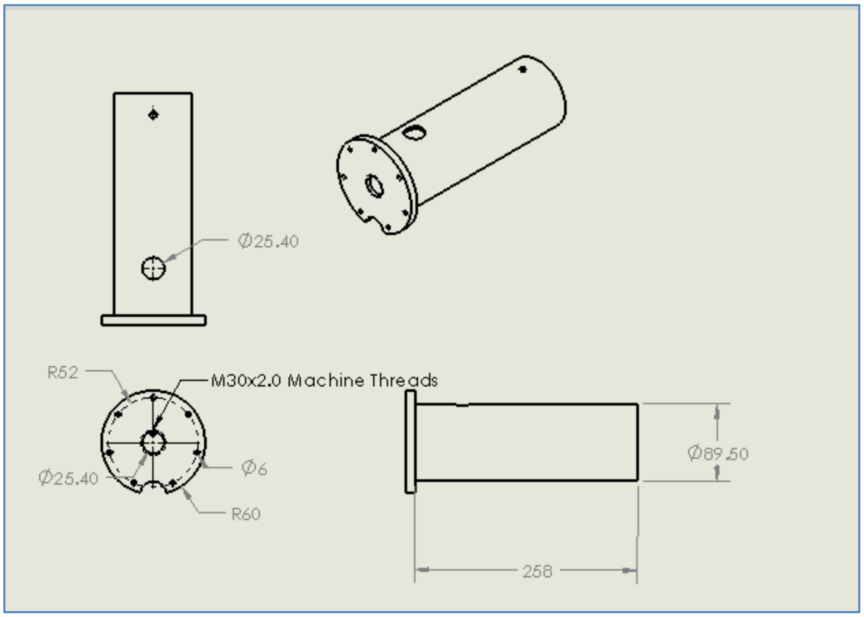

Figure 30. Overall Dimensions Humidification Chamber.

As an additional step, a 2D simulation analysis using ANSYS 15.0 Software was conducted on a humidification chamber to verify the proposed design. ANSYS was chosen because of its capability to conduct transient analysis with phase change and thermal energy. A tutorial provided by ANSYS [47] regarding the modeling of heat transfer with the evaporation-condensation mass transfer mechanism was used as a guideline to set up the model.

Figure 31 shows the general configuration of the simulation model in Simulink; a transient analysis was conducted to see the behavior of the liquid and vapor phases on the humidification chamber. Figure 32 shows the setup for the analysis that was conducted. The liquid in the humidification chamber is static; therefore, the laminar option was selected, and two phases were defined for the analysis (water liquid and vapor).

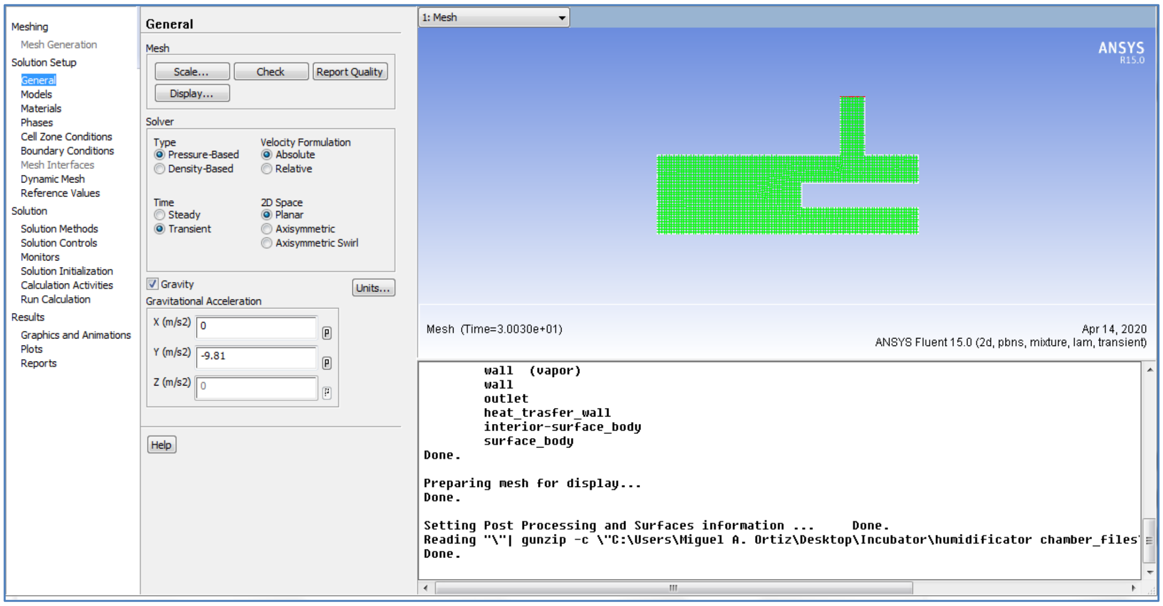

Figure 31. General Configuration.

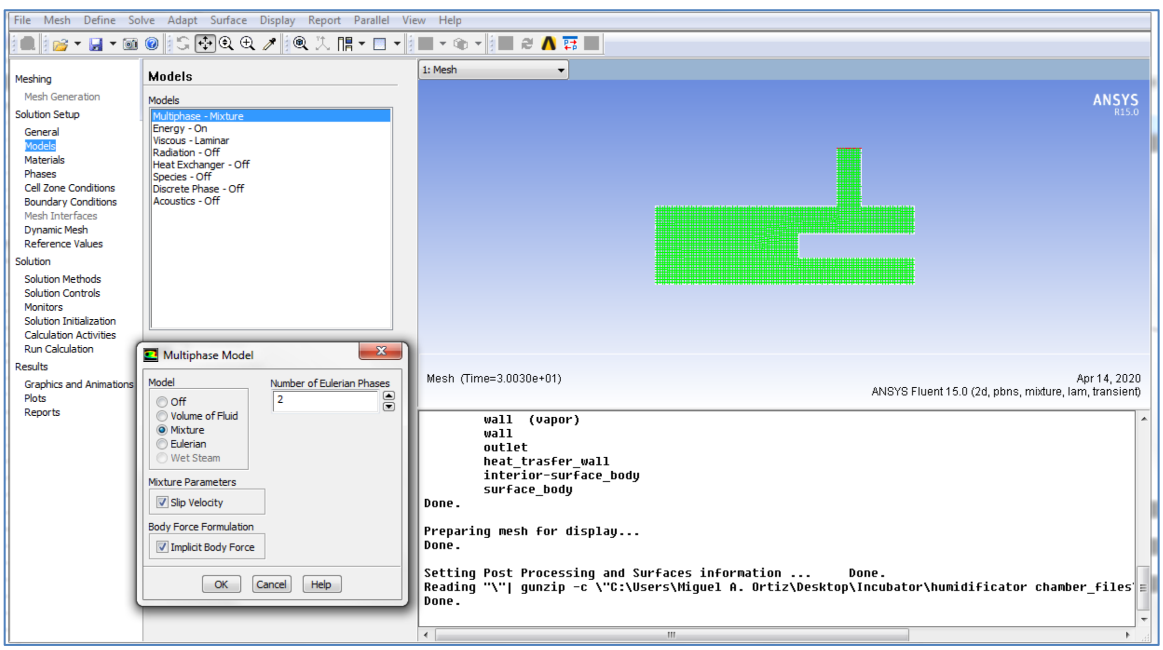

Figure 32. Model Setup.

The analysis considered only mass transfer mechanism to be evaporation-condensation, as shown in Figure 33

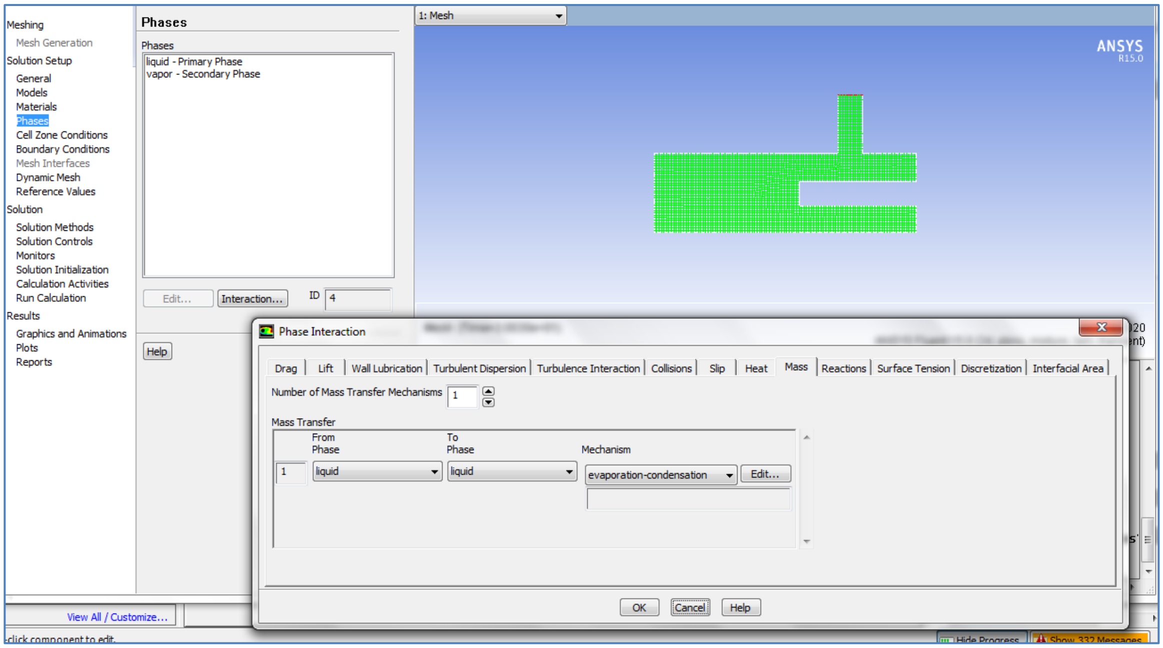

Figure 33. Mass Transfer Mechanism.

Based on the heater's power and dimensions defined previously, it was determined that the heat flux to be transferred through the heating walls would be approximately 86,000 W/m^{2}. This state is captured in the boundary condition for the simulation, as shown in Figure 34.

The solution methods that were run in this simulation were selected following the recommendations from ANSYS on how to solve this type of heat transfer problem [47]. These solution methods are shown in Figure 35.

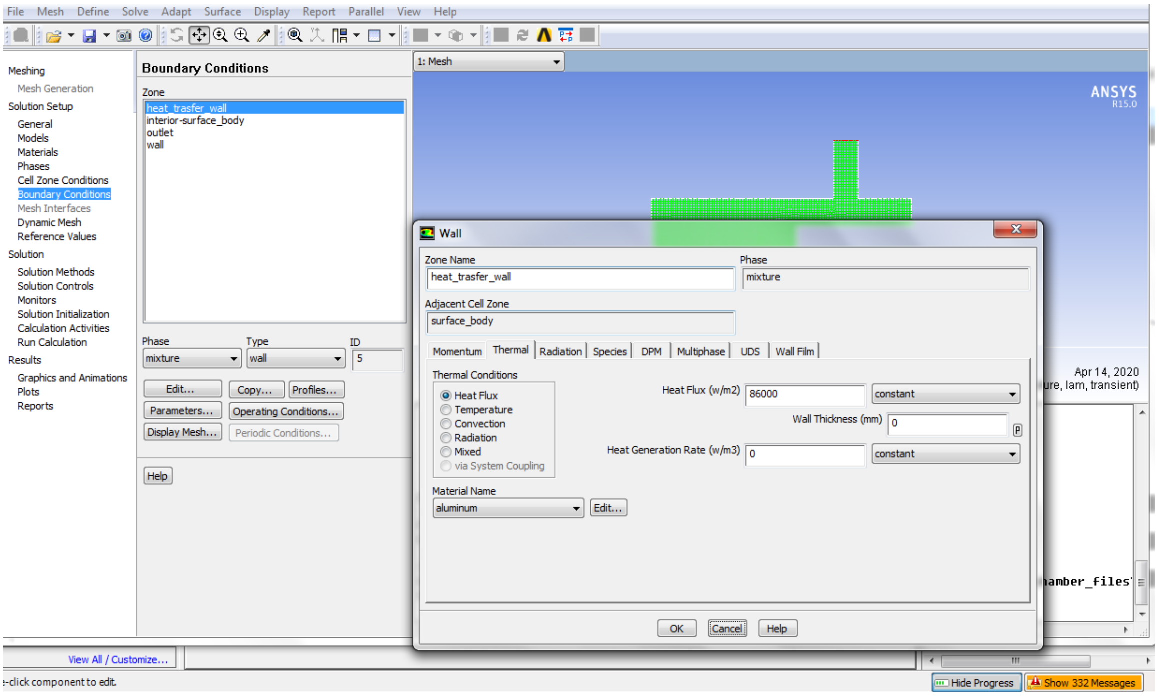

Figure 34. Heat Transfer Configuration.

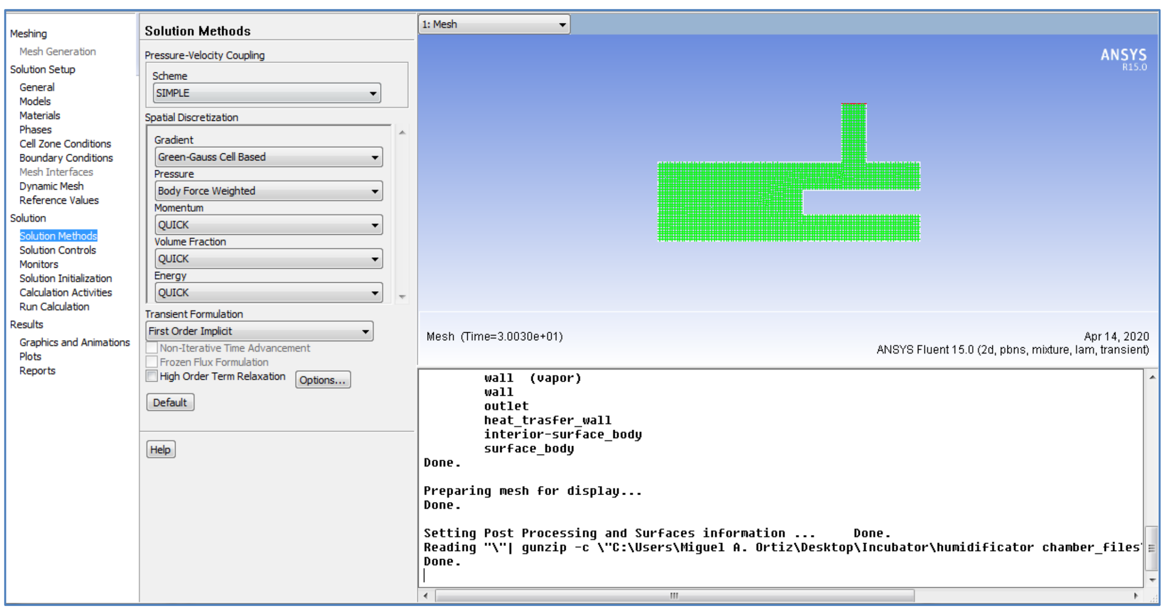

Figure 35. Solution Methods.

The results of the simulation are presented in the Result section of this report.

The Bill of Materials (BoM) for the proposed system is shown in Table 5.

Table 5. Bill of Materials for Humidification System.

ID	Component Description	OEM number	Quantity	Unitary Cost (USD $)	Total Cost (USD $)	Reference
1	Microcontroller*	Arduino: 7630049200067	1	0.00	0.00	[30]
2	Solid State Relay	Watlow: SSR-100-10-AC1	1	30.00	30.00	[35]
3	Temperature Cut-off device	Thermodisc: G4A01110C	1	1.00	1.00	[48]
4	Electrical heater	Omega: EMH-110-120V	1	183.00	183.00	[49]
5	Thermocouple	Omega: M12JSS-M3-U-200-F	1	59.00	59.00	[40]
6	Analog to Digital Converter*	Maxim Integrated: MAX31855	1	0.00	0.00	[41]
7	Humidity Sensor	Adafruit: 4099	1	25.00	25.00	[50]
Total Cost for the System					**298.00**	

**Cost was included in a previous bill of materials* — *Cost was included in a previous bill of materials

The main considerations for selecting the components shown in Table include the following.

Technical Considerations

- Ability to meet the technical specifications (i.e., voltage, current, temperature, accuracy, communication protocols, etc.).
- Online documentation is available for wiring and configuration. This aspect is important because the main objective of this project was to design an incubator that can be maintained in developing nations.

Commercial Considerations

- Price
- Online procurement

Enclosure

As previously stated, the main objective of this project was to design an incubator with a low manufacturing cost for developing nations that is also compliant with applicable standards. Therefore, the methodology to design the physical enclosure needed to consider the following criteria:

- IEC requirements [11]
- Low manufacturing costs
- Simplicity of design

The relevant criteria defined by the IEC standards were used to develop the initial design, and once the concept was developed, the manufacturing cost was validated using online manufacturing cost data. If the prototype idea resulted in a high manufacturing cost, a redesign process would have needed to take place, until the manufacturing cost would fall into the expected price range of less than $3,000 U.S., which was an important design goal.

Materials suitable for medical devices were considered, as suggested by Sastri [51]. The list of suitable materials includes Polyvinyl Chloride (PVC), Polypropylene (PP), Low-Density Polyethylene (LDPE), Polytetrafluoroethylene (PTFE), among others.

Figure 36 shows a graphical representation of the relation between yield strength and density for the different materials that were considered for this project.

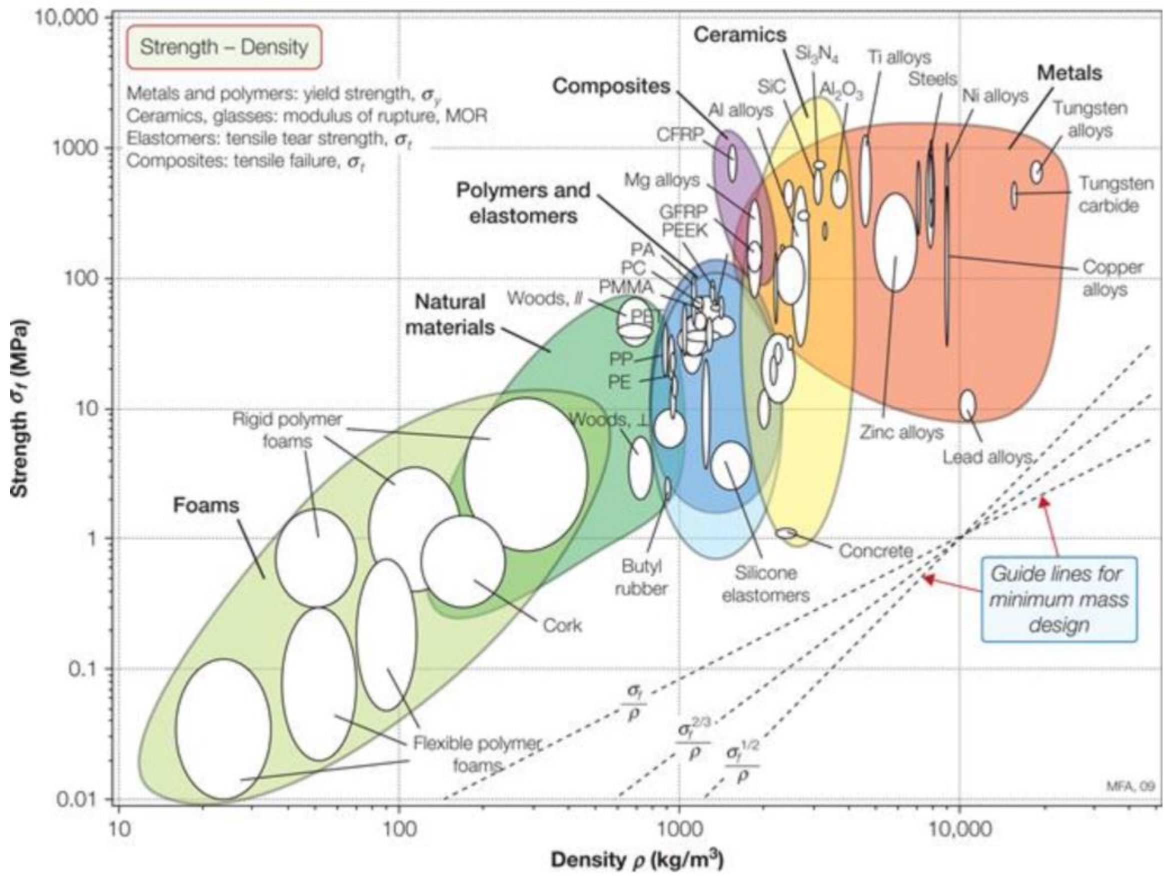

Figure 36. Strength - Density for Different Materials [52].

After considerable research, it was decided to use the following manufacturing providers based on their reputation and their ability to provide instant quotes:

- Sculpteo [53]: Online provider of design and additive manufacturing and laser cutting services.
- Xometry [54]: Provides CNC machining, 3D Printing, sheet metal and injection molding services in one central location.
- 3D Hubs [55]: Offers online quotes for the same services as Xometry.

The providers listed above can provide any medical facility with the capability to manufacture the components for the proposed incubator, which is a key objective of this project.

One of the key questions this project sought to explore in this section is the feasibility of using additive manufacturing (3D Printing) as a potential low-cost manufacturing method for medical devices for developing nations.

Additive manufacturing, or 3D printing, is the process of manufacturing three-dimensional solids from a digital model through the addition of material in small layers until the whole model is complete, as shown in Figure 37.

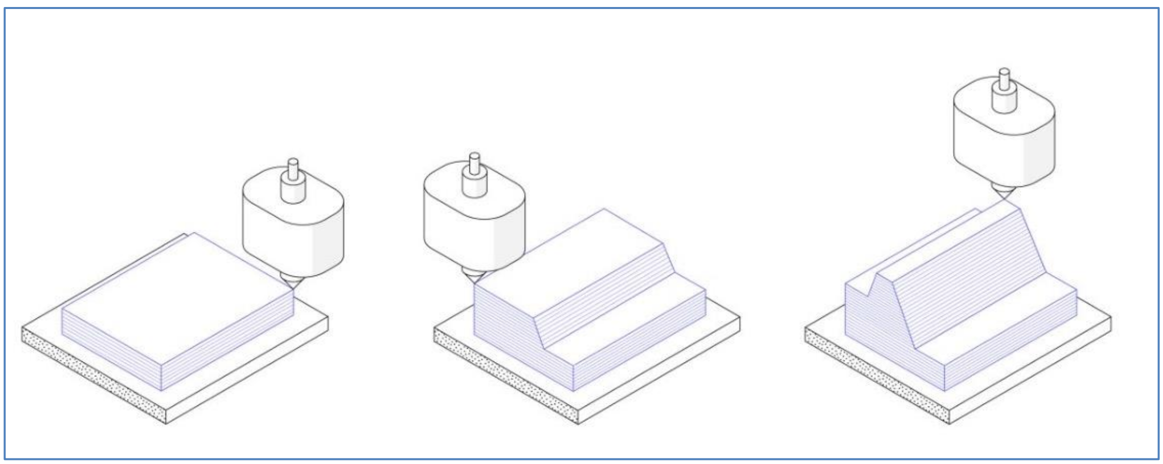

Figure 37. 3D Printing Technology [56].

The first 3D printer was released in 1987 by Chuck Hull [56], so the technology is not new, but its commercial availability has increased in the last decade, and it is expected to grow as the Digital Revolution, also known as Industry 4.0, continues to transform the supply chains of the future [57].

This project first explored the feasibility of using 3D printing as the main manufacturing process to minimize production time and to reduce the total amount of components required for the incubator. As explained below, however, this approach proved to be cost-prohibitive, and thus, traditional manufacturing processes were investigated.

For the development of an enclosure prototype, the design focused on the following requirements articulated in the IEC standards [11]:

1. "The infant shall be safely retained within the COMPARTMENT by barriers such as walls or side panels."[13]
2. "If a water reservoir is provided as an integral part of the INFANT INCUBATOR, it shall have a water level indicator with "max" and "min" markings if the level of the water in the tank cannot be seen."[14]
3. "INFANT INCUBATOR shall be constructed that spillage does not wet parts which, if wetted, might cause a safety hazard."[15]
4. "The INFANT INCUBATOR shall have means by which the infant can be taken in and out without the need to remove the canopy completed, or to disconnect tubes, cords, leads and the like from the infant."[16]

[13] Section: 201.9.8.3.101, page 14.
[14] Section: 201.11.6.2, page 16.
[15] Section: 201.11.6.3, page 16.

5. “Temperatures of the surfaces intended to be in contact with the patient shall not exceed 40 degrees Celsius [17]

Requirements Numbers 1 through 4 were addressed during the designing process in SolidWorks, and the discussion on how each requirement is met by the proposed design will be addressed in the “Results” section of this report.

The requirement specified in Number 5 will be addressed below in the heat transfer analysis for the supporting bed of the incubator.

For this project, it was decided to use PVC as an insulator material to cover all surfaces that will be in contact with the infant inside the incubator. PVC was selected because it is an excellent thermal insulator, and it is commercially available and suitable for medical equipment.

A steady-state analysis of the heat transfer process for the supporting bed was conducted using Simscale Simulation Software [58] to determine the steady-state temperatures of the incubator bed.

The schematics for the heat transfer process are shown in Figure 38. The supporting bed is subjected to heat convection on the top side, which is exposed to the heated air in the incubator chamber at atmospheric pressure, and the heating control system is keeping the air chamber at approximately 36° C. The airstream velocity is 2 m/s, which is the same value used in the mathematical model proposed by Fraguela *et al.* [23], and was used in the simulation model to calculate the heating control system.

---

[16] Section: 201.15.3.101.
[17] Section 201.11.1.2.2, page 25.

Conduction heat transfer takes place between the PVC and aluminum layer of the bed, and finally, at the bottom of the aluminum board, heat transfer by natural convection takes place.

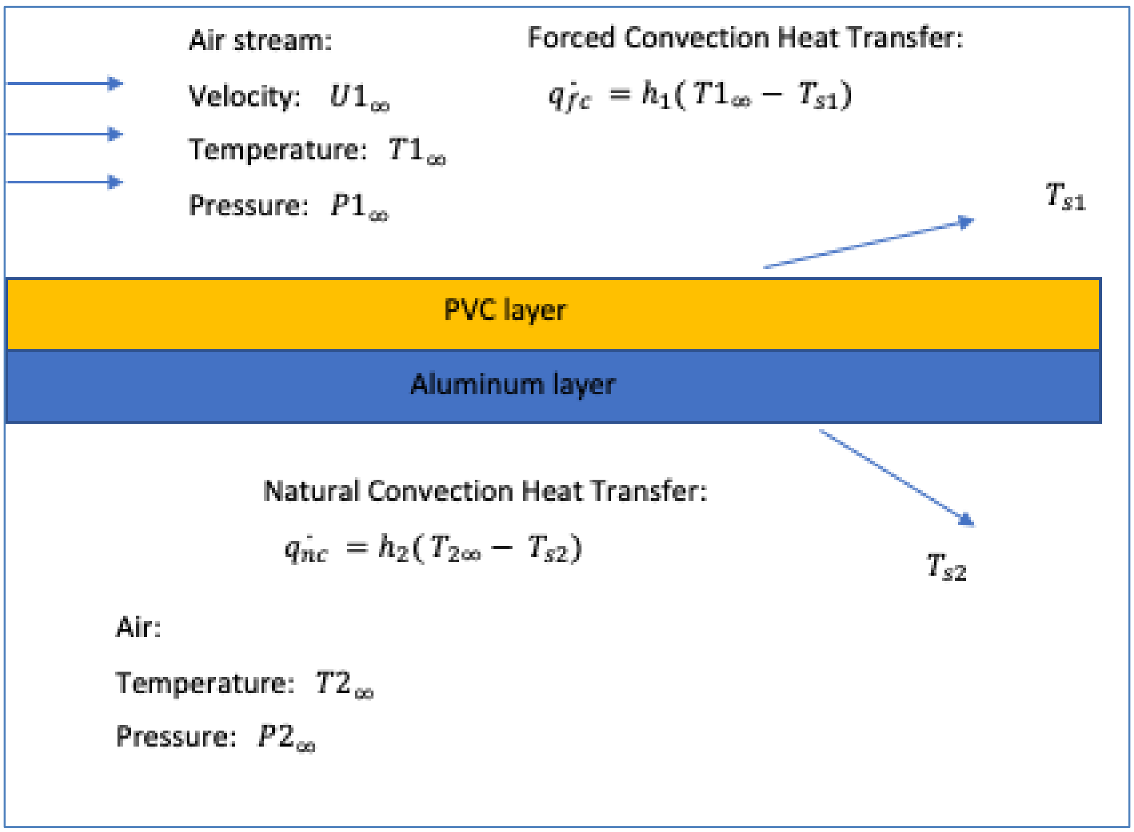

Figure 38. Heat Transfer Mechanism for Supporting Bed.

Equations (22), (23), and (24) were used to determine convection coefficient h_1 with the following data:

Velocity: $U1_{\infty}$ = 2 m/s

Temperature: $T1_{\infty}$ = 36 degrees Celsius (309.15 K)

Pressure: $P1_{\infty} = P1_{\infty} = 101.325\ kPa$

Temperature: T_{s1} = 35 degrees Celsius (308.15 K), (assumed to be one degree less than the air temperature)

Then, from Equation (30), the median temperature T_{f1} is obtained:

$$T_{f1} = \frac{(309.15 + 308.15)}{2} = 308.65\ K,$$

Using Table A.4 from *Introduction to Heat Transfer* by Incropera *et al.* [28], the following values were determined by linear interpolation:

Kinematic viscosity $(\nu) = 16.76\ x\ 10^{-6}\ {m^2}/{s}$

Conduction Coefficient $(k) = 26.94\ x\ 10^{-3}\ {W}/{m\ K}$

Prandtl number $(P_r) = 0.70579$

Using Equation (22), the Reynolds number was obtained, knowing that the length of the supporting bed (L) is expected to be 0.677 m:

$$Re_L = \frac{2(0.677)}{16.76\ x\ 10^{-6}} = 8.07x\ 10^4\ .$$

Based on the criteria expressed by White [59][18], the Reynolds value obtained above falls in the laminar flow category. Therefore, it is possible to use Equation (25) to determine the Nusselt number as follows:

$$Nu_L = 0.664 Re_L^{\frac{1}{2}} \Pr(T_f)^{\frac{1}{3}} = 0.664(8.07x\ 10^4)^{0.5}(0.70579)^{0.33} \cong\ 168.03.$$

The value for the average convection coefficient was obtained using Equation (26):

$$\boldsymbol{h_1 = \frac{Nu_L k_a(T_f)}{L} = \frac{168.03(26.94\ x\ 10^{-3})}{0.677} \cong 6.68\ {}^{W}/_{m\ K}}.$$

To calculate the convective heat coefficient for the bottom plate, the empirical equation suggested by Incropera *et al*. [28] for natural convection was used, which required the calculation of the Rayleigh number:

$$\boldsymbol{R_{aL} = \frac{g\beta(T_s - T_\infty)L^3}{\alpha\nu}}, \qquad (33)$$

$$\boldsymbol{\beta = \frac{1}{T_f}}, \qquad (34)$$

[18] Chapter 7, page 482.

$$\boldsymbol{Nu_L = 0.15\left({R_{aL}}^{1/3}\right)}, \tag{35}$$

$$\boldsymbol{h_2 = \frac{k(Nu_L)}{L}}, \tag{36}$$

where

$k =$ Conduction Coefficient for air at T_f,

$Nu_L =$ Nusselt number,

$g =$ gravity,

$T_s =$ temperature of the flat surface,

$T_\infty =$ ambient temperature,

$L =$ length of the flat surface,

$\beta =$ volumetric thermal expansion coefficient,

$\alpha =$ thermal diffusity,

$T_f =$ median temperature,

$\nu =$ kinematic viscosity,

$h_2 =$ convection coefficient for the bottom plate.

In this case, the temperature of the bottom surface is unknown. Therefore, the lowest operational ambient temperature specified for the incubator was used, which is 25°

Celsius (≅ 300 K) as the T_f temperature, to obtain the corresponding air property values for calculating the Rayleigh number. The assumption was also made that the difference between the surface temperature of the bottom plate and the ambient temperature is not greater than 5° Celsius. Thus:

$$g = 9.8 \frac{m}{s^2},$$

$$L = 0.677\ m,$$

$$\beta = \frac{1}{(300)} \cong 0.00333\ K^{-1},$$

$$\alpha = 22.5\ x\ 10^{-6}\ \frac{m}{s^2},$$

$$\nu = 15.89\ x\ 10^{-6}\ \frac{m}{s^2},$$

$$k = 26.3\ x\ 10^{-3}\ .$$

The following results are obtained using Equations (33), (34), and (35):

$$\boldsymbol{R_{aL}} = \frac{\mathbf{9.8(0.00333)(5)0.677^3}}{\mathbf{22.5\ x\ 10^{-6} * 15.89\ x\ 10^{-6}}\ \frac{m}{s^2}} \cong \mathbf{1.4161\ x\ 10^8}\ ,$$

$$Nu_L = 0.15\left(1.4161\ x\ 10^{8}{}^{1/3}\right) \cong 78.18,$$

$$h_2 = \frac{26.3\ x\ 10^{-3}(78.18)}{0.677} = 3.03\ {}^{W}/_{m^2K}.$$

The calculated convective coefficients were used in the heat transfer simulation to validate the temperature of the support bed in Simscale Software. It was believed that the assumptions used to determine the values for the convection coefficient are valid because they represent the worst-case scenario of conduction and, therefore, they provide the highest possible temperatures in the supporting bed.

Results

The purpose of this project was to study the feasibility of building a standard-compliant, infant incubator with open-source technology at a lower manufacturing cost than a commercial option, and with the potential to be built locally.

Crucial design characteristics for the incubator -- temperature and humidity control – were the focus of the project, as well as the design of a proper control mechanism for both systems based on some essential requirements of the IEC standards. Selected hardware components were also researched that would be necessary to build the required systems, which provided a clear picture regarding the manufacturing cost.

The summary of the results for each critical system researched in this project is featured next.

Temperature Control System

The temperature control system needs to comply with some critical requirements based on the IEC standards. The main requirements that were considered for this project include the following:

1. "The overshoot in incubator temperature shall not exceed 2 degrees Celsius and Steady-Temperature condition shall be restored within 15 minutes."[19]

    - The IEC standard indicates that to test for this point, the infant incubator should be operated as an air-controlled incubator at a controlled temperature of 32 degrees Celsius until the steady-state temperature is reached and then the temperature control should be adjusted to a new setpoint of 36 degrees Celsius to observe the response of the temperature. Figure 39 shows the model for an air controlled incubator, in which the skin temperature of the infant is not controlling the heating system; instead, it is controlled by the temperature sensor inside the incubator.

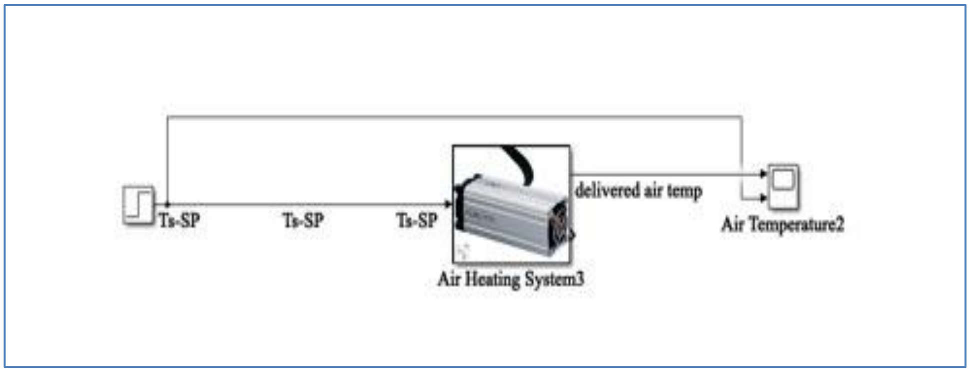

Figure 39. Air Controlled Incubator.

[19] Section 201.12.1.108, page 18.

To simulate this test in Simulink, a change of setpoint was defined using a step block, which would change the setpoint value at a predefined amount of time, as shown in Figure 40.

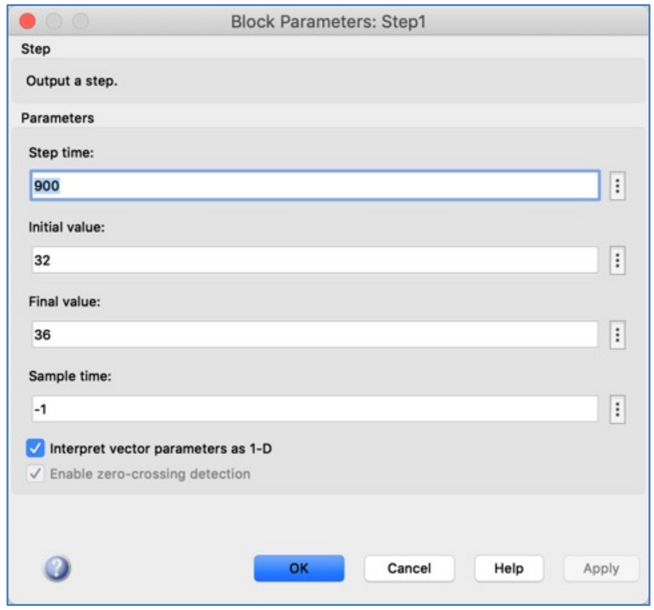

Figure 40. Step Block Configuration.

Figure 41 shows the time response of the system once the change in setpoint is made. The peak value is thirty-six and twenty two-hundredths of degrees Celsius, meaning an overshoot of approximately 0.6 percent. The stabilization time after the change of setpoint value is less than 15 minutes, as specified by the standard.

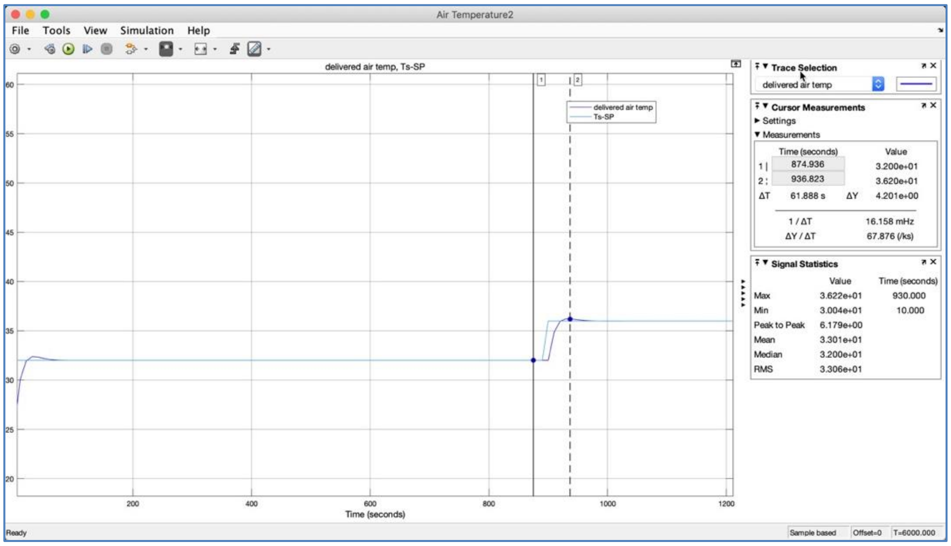

Figure 41. Temperature Response.

2. A baby-controlled incubator shall be equipped with a thermal cut-out that operates independently of any thermostat.”[20]

   - The design includes a thermal cut-out for both the air heating and humidification control system that would interrupt electrical power if the incubator’s temperature reaches a value equal to or greater than 40 degrees Celsius. In addition to the physical devices, electronic switches can be deployed inside the microcontroller via software, as a redundant safety system.

---

[20] Section 201.15.4.2.1, numeral bb, page 24.

Humidification System

The results of the ANSYS simulation for the transient response are presented in this section.

After conducting a transient analysis of 90 seconds, the results of the heat transfer process inside the chamber were obtained.

Figure 42 shows the volume fraction of the liquid phase. It is possible to observe that evaporation has started to occur in the upper section of the liquid volume.

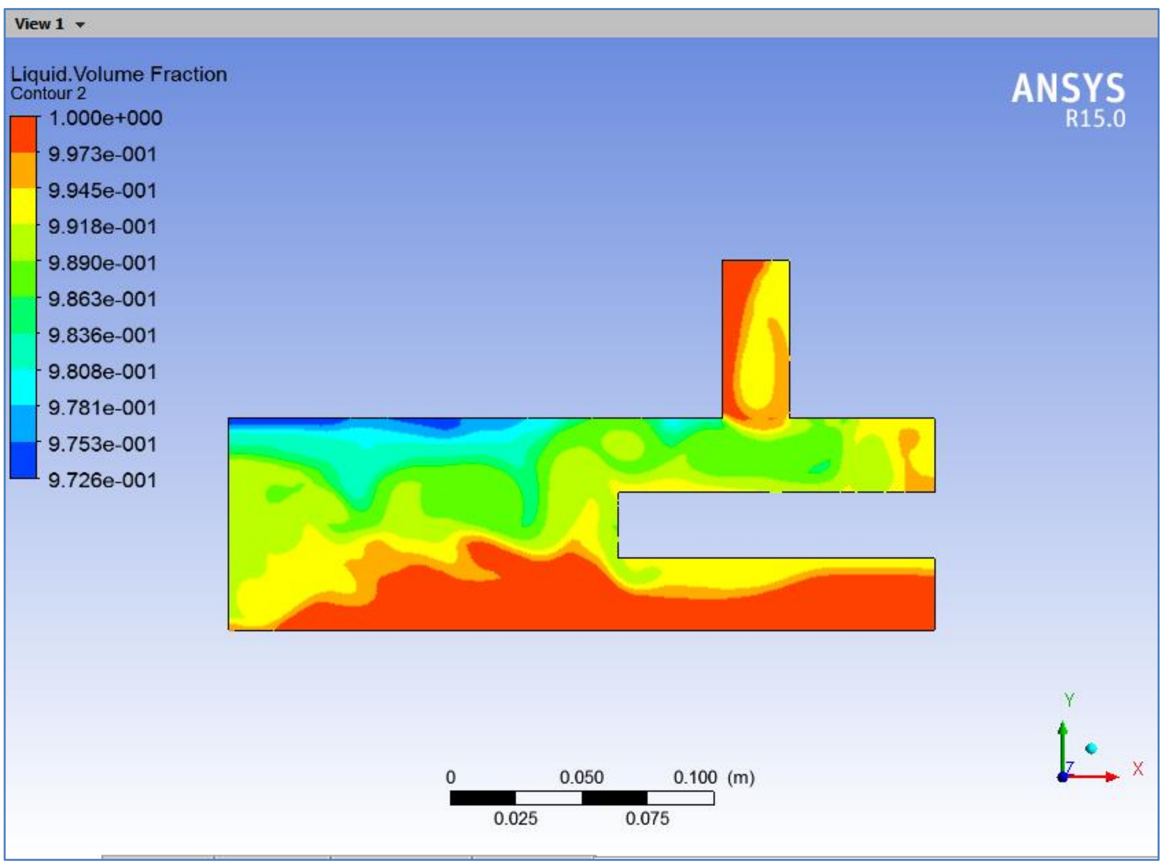

Figure 42. Liquid Volume Fraction.

Figure 43 provides a view of the profile velocity in the exit port that conveys the steam to the incubator chamber; as expected, the positive and negative velocity profiles in the outlet port indicate a convection process taking place in this section.

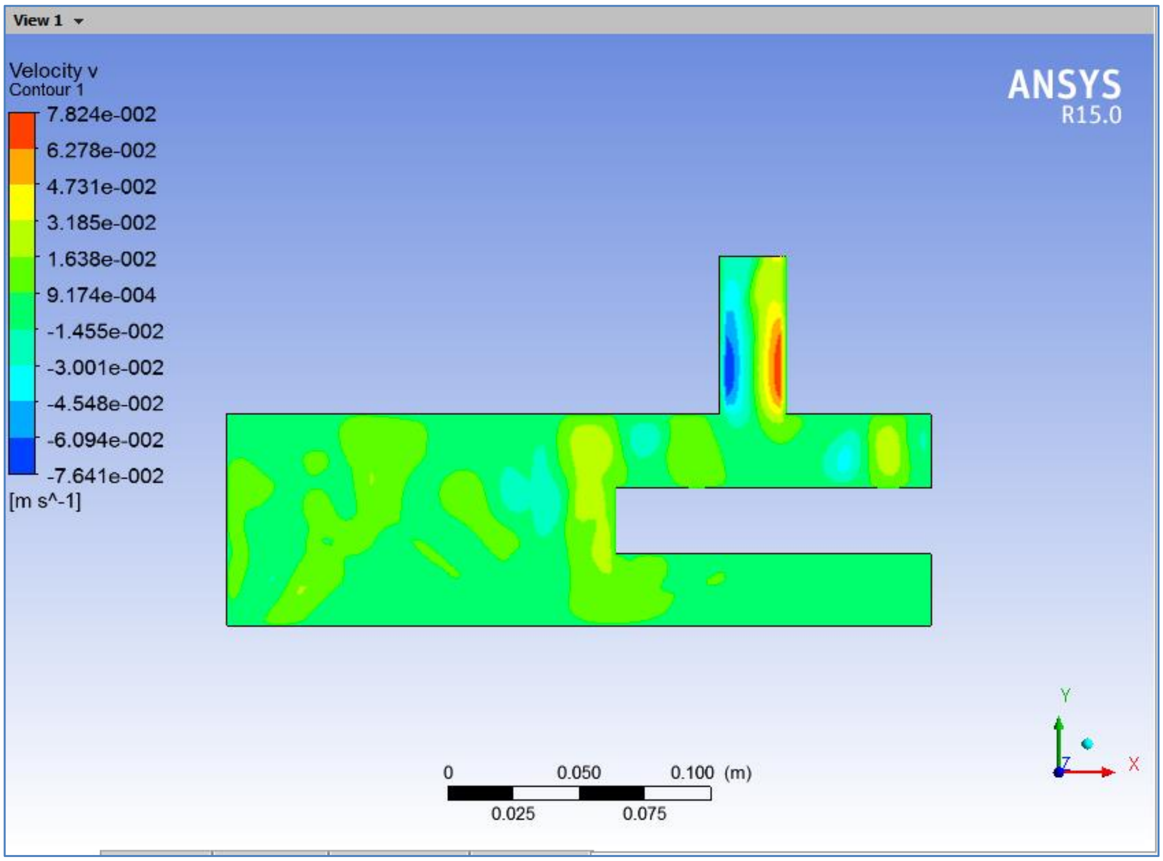

Figure 43. Velocity Contour.

Figure 44 shows the average temperature profile inside the chamber, by the elapsed time (90 seconds), most of the liquid's temperature is close to the boiling point, which is consistent with the calculations developed previously.

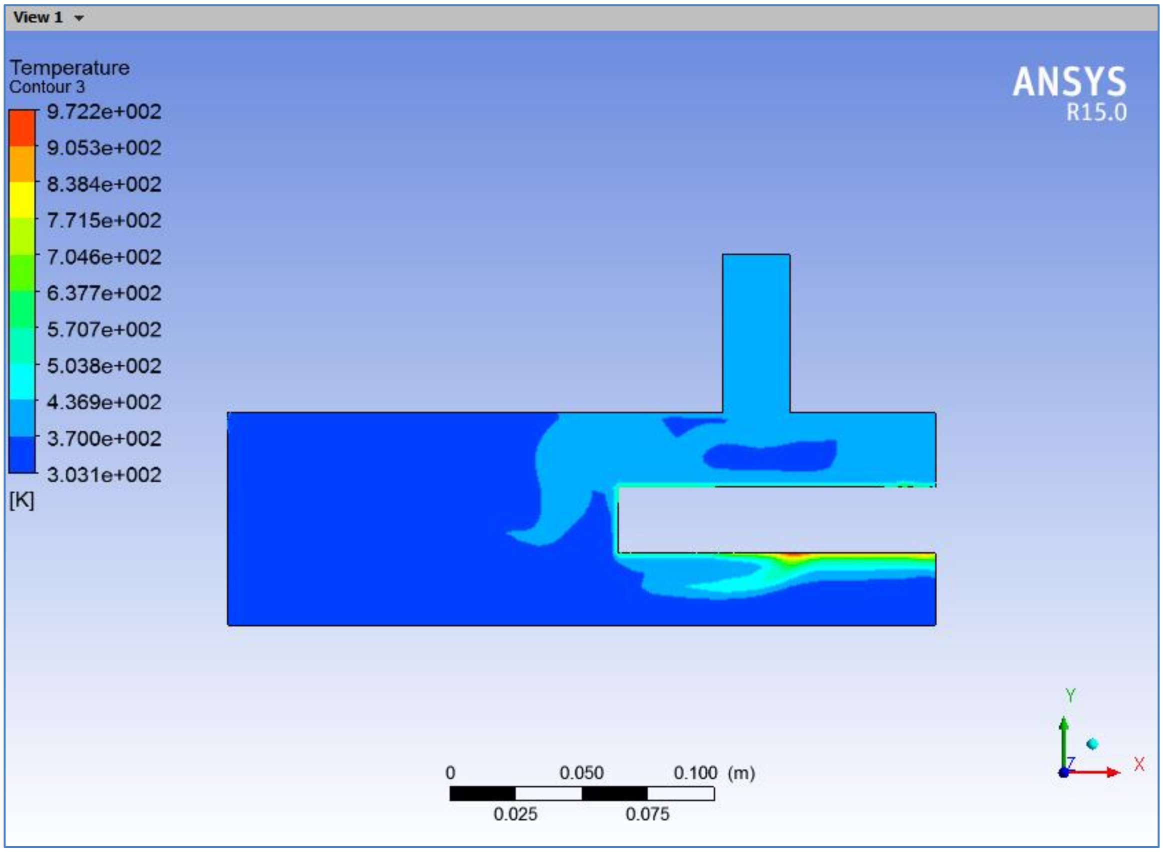

Figure 44. Temperature Profile.

Enclosure

A preliminary design for the incubator enclosure was developed using SolidWorks software, and is shown in Figure 45.

Figure 46 and Figure 47 show a rendered view of the preliminary design of the incubator's enclosure and its cross-section view.

The guiding principle for the initial design was to develop a monolithic block that could be 3D printed, thus minimizing assembly time, moving parts, and required components.

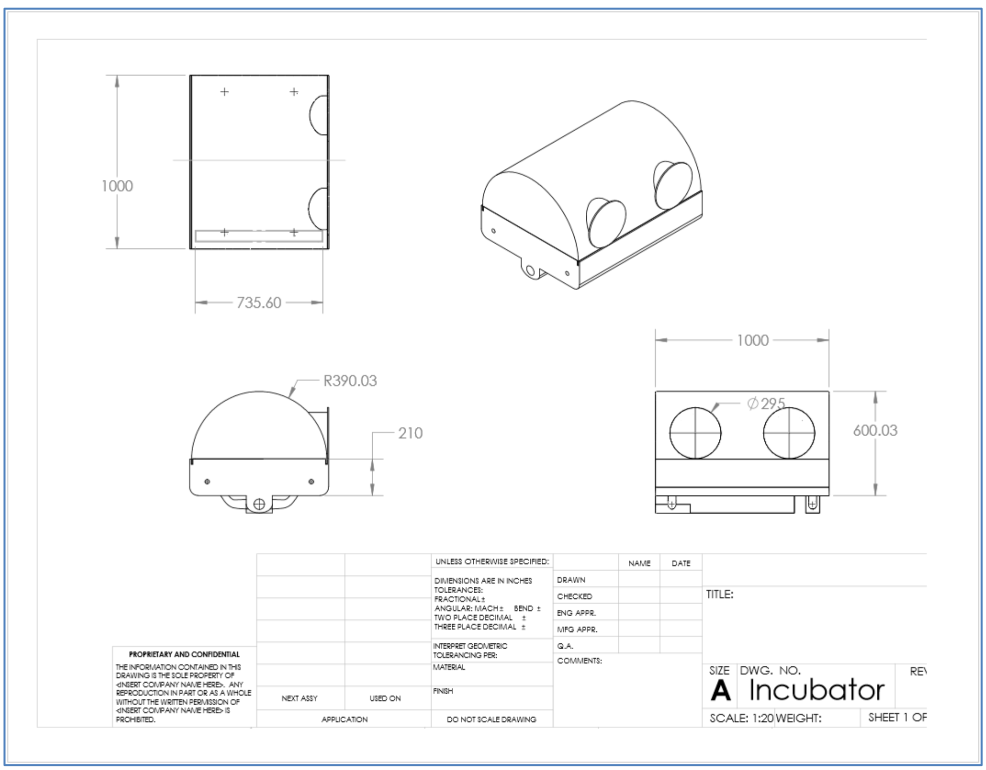

Figure 45. Preliminary Design of Incubator Enclosure [25].

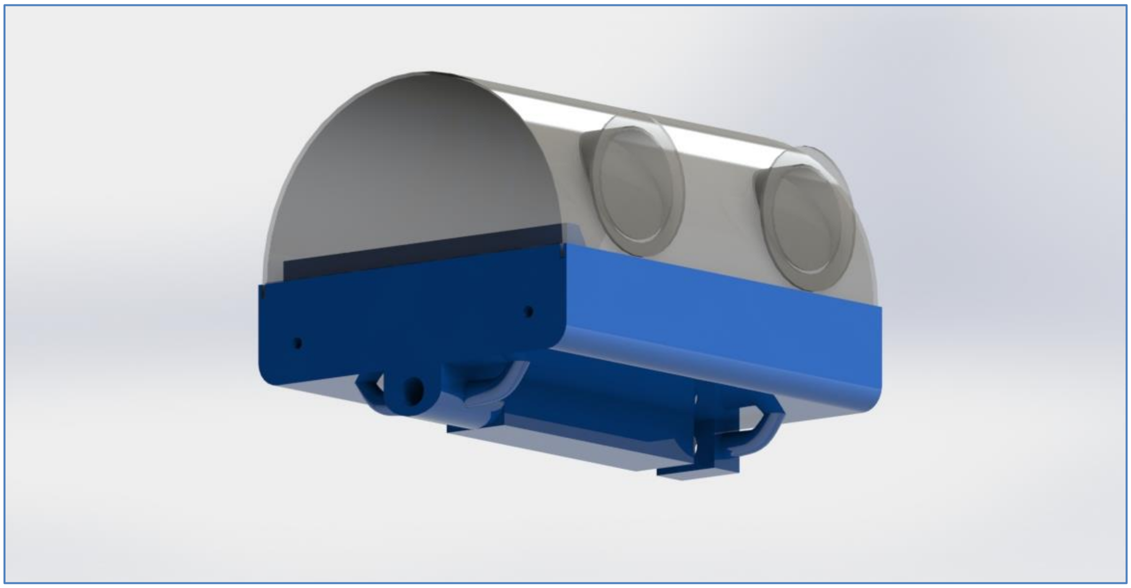

Figure 46. Rendering of Isometric View of Incubator.

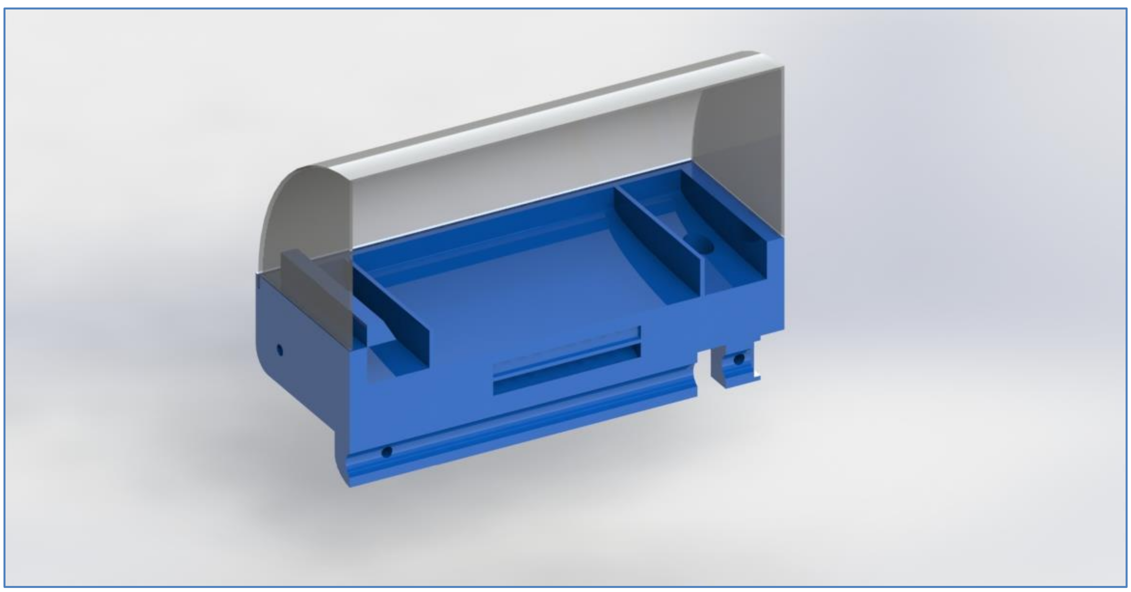

Figure 47. Cross-Section View of Incubator.

After finalizing the initial design, the bed part was submitted to the manufacturing services selected for this project, and it was learned that the cost to produce 3D-printed parts was too high. Figure 48 shows the cost of a small section of the bed.

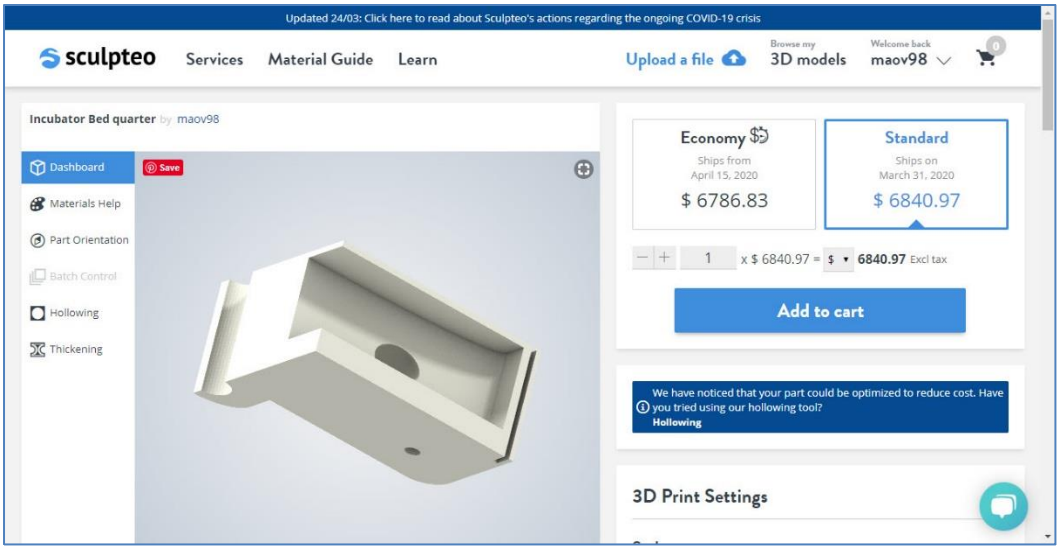

Figure 48. 3D Manufacturing Cost for Partial Bed Section.

Considering that 3D manufacturing was not an option, it was decided to follow a different path, which consisted of using standard and commercial components to minimize manufacturing cost and to use traditional manufacturing methods for building the design parts.

A new incubator enclosure design was developed using the guidelines described above and is shown in Figure 49.

A rendered view of the interior of the incubator is shown in Figure 50, and an exploded view is shown in Figure 51

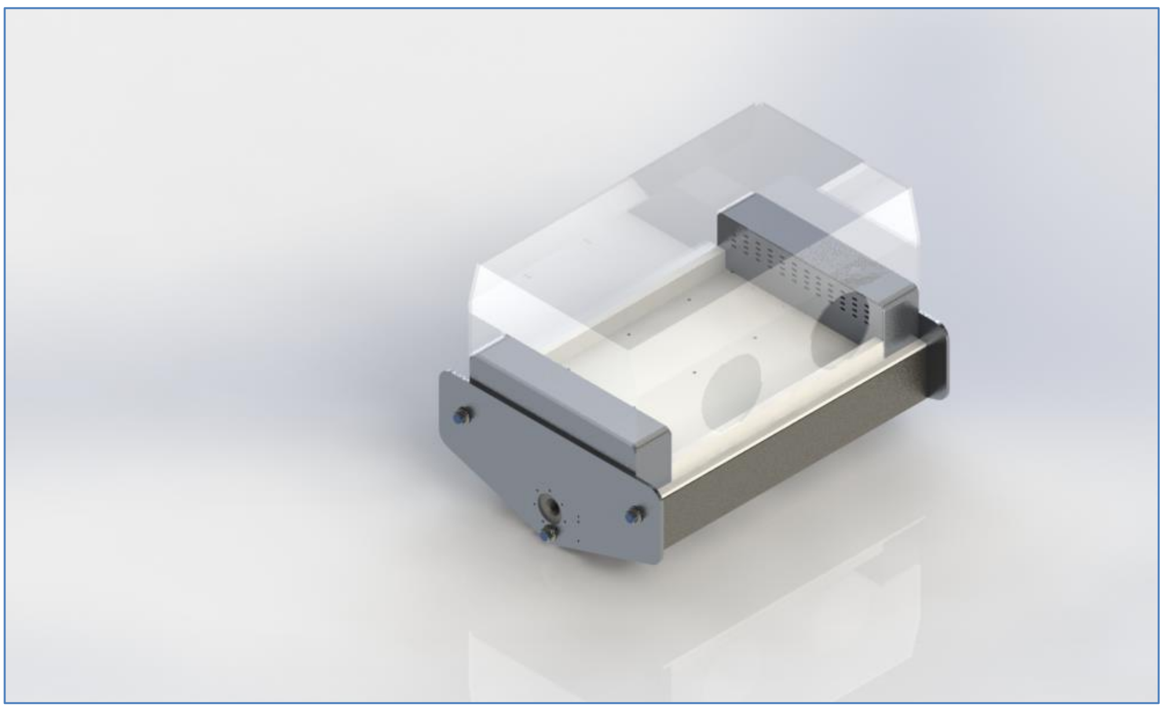

Figure 49. Isometric View of Final Incubator Design.

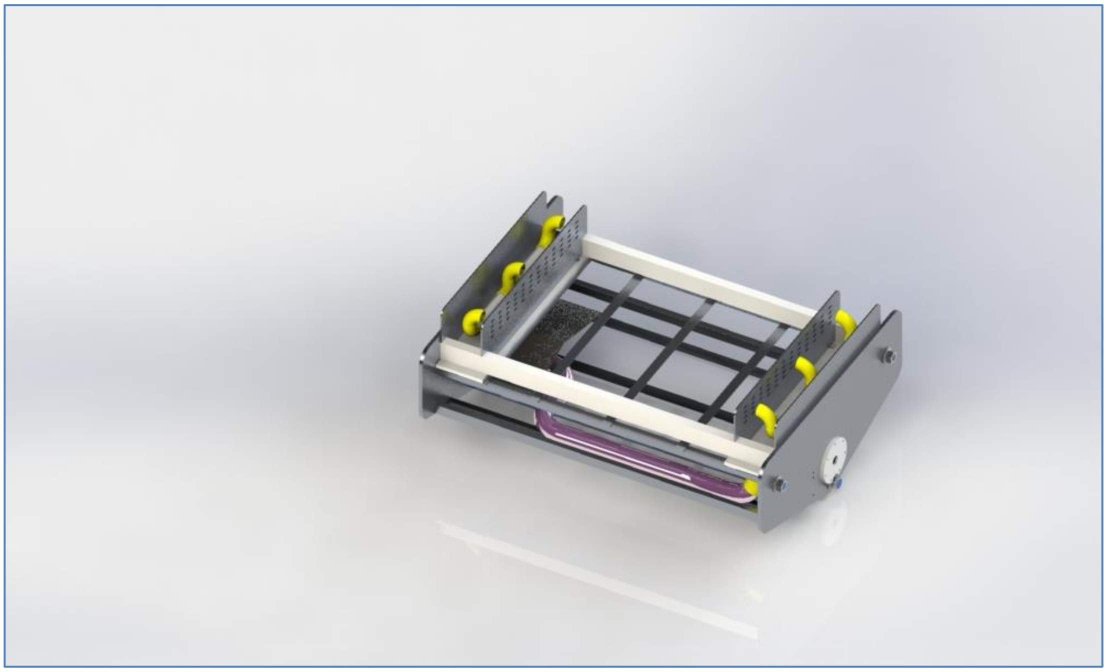

Figure 50. Interior View of Final Design of Incubator.

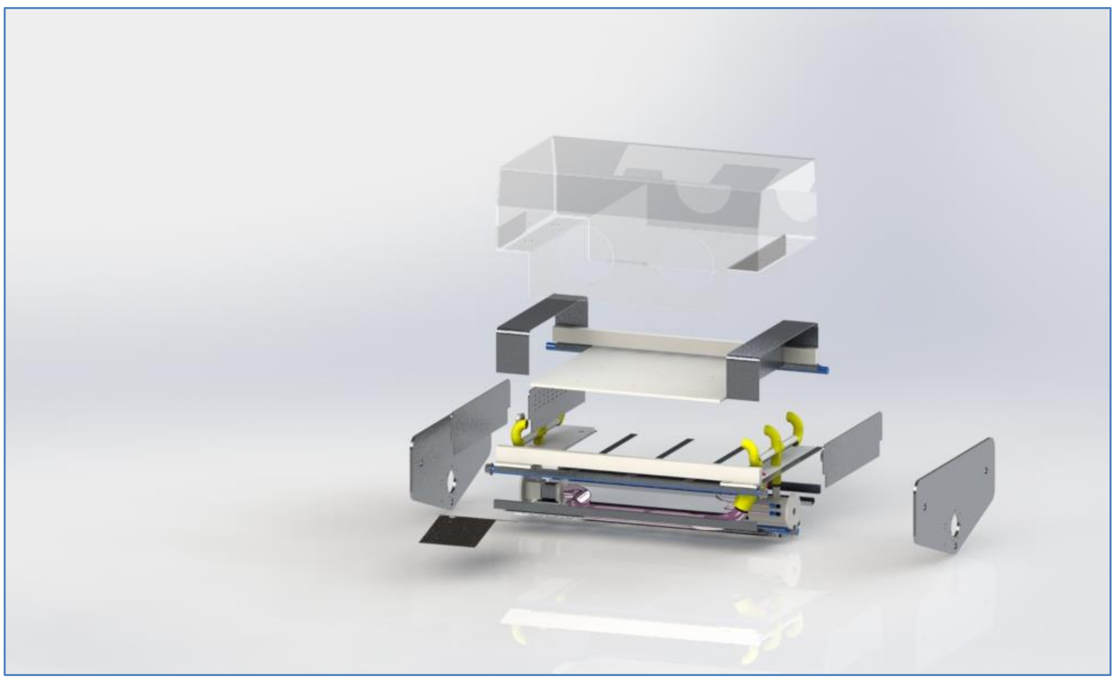

Figure 51. Exploded View of Incubator.

The Bill of Material (BoM) for the enclosure component, requires laser cutting manufacturing processes, is listed in Table 6.

Table 6. Bill of Materials for Incubator Enclosure – Laser Cutting Process [55].

Component Description	Picture	Quantity	Manufacturing Method/Material	Unitary Cost (USD $)	Total Cost (USD $)
Front Cover	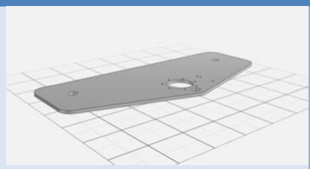	2	Laser Cutting/Aluminum 5052	128.00	256.00
Vertical Vent A	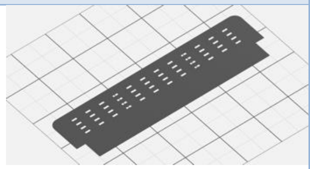	2	Laser Cutting/Aluminum 5052	80.00	160.00
Vertical Vent B	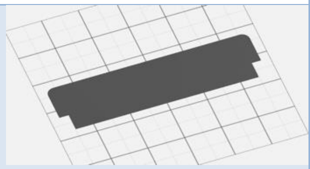	2	Laser Cutting/Aluminum 5052	71.00	142.00
Heater Cover	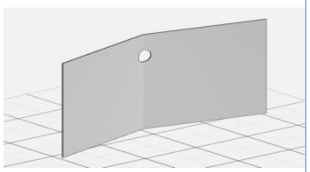	1	Laser Cutting/Aluminum 5052	130.00	130.00
Bed	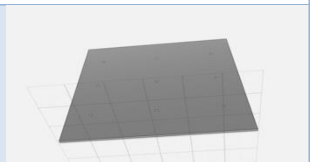	1	Laser aluminum 5052	169.00	169.00
	Sub Total				**857.00**

The Bill of Materials (BoM) and costs for all of the enclosure components that require manufacturing process using Computer-Numerical Control (CNC) are listed in Table 7.

Table 7. Bill of Materials for CNC Manufacturing Process [55].

Component Description	Picture	Quantity	Manufacturing Method/Material	Unitary Cost (USD $)	Total Cost (USD $)
Heater Adaptor inlet	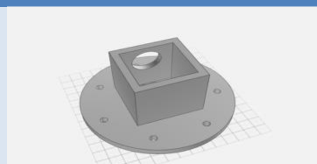	1	CNC/PVC	260.00	256.00
Heater Adaptor Outlet	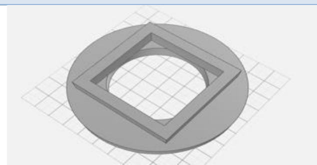	1	CNC/PVC	136.00	136.00
Humidification Chamber	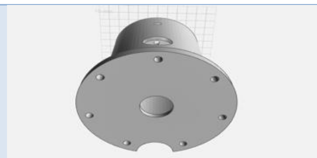	1	CNC/PTFE	642.00	642.00
	Sub Total				**1034.00**

To minimize the total manufacturing cost, the incubator was designed with commercial off-the-shelf elements that require no or minimal manufacturing processes. The objective is that these components can be acquired online and used directly in the incubator assembly. The complete list of off-of-the-shelf components is shown in Table 8.

In addition, an item list was compiled for all other construction elements that were not previously detailed in the project (e.g., bolts, fasteners).

Table 8. Off-the-Shelf Components.

Component Description	Picture	Quantity	Manufacturing Method/Material	Unitary Cost (USD $)	Total Cost (USD $)
PVC Sheet ¼” x 48” x 96” [60]		1	NA/PVC	174.00	174.00
Square Bar [61]		6	NA/PVC	5.00	30.00
Aluminum Channel [62]		2	NA/Aluminum	33.00	66.00
Other Unaccounted elements (Estimation)	NA	1	NA	500.00	500.00
	Sub Total				**770.00**

A summary of the total enclosure cost is shown in Table 9.

Table 9. Total Enclosure Cost.

No	System Description	Cost ($ USD)
1	Laser-Cutting Components	857.00
2	CNC-Machining Components	1,034.00
3	Out-of-shelf Components	770.00
	Total Enclosure Cost	2,661.00

In addition to the compilation of cost data, a stress analysis was undertaken to verify that the proposed incubator can bear the average weight of a premature baby. The Finite Element Analysis (FEA) capabilities in SolidWorks were employed to conduct the stress analysis of the weakest supporting element in the design (i.e., the plastic supporting bed).

The analysis was conducted for the worst-case scenario: a plastic bed supporting the uniformly distributed weight of a baby with a fixed support at the ends only. Based on data from Mayo Clinic [63], the average weight of a 40-week premature baby is 7 pounds and 15 oz. A 10-pound (44 N) distributed force was employed for the analysis. Both PVC and Acrylonitrile Butadiene Styrene (ABS) were considered as viable alternatives for manufacturing the bed, but since ABS has a lower yield strength [64], it was selected for this simulation. ABS is an opaque thermoplastic and amorphous polymer.

The summary of the model information and material properties from SolidWorks is shown in Table 10.

Table 10. Model Summary and Material Properties for Supporting Bed.

<table>
<tr><td colspan="4">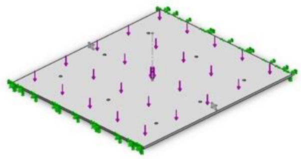
Model name: bedA</td></tr>
<tr><th>Load name</th><th>Load Image</th><th colspan="2">Load Details</th></tr>
<tr><td>Force-1</td><td>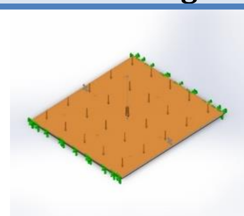</td><td colspan="2">Entities: 1 face(s)
Type: Apply normal force
Value: 44 N
Phase Angle: 0
Units: deg</td></tr>
<tr><th>Fixture name</th><th>Fixture Image</th><th colspan="2">Fixture Details</th></tr>
<tr><td>Fixed-1</td><td>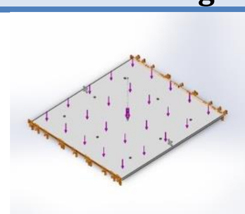</td><td colspan="2">Entities: 2 face(s)
Type: Fixed Geometry</td></tr>
<tr><th>Document Name and Reference</th><th>Treated As</th><th>Volumetric Properties</th><th>Document Path/Date Modified</th></tr>
<tr><td rowspan="3">Boss-Extrude1
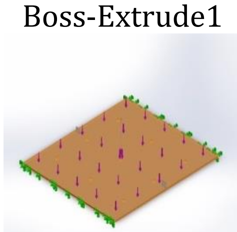</td><td>Solid Body</td><td>Mass:4.12222 kg
Volume:0.00404139 m^3
Density:1020 kg/m^3
Weight:40.3977 N</td><td>Mar 24 11:39:06 2020</td></tr>
<tr><th colspan="2">Properties Components</th><th>Components</th></tr>
<tr><td colspan="2">Name: ABS
Model type: Linear Elastic Isotropic
Default failure criterion: Unknown
Tensile strength: 30 N/mm^2</td><td>SolidBody 1(Boss-Extrude1)(bedA)</td></tr>
</table>

The results for the stress analysis and displacement for the supporting beds are shown in Figure 52 and Figure 53, respectively. The max yield strength experienced by the supporting bed was 0.22971 Mpa, which is much lower than the tensile strength for ABS (30 Mpa). The max deformation is approximately 0.35 mm.

Name	Type	Min	Max
Stress	VON: von Mises Stress	0.000164487 N/mm^2 (MPa) Node: 14898	0.22971 N/mm^2 (MPa) Node: 19263

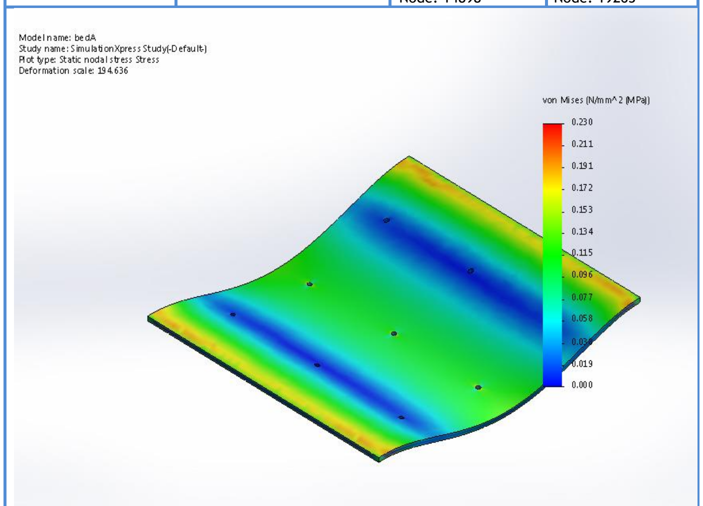

bedA-SimulationXpress Study-Stress-Stress

Figure 52. Stress Analysis for Supporting Bed.

Name	Type	Min	Max
Displacement	URES: Resultant Displacement	0 mm Node: 135	0.347829 mm Node: 18508

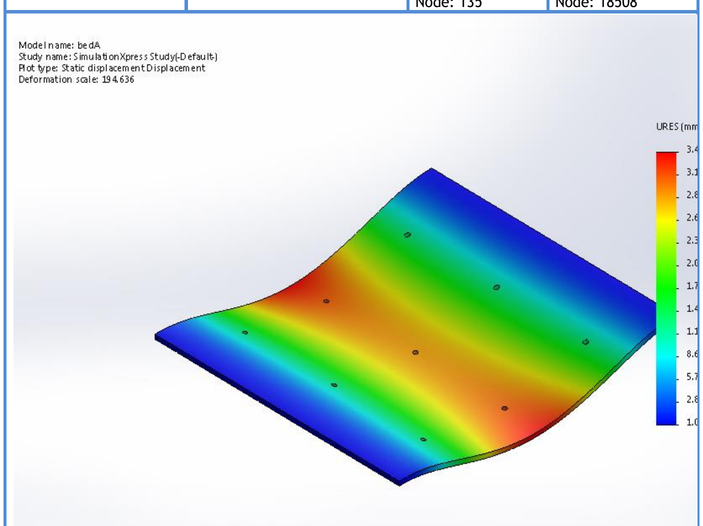

bedA-SimulationXpress Study-Displacement-Displacement

Figure 53. Displacement Analysis for Supporting Bed.

Based on these results, it is possible to conclude with confidence that the supporting bed is safe. Therefore, it can be stated with a high degree of confidence that the whole structure is capable of supporting the weight of the infant and equipment safely.

The compliance of the design with IEC requirements [11] associated with the enclosure is addressed in the next section.

1. "The infant shall be safely retained within the COMPARTMENT by barriers such as walls or side panels."[21]
   - Containment is achieved through the barriers shown in Figure 54. Besides, the acrylic cover will swing open only along the dashed line, providing the necessary barriers to prevent a fall for the infant inside the unit.
   - 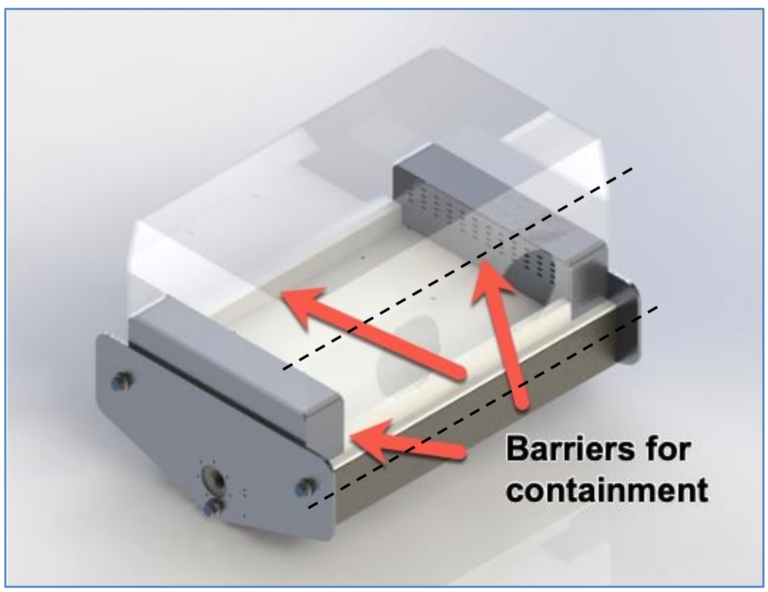

Figure 54. Incubator Containment.

[21] Section: 201.9.8.3.101, page 14.

2. "If a water reservoir is provided as an integral part of the INFANT INCUBATOR, it shall have a water level indicator with "max" and "min" markings if the level of the water in the tank cannot be seen."[22]
   - A water reservoir has been considered for the humidification chamber. The max-min levels would be indicated via a sight glass mounted on the front cover of the incubator, as shown in Figure 55.
   - 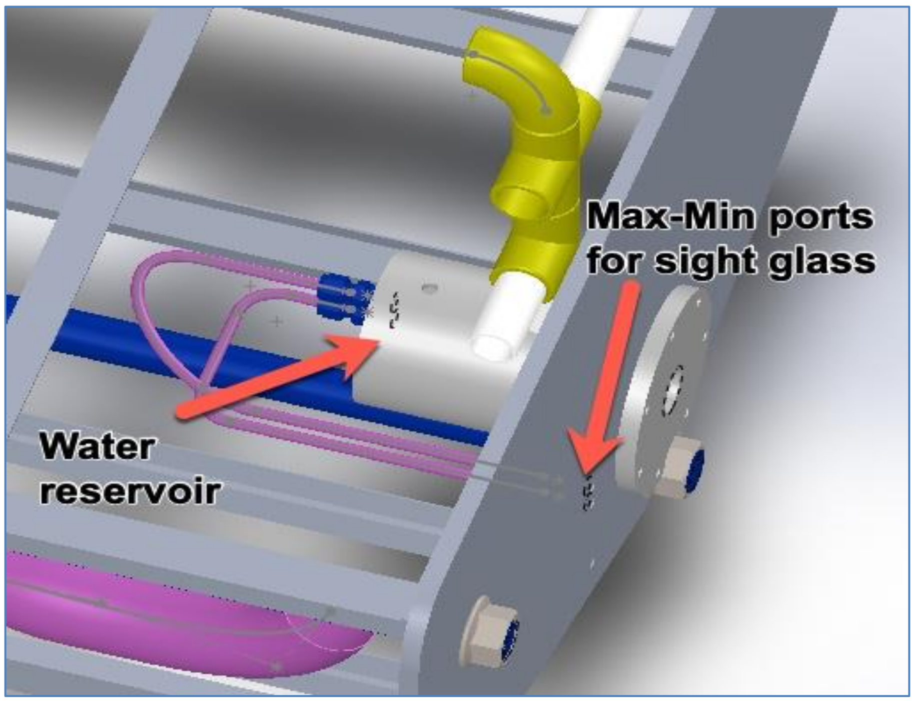

Figure 55. Max-Min Water Levels.

[22] Section: 201.11.6.2, page 16.

3. “INFANT INCUBATOR shall be constructed such that spillage does not wet parts which, if wetted, might cause a safety hazard.”[23]

   - The test used to comply with this point consists of pouring 200 ml of water on any point of the top surface of the equipment. The design provides for draining holes on the supporting bed that would allow any liquid to be drained to the component section below and subsequently be drained. The only electrical component susceptible to any spillage is the heater, for which a spillage cover has been considered to avoid any water coming from above to come into contact with the component, as shown in Figure 56.

   - 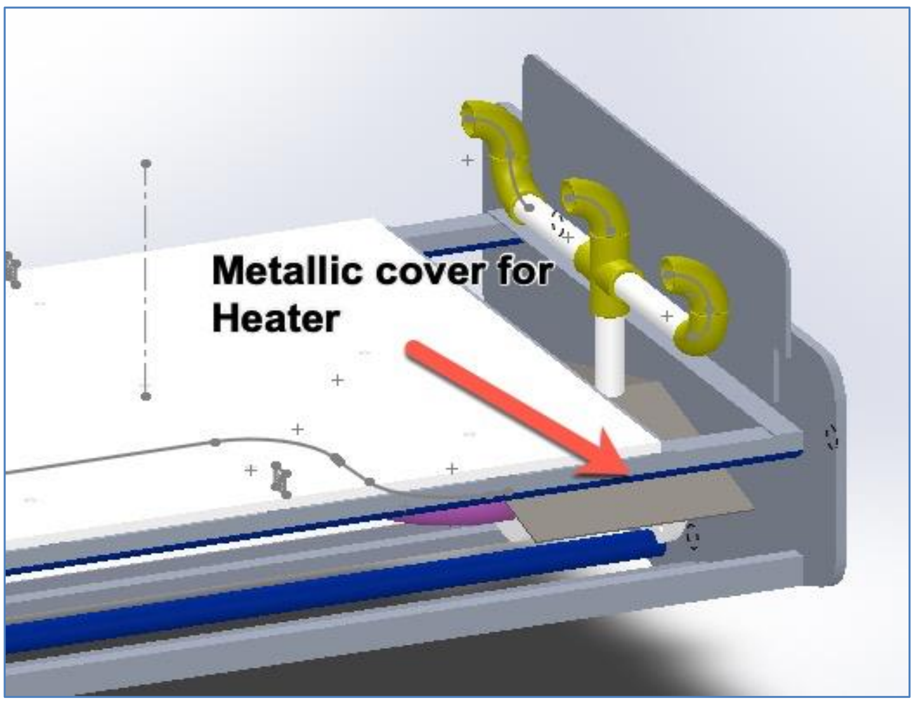

Figure 56. Spillage Cover for Heater.

[23] Section: 201.11.6.3, page 16.

4. "The INFANT INCUBATOR shall have means by which the infant can be taken in and out without the need to remove the canopy completed, or to disconnect tubes, cords, leads and the like from the infant."[24]
    - The acrylic cover shown in Figure 54, allows an infant to be placed inside the incubator without disconnecting any device, wire, or any of the sorts.

[24] Section: 201.15.3.101.

5. “Temperatures of the surfaces intended to be in contact with the patient shall not exceed 40 degrees Celsius [25].

   - In the “Methods” section of this report, the necessary calculation of critical values to conduct a heat transfer analysis was described. Simscale software [58] was used to conduct a steady-state simulation of the temperatures. A heat transfer analysis was defined in the Simscale workbench, and the material configuration, contact properties and boundary conditions using the convection coefficient values determined previously also were defined in the workbench, as shown in Figure 57.
   - 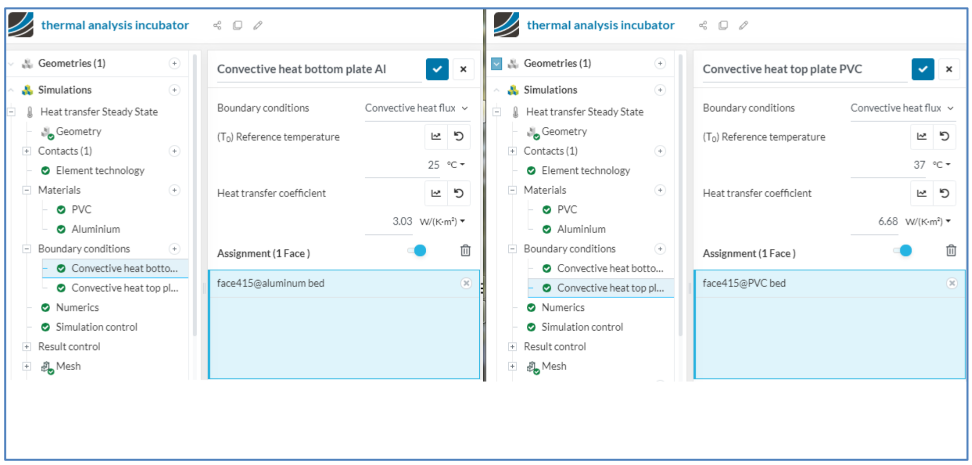

Figure 57. Boundary Conditions for Heat Transfer Simulation.

[25] Section 201.11.1.2.2, page 25.

The meshing configuration defined for the model is shown in Figure 58. The recommended Simscale setting for creating a mesh was employed, given the simplicity of the design.

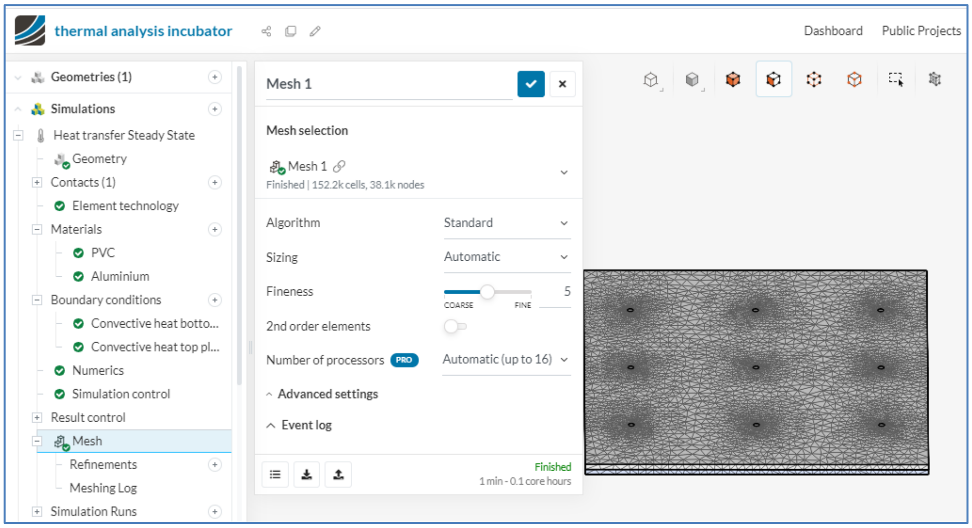

Figure 58. Meshing Configuration.

The temperature profile calculated by the software is shown in Figure 59. The results of the simulation indicate that the maximum value reached by the contact surface for the infant is 306 K (≅ 33 °C). Therefore, the proposed design complies with IEC requirements.

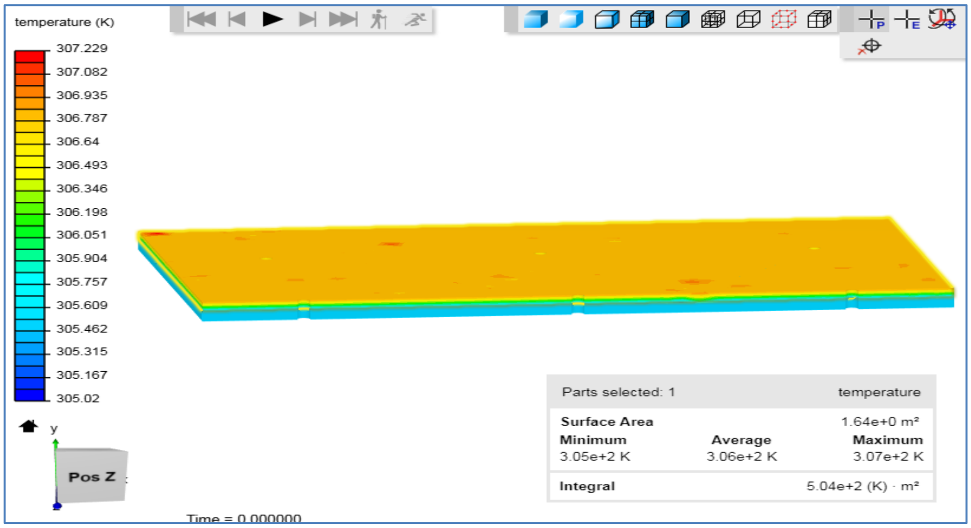

Figure 59. Temperature Profile.

Conclusions

The purpose of this project was to determine if it is feasible to develop a low-cost, a standard-compliant incubator for developing nations to help mitigate the infant mortality rate in those regions. A key project goal was to develop a design that could be built and assembled using open-source and available manufacturing technologies.

In this project, an incubator prototype was successfully developed – one that can meet the standardized requirements associated with temperature, humidity, and enclosure characteristics.

The use of simulation software showed that the proposed mechanisms in the prototype are feasible and able to meet the project's functional requirements.

The total cost for the system developed for this project is shown in Table 11. This cost is very similar to the entry-price of infant incubators manufactured in China with similar capabilities. However, the advantage of the approach adopted in this project provides developing nations with the ability to build, to assemble, and to maintain their incubators, which can also benefit local economies. It must be noted that the manufacturing cost explored in this project has the potential for a reduction, since the cost obtained reflects the manufacturing cost in the United States, but which is significantly lower in developing nations because of less expensive labor costs.

Table 11. Total Manufacturing Cost for Incubator.

System No	Component Description	Total Cost (USD $)
1	Air Heating System	696.02
2	Humification System	298.00
3	Enclosure	2,661.00
	Total Manufacturing Cost	**3,655.02**

Based on the estimated cost, the use of open source technology, and the development of detailed prototype schematics, it is concluded that the project was able to achieve its objective to provide a feasible prototype for an infant incubator that can be built and assembled in developing nations using traditional manufacturing technologies.

At the beginning of the project, it was expected that the use of additive manufacturing could be an important factor in decreasing manufacturing cost and enable unitary production of incubators as needed. As discussed previously, the expectation was not met. Additive manufacturing is not yet able to reduce manufacturing cost for these types of projects, although it is believed that this technology would become more available and affordable in the future, leading to wider adoption to solve complex problems related to manufacturing of health care equipment.

The COVID-19 Pandemic and the shortage of critical medical equipment like ventilators have shown the relevance of initiatives like the one explored in this project. The capability of nations to build and to manufacture medical equipment can make the difference between life and death, economic disruptions, and social chaos. Therefore, this project additionally points to the need for additional research on low-cost solutions for medical equipment to fight global pandemics.

Recommendations

One of the key challenges encountered during this project was the lack of an integrated design platform to design and test the prototype ideas. This project, even though it was simple in concept, required the use of CAD software to develop the mechanical parts and assemblies, mathematical software like MATLAB to develop models and to solve equations, and computational fluid dynamics (CFD) software to simulate the physical behaviors of the components, such as heat transfer associated with the components. This proved to be a challenging effort, due to the lack of integration between the different software packages and also due the lack of cloud solutions that could facilitate this effort [65].

In retrospect, it is clear that had more time been invested in reviewing additive manufacturing during the initial stages of this project, that manufacturing option would have been discarded esrly on, reducing the time and effort spent on developing a prototype suitable for this technology.

This aspect points to the future of cloud-based integrated end-to-end platforms that allow the integration of different solutions to create digital twins to optimize the design process. A digital twin is a digital representation of a physical object or system [66], and it has been identified by the consulting group Gartner as one of the top ten technology trends for the future [67]. It is a recommendation for MSOE to invest in this type of platform, which could lead to more research and development in an integrated way and facilitate similar projects in the future.

Because of the shortage of mechanical ventilators caused by COVID 19, Medtronic [65] has released its design specifications for this type of equipment. In a similar manner, it is recommended that future research should be undertaken to use the materials and approach in this project, along with the Medtronic specifications, to develop a simplified version of a mechanical ventilator for developing countries.

With respect to this capstone project, it is recommended that the building of a physical prototype of the proposed incubator should be undertaken to refine the design. Once the design has been suitably refined, it would be possible to seek FDA approval, with the goal of eventually conducting clinical testing in a health care facility in a developing nation.

References

[1] WHO-MCEE, "Methods and Data Sources for Child Cause of Death 2000 - 2016," [Online]. Available: http://www.who.int/maternal_child_adolescent/data/causes-death-children/en/. [Accessed 5 October 2018].

[2] UNICEF, "Levels and Trends in Child Mortality," UN Inter-Agency Group for Child Mortality Estimation, 2018.

[3] K. Lunze, D. E. Bloom, T. D. Jamison and H. D. Hamer, "The Global Burden of Neonatal Hypothermia: Systematic Review of a Major Challenge for Newborn Survival," 24 November 2013. [Online]. Available: https://bmcmedicine.biomedcentral.com/articles/10.1186/1741-7015-11-24#Abs1. [Accessed 10 October 2018].

[4] L. Mulany, J. Katz, S. Khatry, S. Leclerq, G. Darmstadt and J. Tielsch, "Neonatal hypothermia and associated Risk Factors Among Newborns," BMC Med, 2010.

[5] K. Lunze and D. Hamer, "Thermal Protection of the Newborn in Resource-Limited Environments," J Perinatol, vol. 32, pp. 317-324, 2012.

[6] A. Bergstrom, R. Byaruhanga and P. Okong, "The Impact of Newborn Bathing on the Prevalence of Neonatal Hypothermia in Uganda: a Randomized, Controlled Trial," Acta Paediatrica, vol. 94, pp. 1462-1467, October 2005.

[7] D. Hamer, K. Lunze, J. Herlihy, A. Mazimba, C. Grogan, M. Nkimberg, L. Owens, K. Yeboah-Antwi and K. Semrau, "Prevention of Neonatal Hypothermia in Southern Province, Zambia," in 61st Annual Meeting, American Society of Tropical Medicine and Hygiene, Atlanta, 2012.

[8] American Public Health Association, "Strengthening Health Systems in Developing Countries," October 2008. [Online]. Available: https://www.apha.org/policies-and-advocacy/public-health-policy-statements/policy-database/2014/07/23/09/09/strengthening-health-systems-in-developing-countries. [Accessed 22 October 2018].

[9] A. Gomez, Interviewee, Resident Doctor Hospital Escuela. [Interview]. June 2018.

[10] Alibaba, "Alibaba Incubator Search Results," [Online]. Available: https://www.alibaba.com/trade/search?IndexArea=product_en&SearchText=baby_incubator_price&viewtype=L&f0=y&pricef=3000&pricet=15000. [Accessed 25 October 2018].

[11] IEC, "Medical electricla equipment Part 2-19: Particular Requirements for the basic and essential performance of infant incubators," International Electrotechnical Comission, 2009.

[12] IEC, "Medical electrical equipment. Part 1 General requirements for basic safety and essential performance.," IEC, 2007.

[13] W. H. Organization, "Country profiles - Global atlas of medical devices (2017 update)".

[14] W. H. Organization, "Medical devices".

[15] U. N. D. Program, "Human Development Report," [Online]. Available: http://hdr.undp.org/en/composite/HDI. [Accessed 10 November 2018].

[16] J. Ellis, "Neonatal hypothermia," Journal of Neonatal Nursing, vol. 11, no. 2, pp. 76-82, 24 August 2005.

[17] F. Weithöner, "Franks hospital," [Online]. Available: http://www.frankshospitalworkshop.com/.

[18] "James Dyson Award," 2014. [Online]. Available: https://www.jamesdysonaward.org/en-GB/2014/project/mom/. [Accessed October 2018].

[19] E. Innovation, "Embrace Innovation," [Online]. Available: https://www.embraceinnovations.com/#home. [Accessed October 2018].

[20] Y. Molgan-Seon, T. Daboval, S. Chou and O. Jay, "Accidental Overheating of a Newborn Under an Infant Radiant Warmer: a Lesson for Future Use," Journal of perinatology: official journal of the California Perinatal Association, vol. 33, no. 9, 2013.

[21] FDA, "Premarket Information - Device Design and Documentation Processes," [Online]. Available: https://www.fda.gov/medical-devices/human-factors-and-medical-devices/premarket-information-device-design-and-documentation-processes.

[22] C. Barbosa Pereira, H. Konrad, M. Czaplik, V. Balzek, V. Bouewijn and S. Leonhardt, "Thermoregulation in Premature infants: A mathematical model," Journal of Termal Biology, vol. 62, pp. 159-169, 2016.

[23] A. Fraguela, F. D. Matlalcuatzi and Á. M. Ramosc, "Mathematical modeling of thermoregulation processes for premature infants in closed convectively heated incubators," Computers in Biology and Medicine, vol. 57, pp. 159-172, 2015.

[24] M. Hitu, M. Lini and G. Ashish, "Design and Development of an Infant Incubator for Controlling Multiple Parameters," National Institute of Technical Teachers, Chennai, India.

[25] M. A. Ortiz Valdez, "Github," [Online]. Available: https://github.com/maov98/Incubator_Project.

[26] F. G. Franklin, J. D. Powell and A. Emami-Naeimi, Feedback Control of Dynamics Systems, Seventh ed., Pearson.

[27] N. S. Nise, "Control Systems Engineering," 7th ed., Wiley.

[28] F. P. Incropera, D. P. Dewitt, L. T. Bergman and S. A. Lavine, Introduction to Heat Transfer, Indiana: John Wiley & Sons.

[29] Š. Bucz and A. Kozáková, "Advanced Methods of PID Controller Tuning for Specified Performance," ntechOpen, 2018.

[30] Arduino, "Arduio Official Site," [Online]. Available: https://store.arduino.cc/usa/mega-2560-r3. [Accessed 01 03 2020].

[31] MAxin Integrated, "Technical Documentation," [Online]. Available: https://www.maximintegrated.com/en/design/technical-documents/app-notes/4/4026.html. [Accessed 03 03 2020].

[32] Maxim Integrated, "Sensors," [Online]. Available: https://www.maximintegrated.com/en/products/sensors/MAX31856.html. [Accessed 03 03 2020].

[33] OMROM, "Support Guide," [Online]. Available: https://www.ia.omron.com/support/guide/18/overview.html. [Accessed 02 03 2020].

[34] Crydom, "SSR," [Online]. Available: http://www.crydom.com/en/tech/newsletters/solid%20statements%20-%20ssrs%20switching%20types.pdf. [Accessed 01 03 2020].

[35] F. N. C. Inc, "Heater Supply," [Online]. Available: https://www.heater-supply.com/SOLID-STATE-RELAYS-SSR_c_222.html. [Accessed 01 3 2020].

[36] MROcrib, [Online]. Available: https://mrocrib.com/en/accessories/1000818-watlow-rpc-5399-42-000.html. [Accessed 01 03 2020].

[37] OMEGA, "Compact Fan Heaters," [Online]. Available: https://www.omega.com/en-us/industrial-heaters/duct-and-enclosure-heaters/enclosure-heaters/fch-fgc1/p/FCH-FGC10262R. [Accessed 02 03 2020].

[38] Digi-Key, "Products," [Online]. Available: https://www.digikey.com/product-detail/en/sensata-crydom/DR24D03/CC2069-ND/3915212. [Accessed 02 03 2020].

[39] NGD, "NGD Products," [Online]. Available: https://store.ncd.io/product/ad5696-4-channel-4-20ma-16-bit-current-loop-transmitter-with-iot-interface/. [Accessed 2 03 2020].

[40] Omega, "Omega," [Online]. Available: https://www.omega.com/en-us/sensors-and-sensing-equipment/temperature/sensors/thermocouple-probes/m12probes/p/M12JSS-M3-U-200-F. [Accessed 01 03 2020].

[41] Playing with Fusion, [Online]. Available: https://www.playingwithfusion.com/productview.php?pdid=76. [Accessed 01 03 2020].

[42] Adafruit, "Adafruit Displays," [Online]. Available: https://www.adafruit.com/product/2050.

[43] Planet Technology, [Online]. Available: https://planetechusa.com/product/pwr-15-12-industrial-12vdc-din-rail-power-supply?campaignid=2044569076&adgroupid=75017196369&creative=357882966705&matchtype=&network=u&device=c&keyword=&gclid=Cj0KCQjwx7zzBRCcARIsABPRscPBR8m48jDrH24sVZ45NBdk-RL307hHnvyQFf. [Accessed 01 03 2020].

[44] V. A. Harpin and N. Rutter, "Humidification of Incubators," Archives of Disease in Chilhood, vol. 60, pp. 219-220, 1985.

[45] World Health Organization, "Medical Device Specification," [Online]. Available: http://www.who.int/medical_devices/management_use/WHO_TS_61_MDs_web.xlsx. [Accessed October 2018].

[46] WOLFRAM, "Demonstration Project," [Online]. Available: https://www.wolframcloud.com/objects/demonstrations/ReadingAPsychrometricChart-source.nb. [Accessed 26 02 2020].

[47] Ansys, "ACADEMIA," [Online]. Available: https://www.academia.edu/24133202/Tutorial_Heat_and_Mass_Transfer_with_the_Mixture_Model_and_Evaporation-Condensation_Model. [Accessed 01 04 2020].

[48] Testco, "Testco," [Online]. Available: https://www.testco-inc.com/thermodisc/G4A01110C. [Accessed 01 03 2020].

[49] OMEGA, "OEMGA Catalog," [Online]. Available: https://www.omega.com/en-us/industrial-heaters/immersion-heaters/emh-heater/p/EMH-110-120V. [Accessed 04 03 2020].

[50] Adafruit, "Adafruit," [Online]. Available: https://www.adafruit.com/product/4099. [Accessed 01 03 2020].

[51] V. R. Sastri, Plastics in Medical Devices, William Andrew, 2014, p. 336.

[52] M. F. Ashby, Material Selection in Mechanical Design, Elsevier, 2017.

[53] Sculpteo, "Sculpteo," [Online]. Available: https://www.sculpteo.com/en/.

[54] Xometry, [Online]. Available: https://www.xometry.com/. [Accessed 04 2020 03].

[55] 3d Hubs, [Online]. Available: https://www.3dhubs.com/. [Accessed 04 03 2003].

[56] 3. Hubs, "Printing Basics," [Online]. Available: https://www.3dhubs.com/guides/3d-printing/#basics. [Accessed 03 03 2020].

[57] Deloitte, "The Industry 4.0 Paradox," [Online]. Available: https://www2.deloitte.com/us/en/insights/focus/industry-4-0/challenges-on-path-to-digital-transformation/summary.html?id=us:2ps:3gl:confidence:eng:cons:050519:nonem:na:XCndYSKw:1150326370:346939503340:e:Internet_of_Things:Industry_4.0_Paradox_Exact:nb. [Accessed 03 03 2020].

[58] SImscale, "Simulation Cloud," [Online]. Available: https://www.simscale.com/. [Accessed 05 03 2020].

[59] F. M. White, Fluid Mechanics, McGraww Hill, 2011.

[60] USA PLastic Corps, "Polypropylene," [Online]. Available: https://www.usplastic.com/catalog/item.aspx?itemid=44114&catid=733. [Accessed 02 03 2020].

[61] US Plastics Corp, "Square Bars," [Online]. Available: https://www.usplastic.com/catalog/item.aspx?itemid=25662&catid=733. [Accessed 02 03 2020].

[62] Orange Aluminum, "Channel," [Online]. Available: https://www.orangealuminum.com/channels-oa2900.html. [Accessed 03 03 2020].

[63] Mayo Clinic, "Premature Birth," [Online]. Available: https://www.mayoclinic.org/diseases-conditions/premature-birth/symptoms-causes/syc-20376730. [Accessed 04 03 2020].

[64] Engineering ToolBox, "Thermoplastics," [Online]. Available: https://www.engineeringtoolbox.com/physical-properties-thermoplastics-d_808.html. [Accessed 04 03 2020].

[65] Medtronic, "Home Page," [Online]. Available: https://www.medtronic.com/us-en/. [Accessed 03 04 2020].

[66] NetWorkLoad, "What is a Digital Twin," [Online]. Available: https://www.networkworld.com/article/3280225/what-is-digital-twin-technology-and-why-it-matters.html. [Accessed 03 04 2020].

[67] NetWorkWorld, "Top 10 Technology Trends," [Online]. Available: https://www.networkworld.com/article/3132363/gartner-top-10-strategic-technology-trends-you-should-know-for-2017.html. [Accessed 03 04 2020].

Bibliography

American Society of Quality (ASQ), "Resources-FMEA," [Online]. Available: https://asq.org/quality-resources/fmea. [Accessed 11 December 2018].

A. Ahmed, J. Cabello, D. Patel, D. Russo, K. Tseng, G. Facas and B. F. Busha, "Low Cost Transportable Infant Incubator," in 39th Annual Northeast Bioengineering Conference, 2013.

A. De Silva and A. Galgomuwa, "High Performance Temperature Controller for Infant Incubators," in International Conference on Information and Automation, 2006.

A. Fic, D. Ingham, M. Ginalski, A. Nowak and L. Wrobel, "Heat and Mass Transfer Under an Infant Radiant Warmer - Development of a Numerical Model," Medical Engineerng and Physics, vol. 32, no. 5, 2010.

A. Vilinsky, A. Sheridan and L. Nugent, "Preventing Peri-Operative Maternal and Neonatal Hypothermia After Skin-to-Skin Contact," Neonatal Nursing, vol. 22, no. 4, August 2016.

B. Navaneethakrishnan and P. Neelamegan, "FPGA-Based Temperature Monitoring and Control System for Infant Incubator," Sensors & Transducers, vol. 143, no. 8, August 2012.

C. 77, "Design Rules for 3D Printing," [Online]. Available: https://www.core77.com/posts/74401/Design-Rules-for-3D-Printing.

Design that Matters, "Otter Newborn Warmer," [Online]. Available: https://www.designthatmatters.org/otter. [Accessed 20 10 2018].

E. Edge, "Engineers Edge," [Online]. Available: https://www.engineersedge.com/thermodynamics/enthalpy_entropy_mollier.htm. [Accessed 26 02 2020].

F. Ibrahim, J. Ding and M. Taib, "Safety and Performance Compliance Test of an Infant Incubator," in Student Conference on Research and Development, 2002.

G. Putic, "Low-Cost Incubator May Save More Babies," 2014. [Online]. Available: https://www.proquest.com/. [Accessed October 2018].

Infinite Electronic, [Online]. Available: https://www.infinite-electronic.hk/product/Sanyo-Denki_109P0612M701.aspx. [Accessed 01 03 2020].

International, Transparency, "Corruption Perception Index 2017," 2017. [Online]. Available: https://www.transparency.org/news/feature/corruption_perceptions_index_2017. [Accessed 28 October 2018].

J. Kerstin, P. Isabelle, E. Delgado, N. Kumar and A. N. Datta, "Dynamics and Complexity of Body Temperature in Preterm Infants Nursed in Incubators," University of Basel, vol. 12, 2017.

K. E. Muchowski, "Evaluation and Treatment of Neonatal Hyperbilirubinemia," 1 06 2014. [Online]. Available: https://www.aafp.org/afp/2014/0601/p873.html. [Accessed 24 November 2018].

K. Shin, D. Shin and S. Kim, "Low-Power Hybrid Wireless Network for Monitoring Infant Incubators," Medical Engineering and Physics, vol. 27, no. 8, 2005.

Medical Dictionary, [Online]. Available: https://medical-dictionary.thefreedictionary.com/incubator. [Accessed December 2018].

MedlinePlus, "Oxygen Therapy," [Online]. Available: https://medlineplus.gov/ency/article/007242.htm. [Accessed 25 November 2018].

M. Zermani, E. Feki and A. Mami, "Building Simulation Model of infant Incubator System with Decoupling Predictive Controller," IRBM, vol. 35, no. 4, 2014.

N. Mao, M. Song and D. Pan, "Computational Fluid Dynamics Analysis of Convective Heat Transfer Coefficients for a Sleeping Body," Applied Thermal Engineering, vol. 117, May 2017.

R. Frischer, M. Penhaker, O. Krejcar and M. Kacerovsky, "Precise Temperature Measurement for Increasing the Survival of Newborn Babies in Incubator Environments.," Sensors, no. 14, 2014.

R. Gupta, R. Patel and N. Murty, "Developing Global Health Technologies: Insight from an Initiative to Address Neonatal Hypothermia," Journal of Public Health Policy, vol. 36, no. 1, February 2015.

S. Miller, H. Lee and J. Gould , "Hypothermia in Very Low Birth Weight Infants: Distribution, Risk Factors and Outcomes," Journal of Perinatology, vol. 31, no. S1, April 2011.

S. Mostert, F. Njuguna, G. Olbara, S. Sindano, M. Sitaresmi, E. Supriyadi and G. Kaspers, "Corruption in Healthcare Systems and its Effect on Cancer Care in Africa," Lancet Oncology, vol. 16, no. 8, 2015.

T. Vian, "Review of Corruption in Health Sector: Theory, Methods and Interventions," Health Policy and Planning, vol. 23, no. 2, March 2008.

T. Yamaguchi, S. Hanai and H. Horio, "An Application of Computational Fluid Mechanics to the Air Flow in an Infant Incubator," Annals of Biomedical Engineering, vol. 20, no. 5, 1992.

V. Hall, E. Geise and N. Kashou, "The IncuLight: Solar-Powered Infant Incubator," in IEEE Global Humanitarian Technology Conference, 2014.

Weibull, "Basics-RCM," [Online]. Available: https://www.weibull.com/basics/rcm.htm. [Accessed December 2018].

W. H. Organization, "Medical Devices WHO," [Online]. Available: https://www.who.int/medical_devices/innovation/incubator_infant.pdf.

Engineering

Capstone Report Approval Form

Master of Science in Engineering – MSE

Milwaukee School of Engineering

This capstone report, titled "Design of Economic and Open Source Incubator for Developing Countries," submitted by the student Miguel A. Ortiz, has been approved by the following committee:

Faculty Co-Advisor: ____________________________ Date: _________________

Dr. Icaro dos Santos, Ph.D.

Faculty Co-Advisor: ____________________________ Date: _________________

Dr. Subha Kumpaty, Ph.D.

Faculty Member: ____________________________ Date: ________________________

Gary Shimek, M.L.I.S.